Rock Assemblage Library: MLA Pilot Study

2021

Authors: David Green and Robert Reid
Date: 08/06/2021
Email: info@mrt.tas.gov.au
Website: www.mrt.tas.gov.au

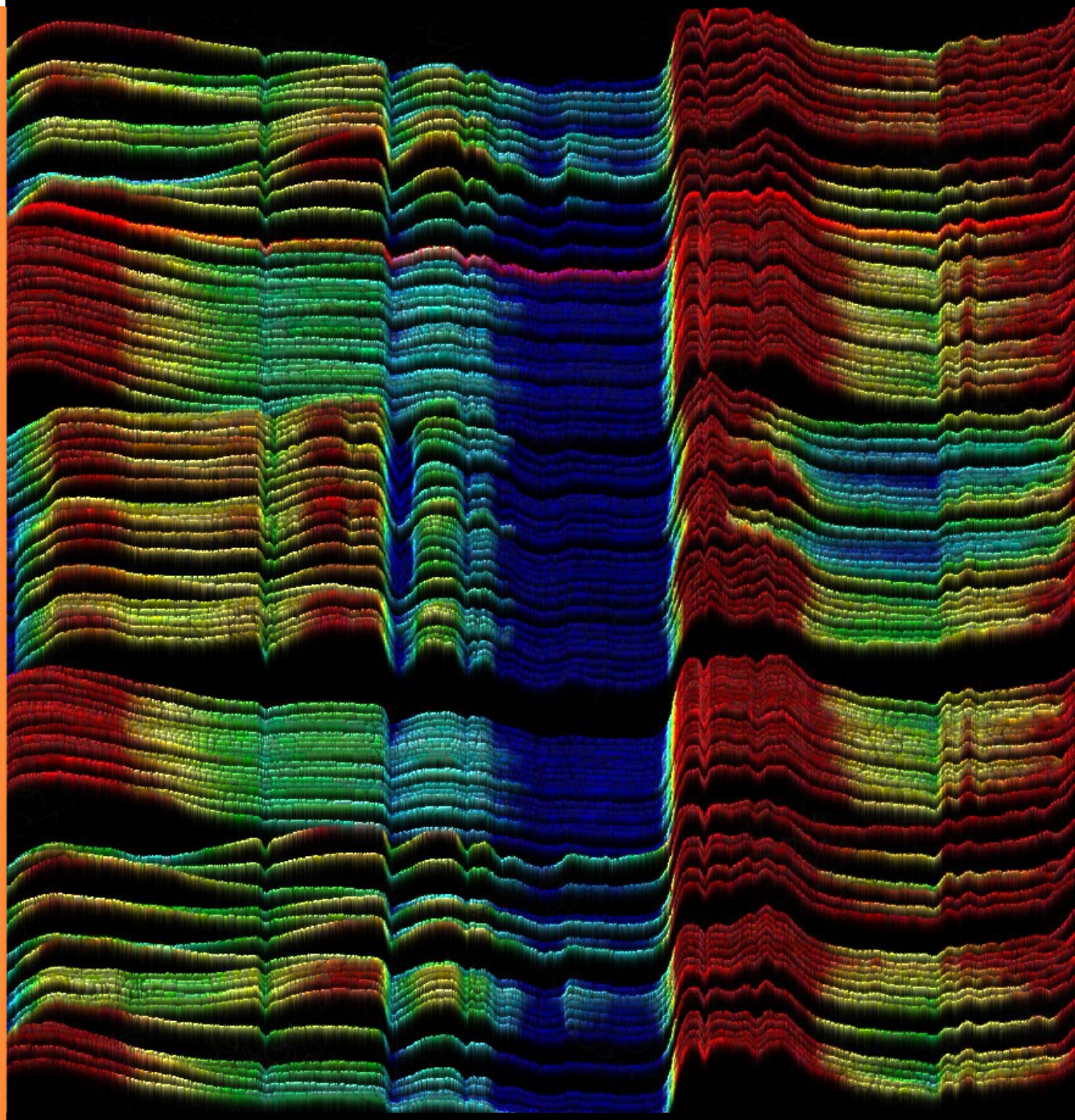

REPORT No: TR23

Geological Survey Technical Report 23

Tasmanian Government

Mineral Resources Tasmania
Department of State Growth

Geological Survey Technical Report 23:

Rock Assemblage Library: MLA Pilot Study

by David Green and Robert Reid

National Virtual Core Library
AuScope
National Collaborative Research Infrastructure Strategy

Contents

Figures

Tables

Acknowledgments

We would like to acknowledge the following for their continued assistance during this project:

Mineral Resources Tasmania staff: Peter Harding, Mirella Terrones, Lia Unwin, Ross King, Steve Newett, Ralph Bottrill, Till Gallagher, Michael Vicary and Chris Large.
Karsten Goeman of the University of Tasmania Central Science Laboratory.
State and Territory Geological Surveys for suggesting test samples.
Andy Green for running MOMA algorithms on the CorStruth database.
CSIRO staff Ian Lau and Carsten Laukamp for their support. Carsten also reviewed the manuscript.

This work was supported by AuScope Pty Ltd and the National Virtual Core Library (NVCL) project, managed by CSIRO Mineral Resources.

"And yes, I tend to disrespect labels because the artificial reality of labels is a significant factor in the demise of the human race"

Peter Mason

What's new in TSG, April 2008

1. Introduction

The AuScope NVCL Rock Assemblage Library project aims to validate the interpretation of HyLogger spectra for representative mineralogies (Moltzen & Bottrill 2018, Moltzen *et al.* 2020). The project has up until now validated HyLogging interpretations primarily by calculating mineral proportions using the MINSQ algorithm from (a) XRD analysis to provide the mineral assemblage, (b) microprobe analysis to provide mineral compositions and (c) XRF analysis of the whole sample (Herrmann and Berry, 2002). Additional validation was provided by quantitative XRD and petrological thin section.

Although the results indicate that the interpretation of HyLogging data has been largely validated, unresolved inconsistencies between the MINSQ, XRD and petrological results reveal significant uncertainty in our best estimate of true mineral abundance composition. In addition, HyLogger scanning, XRD/XRF and thin sections analyse different parts of the sample. Selecting homogeneous samples attempted to minimise consequent errors, but this required a large amount of work and severely filtered the sample candidates. In addition, crushing can result in the loss of fine grained or clay material and the destruction of the sample limited opportunities for repeat, alternative or complementary analysis (e.g. mid infrared scanning and microprobe analysis of minerals).

In this study, MLA (Mineral Liberation Analysis) was used in an attempt to improve the accuracy of the validated results and to better replicate the volume sampled by HyLogging, as was done on small samples by Huntington *et al.* (2009). It was proposed that a representative, homogeneous slab cut from drill core would be analysed by HyLogger and the same surface then analysed by MLA. The advantages and disadvantages of MINSQ and MLA are summarised in Table 1. Despite the cost, the rewards offered by MLA for establishing an accurate analysis (i.e. close to truth) and replicating the sampling volume of HyLogger scanning far outweigh the risks.

Table 1. Summary of the advantages and disadvantages of the MINSQ and MLA methods.

MINSQ

Advantages	Disadvantages
Easy to apply across a large number of samples (usually the most expensive part is the chemical analysis and this has often been done for other purposes).	There can be alternative mineral combinations that cover the same composition space, resulting in non-unique solutions (e.g. chlorite-muscovite-biotite-K feldspar).
Robust for major minerals and minerals with distinctive chemistry.	Individual samples or parts of samples crystallised at different conditions may be incorrectly interpreted.
Not affected by grainsize or intergrowths.	Disequilibrium assemblages (e.g. partly altered or weathered rocks) are poorly handled.
Easier to get estimates of uncertainty.	Variations in mineral composition lead to errors in abundance.

Polished slab MLA

Advantages	Disadvantages
Accurate mineralogy down to 0.1% abundance.	High cost per sample, approaching $1000 (including preparation of the large polished slab). The cost can be significantly reduced by crushing the sample and preparing representative grain mounts. However, (i) the sample is then of the bulk rather than just the surface and (ii) the grain mount may not be the same composition as the original rock as crushing can produce fractionation (e.g. clays and sulphides).
Rapid changes in mineral assemblages are easily recognised.	Very small grains (<10um) may be missed unless they have very distinctive compositions.
	Identified minerals may actually be intergrowths (e.g. nominal muscovite may be micrographic K-feldspar + quartz, which is compositionally identical using EDS). Backscatter images can help to identify these textures.

2. Methods

Sample selection

Candidate rock types and sub-assemblages were identified at the NVCL community workshop, Sydney 2020, then firmed up with emails afterward. The rocks and assemblages were identified because they have been found to be challenging and/or give ambiguous results.

The 15 rocks/mineral assemblages identified for targeting (with the 6 selected for the initial round of work indicated by *) were:

- Sandstone - micaceous
- Sandstone - calcareous
- (Black) shale – micaceous
- (Black) shale - crypto-micaceous *
- Kaolin + White-mica *
- Carbonate + White-mica
- Carbonate + Chlorite
- K-Feldspar + Plagioclase + Quartz *
- K-Feldspar + White-mica + Plagioclase *
- Chlorite + Carbonate + White mica
- Chlorite + Amphibole
- Chlorite + Biotite *
- Chlorite + Biotite + Amphibole
- Chlorite + Epidote + Amphibole
- Biotite + Epidote + Amphibole *

The sandstone and shale targets had been identified in Tasmanian drill core in 2019.

To find suitable examples of the target mineral assemblages, NVCL Analytics was used on Tasmanian drill holes. For a national search, Andy Green kindly built and ran tailored CorStruth MOMA algorithms (Green, 2017) to identify the number of occurrences of candidate assemblages in all drill holes in the CorStruth database (as at April 2020) e.g.

- Kaolin + White-mica
  (White-mica wt > 0.3) AND
  (Kaolin wt > 0.3)
- Chlorite + Biotite
  (0.33 < Chlorite wt < 0.66) AND
  (0.33 < Biotite wt < 0.66)
- K-Feldspar + White-mica + Plagioclase
  (0.2 < White mica wt < 0.4) AND
  (0.2 < Plagioclase wt < 0.4) AND
  (0.2 < K-Feldspar wt < 0.4)
- Chlorite + Carbonate + White mica
  (0.2 < Chlorite wt < 0.4) AND
  (0.2 < Carbonate wt < 0.4) AND
  (0.2 < White mica wt < 0.4)
- Chlorite/biotite (+/- amphibole)
  (0.2 < Chlorite wt < 0.45) AND
  (0.2 < Biotite wt < 0.4) AND
  (0.2 < Amphibole wt < 0.4)

The search used the sjCLST unmixing algorithm with group level mineral weights.

The TSG files of candidate samples were inspected and samples selected based in closeness to equal proportions of the target minerals, mineral assemblage homogeneity, textural simplicity and core condition. The samples were extracted at the relevant state and territory core libraries and gathered at MRT in Tasmania.

The first two samples identified for orientation MLA analysis were selected based on being on hand, their homogeneity, containing a simple mineral assemblage, and having optimal grainsize and an equigranular texture. Later samples were selected to challenge both the technique and the validation task. In total, 6 samples were selected for initial study (indicated by * above, listed in Table 2, and with photographs included in Figure 9). Other samples already on hand were deferred until (i) the technique was bedded down, (ii) more and possibly better examples could be obtained and (iii) samples of other target rocks arrived.

Table 2. Sample details. Start and end refer to TSG dataset sample id numbers. Spectra refers to the total number of HyLogger 4mm samples acquired from the face of the sample selected to be analysed by MLA. MRV – Mt Read Volcanics.

MRT Sample_ID	Target sub-assemblage	Lithology	Location	State	ddh id	Hole name	Start	End	Depth	Length (cm)	Spectra
G408251	Kaolinite + White mica	Mudstone	Tasmania Basin	Tas	6149	Thorp-1	70936	70954	263.25	7.2	165
G408275	K-feldspar + Plagioclase	Altered granodiorite	Gramalote Project	Colombia		Quarry	434	456	1.771	8.8	339
G408243	K-feldspar + Plagioclase + White mica (+ Quartz)	K-feldspar-altered dacite	White Spur, MRV	Tas	24998	WSP-14	102276	102285	347.19	3.6	151
G408265	Biotite + Epidote + Amphibole	Biotite-garnet-altered mafic	Cethana	Tas	29536	CETD4	68737	68748	477.88	8.8	183
G408264	Chlorite + Biotite	Biotite-altered mafic	Cethana	Tas	29536	CETD4	67704	67724	470.95	16	364
G408260	Shale - crypto-micaceous	Micaceous grey shale	Oonah prospect	Tas	15171	DD80OC3	7014	7033	74.658	15.2	219

Sample size

The optimal sample size for HyLogging validation tests should be sufficient to provide statistical robustness, but small enough to ensure homogeneity. An MLA sampling constraint is set by the cost of analysing large samples with sufficient but not excessive (i.e. costly) point density.

The optimum size compatible with the size of typical drill core, that is likely to remain homogeneous and can be completely scanned in 2 dimensions to obtain the hundred or so HyLogger analyses required for sufficient statistical significance, is 10cm x 5cm (compared to 3cm x 0.5cm in a similar study by Huntington *et al.,* 2009). This sample size potentially provides 52 completely independent (i.e. not overlapping) HyLogger spectra, but the scanning procedure actually acquires ~300 spectra, each covering ~1 x 1.4cm and spaced 4mm apart. The signal overlap of adjacent samples, after considering the reflectance intensity function for each sample, is 60% and between every second sample is 10%. Therefore 81 of the original 300 HyLogger samples are 90% independent, and should be the basis for estimating the effective number of spectra used.

The maximum slab size that can be cost effectively analysed by MLA is also 10cm x 5cm. This is also close to the largest that can fit into the SEM sample chamber (15cm x 15cm), which sets a limit on the largest sample that can be analysed in a single overnight session. The scanning is conducted on a raster pattern within tiles that cover an entire sample.

HyLogging

Samples were scanned by the MRT HyLogger-3 (visible, NIR, SWIR and TIR; Schodlok *et al.*, 2016a) with a sample spacing of 4mm in both the down track and cross track directions (i.e. sampling chunked by 1 with tray sections separated by 4mm). Slab samples were scanned on both sides and the HyLogger results were used to select the side with the most homogeneous mineralogy for MLA (Figure 1).

The Spectral Geologist (TSG v8.0.7.4, June 2020, incorporating TSA v7.0 with its dedicated TIR spectral library; Schodlok *et al.* 2016b) was used for basic spectral processing, to mask out compromised spectra (at sample edges and on cracks), calculate useful spectral scalars (e.g. spectral range) and unmix the spectra to mineral proportions (e.g. Figures 2 and 3). The dataset containing all scanned samples (including both the front sides and back sides of each slab) was used to select the surfaces to be analysed by MLA. Each selection was then exported to a separate TSG dataset for final unmixing. Unless otherwise specified, minimum weight and other unmixing parameters are the default TSG settings. The unmixing algorithms used were:

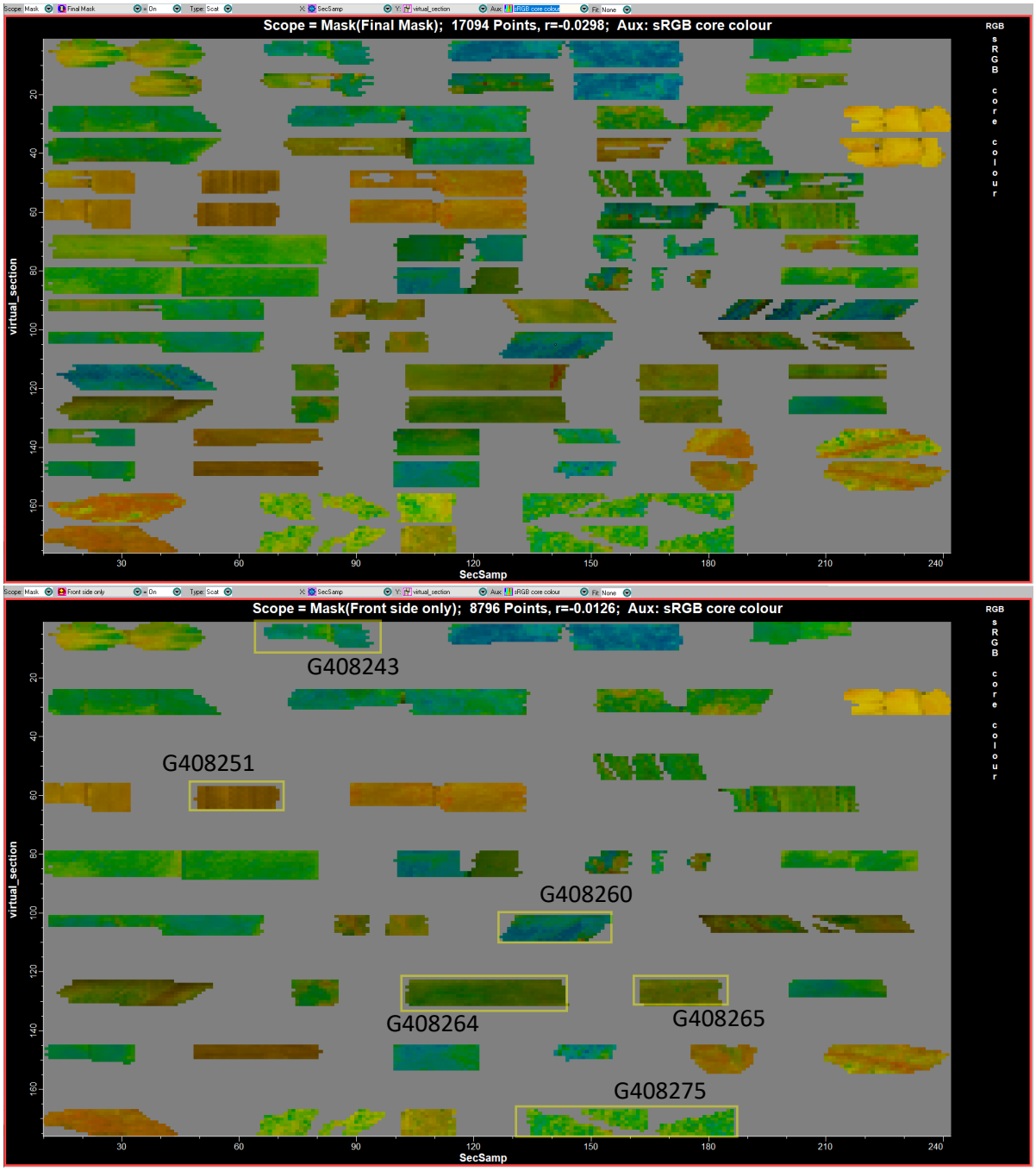

Figure 1. TSG scatter plots showing 34 candidate samples as they were laid out on 16 single-section core trays. Pairs of sections appear like mirror images of each other, resulting from each section pair comprising the same samples, but with the second of each pair having the samples turned over.

The samples are naturally coloured, but with a high saturation enhancement (colour tot_sat (2) in TSG). The top image shows all candidate samples, and the bottom image shows only the sides with more homogeneous mineralogy.

The six sample faces selected for MLA analysis (Table 2) are indicated with a yellow surrounding box.

VNIR-SWIR

- **sTSAS+** (system SWIR TSA+; Berman & Bishof, 1997; Berman *et al.,* 2011, Berman *et al.* 2017; Green, 2015)

  Automatic mixtures of three minerals. TSA+ with all minerals in the spectral library available (except brucite and palygorskite as the default setting in TSG).

- **uTSAS** (user SWIR TSA+)

  Supervised mixtures of up to three minerals. TSA+ with all minerals in the spectral library available except those indicated by sTSA+ that are not supported by diagnostic spectral features, tailored scalars (to seek epidote, prehnite, etc) and/or corresponding TIR spectra or that are mostly aspectral or noisy.

- sTSAV (system VNIR TSA)

  Automatic mixtures of two minerals. TSA with all minerals in the spectral library available (except misc-silicates, carbonates, sulphates, sulphides, and clay-Cu as is standard). All samples were found to contain negligible amounts of VNIR-active minerals, so this was not reported.

- uTSAV (user VNIR TSA)

  Supervised mixtures of two minerals. Usually, no adjustments are made to sTSAV, so uTSAV was not calculated.

TIR

- **sjCLST** (system TIR CLS; Green, 2015)

  Automatic mixtures of three minerals. The restricted mineral set (RMS) is initially informed by sTSAS+, then the algorithm uses scalars and rules to modify the list.

- **dCLST** (user TIR CLS)

  Supervised CLS with mixtures of six minerals using a single domain. Initiate the RMS with entire mineral groups identified by uTSAS+, then add entire mineral groups as needed to fit spectra, mainly using the RMS Error scalar, CLS Residual spectrum, Add 1 function and uTSAT with mix>6 and as many minerals available as possible i.e. all those not black listed by default.

  When adding mineral groups, some individual minerals are turned off by default unless specifically justified, as indicated by their being turned off in the default settings: quartz 4, 5, 6, opal and microcline 4.

  When adding mineral groups, some individual minerals and sub-groups are left turned off unless specifically justified because they are commonly used spuriously: glauconite, axinite, prehnite, pyrophyllite, topaz, amphibole-Na, amphibole-Mg-Fe-Mn-Li, carbonate-Cu, carbonate-Ba-Sr-Pb-Zn, gypsum, anhydrite, retgersite, barite, alunite and jarosite.

- **dTSAT** (user domained TIR TSA)

  Supervised mixtures of six minerals with minimum weight = 0. TSA with an RMS provided by the CLS domain.

- uTSAT (user TIR TSA following the philosophy of SWIR TSA)

  TSA with automatic mixtures > 6 and as many minerals available as possible i.e. all those not black listed by default and excluding only minerals not supported by diagnostic spectral features, tailored scalars and/or corresponding SWIR interpretations. This algorithm (which is computational expensive) was not used in this study.

Carbonates

- Carbonate minerals were further interpreted using the 14000, 11300 and 6500nm features (Green and Schodlok, 2016) and if necessary, appended to the results. (These are only included in the results shown in Appendix 1.)

Figure 2. Candidate samples coloured by dCLST Mineral Group 1 (top) and Mineral Group 2 (bottom). The 6 selected samples are outlined.

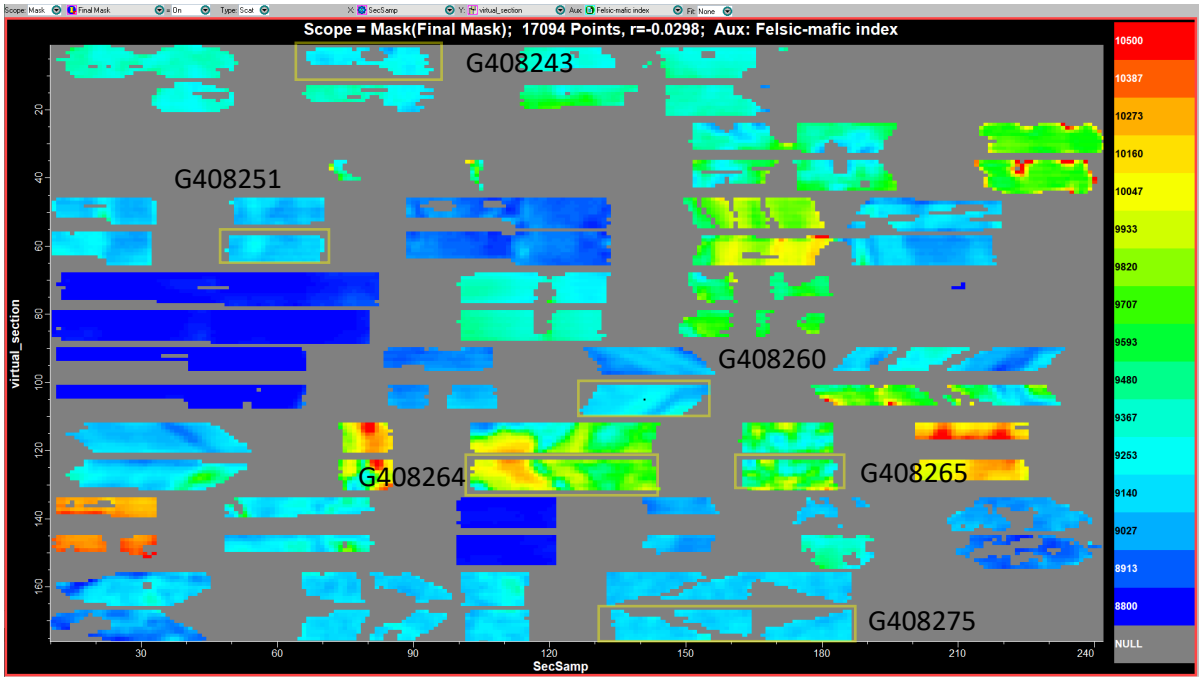

Figure 3. Candidate samples coloured by Felsic-mafic index, with the range of colours in each sample giving an indication of inhomogeneity.

Mineral Liberation Analysis (MLA)

The MLA method uses the EDX (energy dispersive x-ray spectroscopy) and backscatter electron image (BSE) functionality of a SEM to classify tens of thousands of spot analyses using a reference mineral library (Gu and Sugden, 1995). It is an excellent method for obtaining mineral proportions on a sample scale similar to HyLogging and produces a result that is as close to truth as practical. MLA of rock slabs and HyLogging both analyse surfaces and return areal mineral proportions, but they are independent. MLA therefore provides a robust independent reference from which to compare the results of HyLogging unmixing algorithms.

Samples need to be highly polished and carbon coated (Figure 4). Two SEM-based automated mineralogy programs were available at the University of Tasmania Central Science Laboratory: (1) Bruker AMICS which is optimised for textural analysis, producing a very high resolution mineral map of a small area, and (2) XMOD (Fandrich *et al.,* 2007) which is optimised for efficiently point counting large areas, and was therefore selected for this project.

Figure 4. A polished and carbon-coated sample mounted in a holder that has been minutely adjusted, aligning the sample so it is level within the SEM.

The MLA method classifies spot X-ray spectra by matching with a spectral library. Typically, the reference library is based on standard rock-forming minerals and may be modified with information from inspecting the X-ray spectra, acquiring EDX analyses of some of the minerals or from external information. In this project, independence was paramount, so no additional information was provided to the

SEM analyst, who used standard mineral libraries. (It is possible to re-process the data at a later stage using a more informed library.) The SEM analyst was however, informed about the desired specificity of mineral identification, given by HyLogger mineral classes e.g. paragonite, muscovite and phengite, and Fe-chlorite, Fe-Mg-chlorite and Mg-chlorite. The count time per spot was set to provide ~2000 X-ray spectra, just sufficient to reliably match with typical mineral libraries. Table 3 shows how MLA minerals classes were translated into TSG minerals and mineral groups.

Table 3. Translation table mapping MLA minerals to TSG minerals.

XMOD Mineral	TSG Group	TSG Mineral
Actinolite	AMPHIBOLE	Actinolite
Albite	PLAGIOCLASE	Albite
Alumina-Cal	PLAGIOCLASE	
Apatite	PHOSPHATE	Apatite
Biotite	DARK-MICA	Biotite
Ca-Al-Fe-Mg silicate	INVALID	
Calcite	CARBONATE	Calcite
Ca-REE carbonate	CARBONATE	Calcite
Chlorite	CHLORITE	Chlorite-FeMg
Chlorite_Fe	CHLORITE	Chlorite-Fe
Dolomite	CARBONATE	Dolomite
Epidote-Allanite	EPIDOTE	Epidote
Fe-oxide	OXIDE	OXIDE
Galena	OXIDE	OXIDE
Ilmenite-Mn	OXIDE	OXIDE
Kaolinite	KAOLIN	Kaolinite-WX
K-Feldspar	K-FELDSPAR	Orthoclase
Muscovite	WHITE-MICA	Muscovite
Muscovite_minorFe	WHITE-MICA	Phengite
Pl_or_Ab-Cal mix	PLAGIOCLASE	
Plagioclase	PLAGIOCLASE	Oligoclase
Pyrite	INVALID	OXIDE
Quartz	SILICA	Quartz
Rutile	OXIDE	Rutile
Spessartine	GARNET	Spessartine
Titanite	OXIDE	OXIDE
Zircon	MISC-SILICATE	Zircon

The consequent practical constraints on MLA analysis resulted in ~35,000 analyses per sample, which nominally guarantees a mineral proportion uncertainty of less than 1%. However, sensitivity analysis that takes into account errors in matching short count time X-ray spectra to library spectra indicates that a lower bound on uncertainty may be as high as 2% (Ron Berry *pers comm*).

An accelerating voltage of 20 kV was used, resulting in a typical interaction volume diameter and depth on the order of 3-5um in lower density minerals like silicates and carbonates. This is large enough to be representative and small enough to minimise the probability of spots falling on mineral contacts, where the spectra will result from a mix of minerals. Lowering the accelerating voltage would result in less mixed mineral spectra, but reduces peak/background ratio for higher energy X-ray peaks (or completely removes them from the spectrum) which affects classification accuracy.

The actual method used was XMOD_STD, which compared to the basic XMOD mode has the additional feature that it will compare every spectrum during acquisition with a reference spectral library, and if it does not match anything in the library it will assume it is sitting on a grain boundary (leading to a mixed spectrum of two neighbouring minerals) and shift the beam position slightly (by a user adjustable value, typically in the order of 10 microns) and collect another spectrum, which is again compared to the library. If there is a match it will move on to the next grid point, if not it will move the beam position again ... until it has collected up to 5 spectra around the original grid position. If there still is not a match it will assume it is sitting on an additional mineral which is currently not present in the spectral library and collect a higher quality (longer count) spectrum and add it to the library for review afterwards. This way the method will also strongly reduce the number of "mixed spectra" (of more than one mineral).

Details of MLA analytical conditions are detailed in Appendix 2 and the workflow is provided as screen captures in Appendix 3.

Fine grained rock (~20μm) commonly results in 5% or more unknowns because the X-ray spot

is often on two minerals, resulting in a mixed X-ray spectrum that does not match any library spectrum. The sample is best analysed using e.g. X-ray diffraction (XRD). The finer grained samples analysed in this project did not return an excessive number of unknowns.

High resolution backscatter electron (BSE) images were collected primarily as part of the MLA workflow, but were also used to interpret texture and to georeference mineral maps. Example images are provided in Appendix 4.

The BSE images were to verify grain size and textural homogeneity and verify the MLA interpretation (including investigating the likelihood of X-ray spectra from mineral mixtures mimicking pure mineral spectra e.g. plagioclase = albite + calcite). In Figure 5, the BSE image is compatible with the MLA mineral map, together indicating that albite occurs as small, feathery crystals in a K-feldspar host, and as occasional phenocrysts.

The results of MLA were provided as mineral point counts and the derived area percentages. Library mineral compositions were used to also calculate weight percentages. Although XMOD is not designed to produce mineral maps, the located data can nonetheless be displayed in a map view, which were used to check homogeneity and mineral texture (e.g. Figures 6 and 7). Examples of georeferenced MLA data are provided in Appendices 4 and 5.

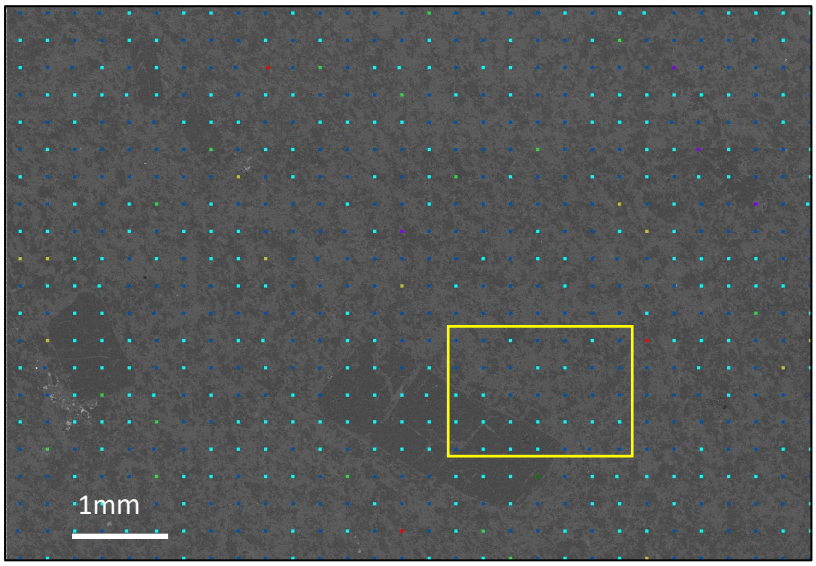

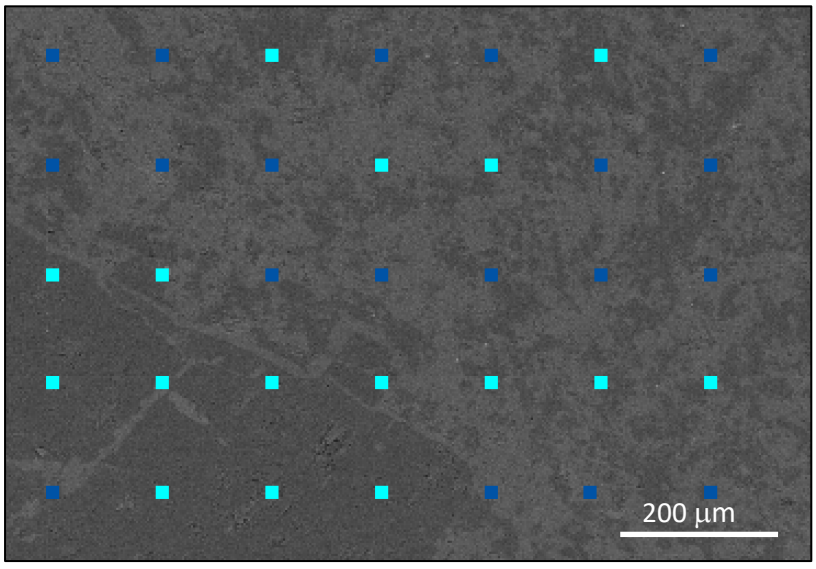

Figure 5. BSE image of G408243 overlain with XMOD EDX spots coloured as in Figure 6.

Enlargement in lower image is indicated with a yellow outline.

The dominant texture is feathery albite (light blue) in a K-feldspar host (dark blue). An albite phenocryst appears at bottom left of the enlarged image.

The scale of the spots (illustrated as squares) is 18 x 18 µm.

The results of MLA were provided as mineral point counts and the derived area percentages. Library mineral compositions were used to also calculate weight percentages. Although XMOD is not designed to produce mineral maps, the located data can nonetheless be displayed in a map view, which were used to check homogeneity and mineral texture (e.g. Figures 6 and 7). Examples of georeferenced MLA data are provided in Appendices 4 and 5.

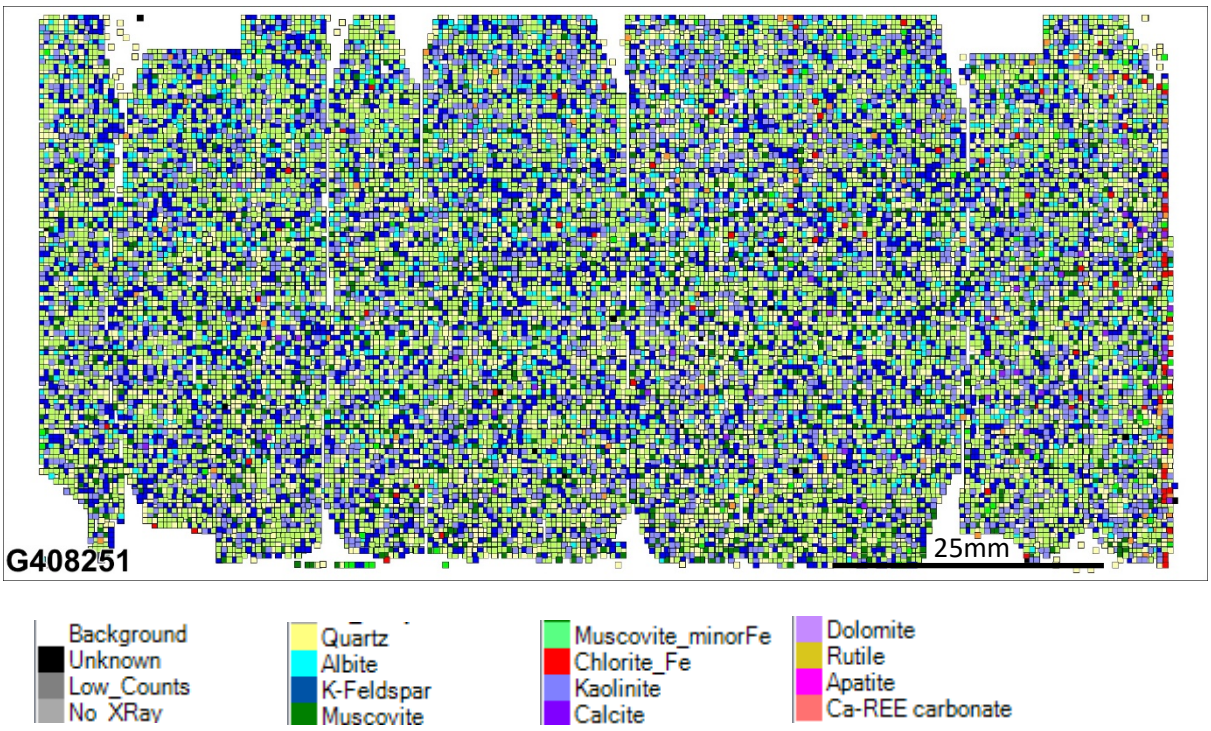

Figure 6. MLA mineral map of sample G408251. The map was produced using MapInfo, as detailed in Appendix 4.

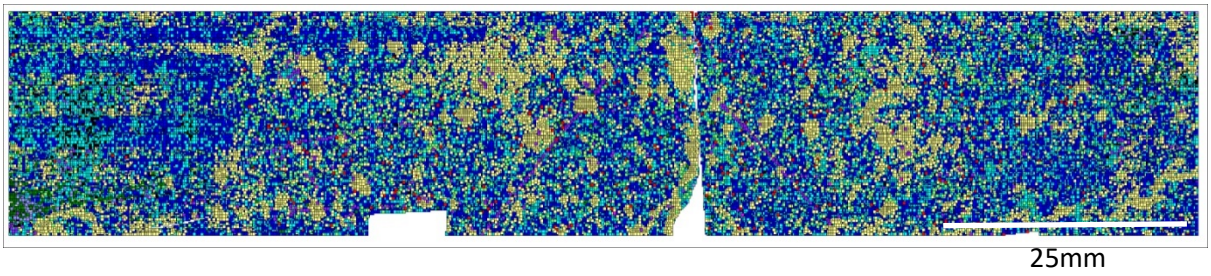

Figure 7.
MLA mineral map of sample G408243. The colour legend is the same as Figure 6.

Figure 8 (below). Spatial summary of G408243 K-feldspar-altered dacite showing the distribution of minerals determined from HyLogging and from MLA. Red lines in the HyLogger tray image indicate sections of hyperspectral data that were masked out prior to mineral interpretation. Pixel size in hyperspectral-based mineral maps is 4mm. XMOD mineral legend (as in Table 3) and HyLogging mineral legend: Alb – Albite, Apat – apatite, Cb – carbonate, Calc – calcite, Chl – chlorite, Kaol – kaolinite, Ksp – K-feldspar, Musc/Mv – muscovite, Mv-Fe – phengite, Mont – montmorillonite, Plag – plagioclase, Qtz– quartz, Rut – rutile. 0% indicates a trace quantity.

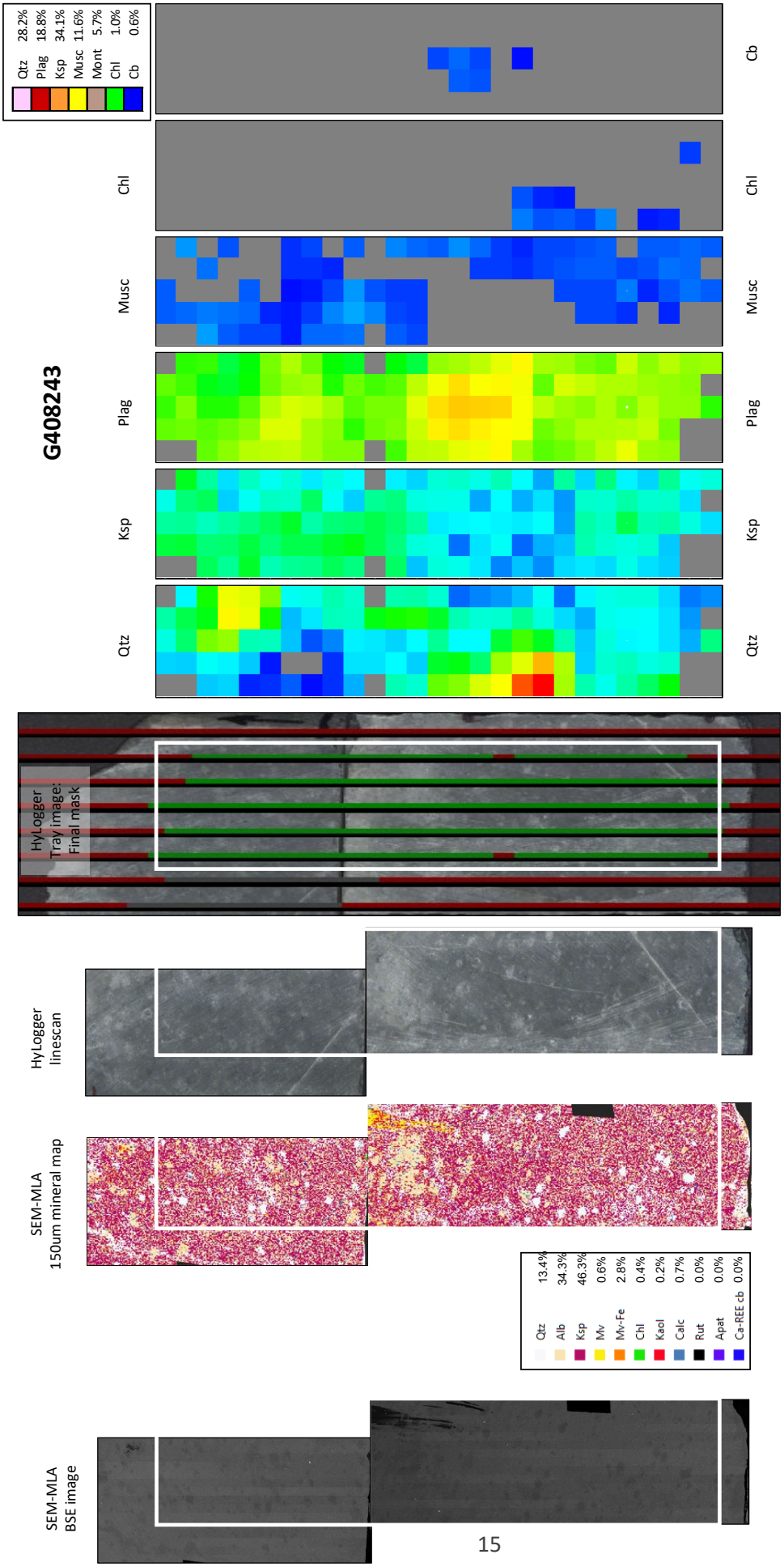
G408243
Qtz
Ksp
Plag
Musc
Chl
Cb
HyLogger
Tray image:
Final mask
HyLogger
linescan
SEM-MLA
150um mineral map
SEM-MLA
BSE image
Qtz 28.2%
Plag 18.8%
Ksp 34.1%
Musc 11.6%
Mont 5.7%
Chl 1.0%
Cb 0.6%
Qtz 13.4%
Alb 34.3%
Ksp 46.3%
Mv 0.6%
Mv-Fe 2.8%
Chl 0.4%
Kaol 0.2%
Calc 0.7%
Rut 0.0%
Apat 0.0%
Ca-REE cb 0.0%

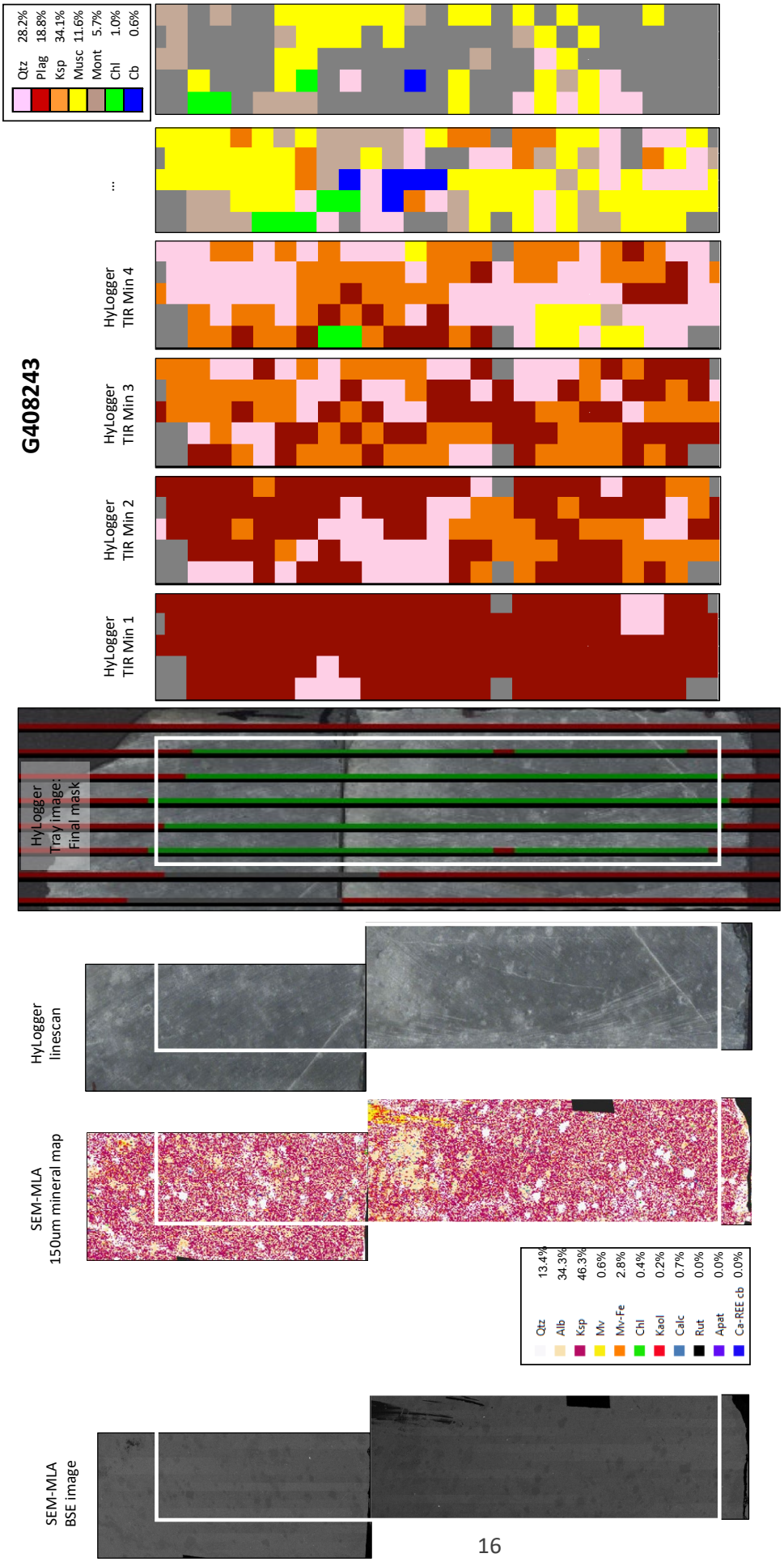
G408243
HyLogger TIR Min 1
HyLogger TIR Min 2
HyLogger TIR Min 3
HyLogger TIR Min 4
...
Qtz 28.2%
Plag 18.8%
Ksp 34.1%
Musc 11.6%
Mont 5.7%
Chl 1.0%
Cb 0.6%
HyLogger Tray image: Final mask
HyLogger linescan
SEM-MLA 150um mineral map
Qtz 13.4%
Alb 34.3%
Ksp 46.3%
Mv 0.6%
Mv-Fe 2.8%
Chl 0.4%
Kaol 0.2%
Calc 0.7%
Rut 0.0%
Apat 0.0%
Ca-REE cb 0.0%
SEM-MLA BSE image

3. Results

Complete mineral proportion results of the unmixing algorithms (sTSAS+, uTSAS+ sjCLST, dCLST and dTSAT) together with our best interpretation of the truth, from MLA using the XMOD program are provided in Appendix 1, with full XMOD results in Appendix 2. Figure 9 summarises the results in graphs, summary tables, representative spectra and line scan images. BSE images are provided in Appendix 6.

Figure 9 (following pages).

Summaries for each sample showing column graphs of SWIR (top) and TIR (bottom), mineral group (left) and mineral species (right) proportion results from the spectral unmixing algorithms and MLA (using the XMOD program), tables summarise the results of the unmixing algorithms and XMOD, representative vis-SWIR and TIR spectra (in black) modelled by uTSAS and dCLST (in colour) respectively and an image.

The minimum proportion illustrated is 5% for the graphs and 1% for the tables. TSAS results classified as Invalid are shown at the Group level, but not at Mineral level, where the mineral proportions are re-normalised to total 100%. Colours are similar to those used in TSG.

G408251 Mudstone

Mineral Group

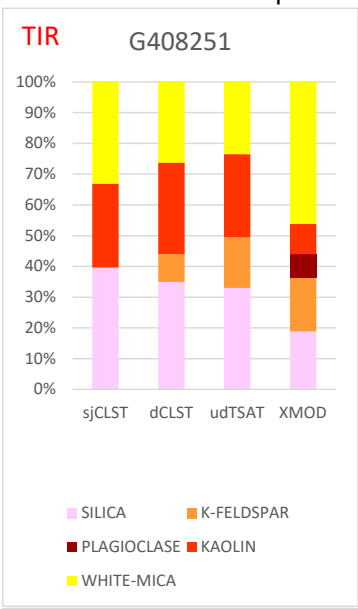

Mineral Species

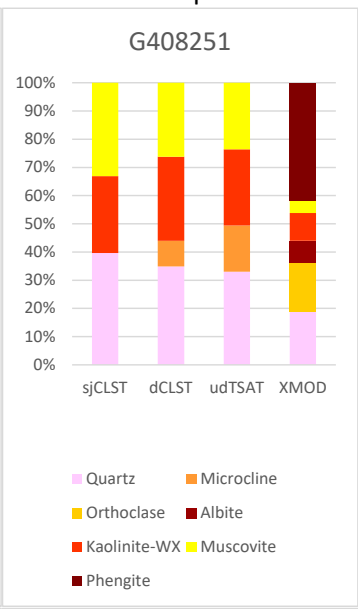

G408251
Kaol+White mica

TIR

Groups	sjCLST	dCLST	udTSAT	XMOD
SILICA	39.5%	34.9%	33.0%	18.6%
K-FELDSPAR		9.1%	16.4%	17.2%
PLAGIOCLASE				7.6%
KAOLIN	27.2%	29.8%	27.0%	9.7%
WHITE-MICA	33.0%	26.2%	23.5%	45.5%

Minerals	sjCLST	dCLST	udTSAT	XMOD
Quartz	39.5%	34.9%	33.0%	18.6%
Microcline		9.1%	16.4%	
Orthoclase				17.2%
Albite				7.6%
Kaolinite-WX	27.2%	29.8%	27.0%	9.7%
Muscovite	33.0%	26.2%	23.5%	4.5%
Phengite				41.1%

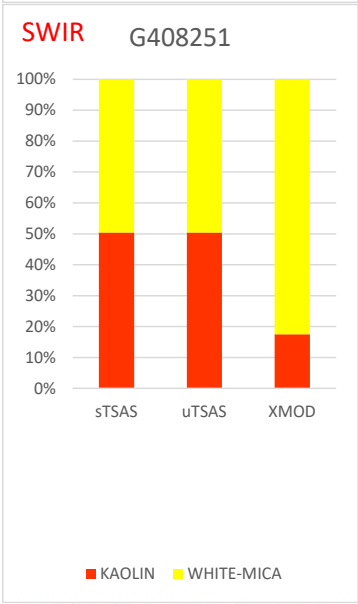

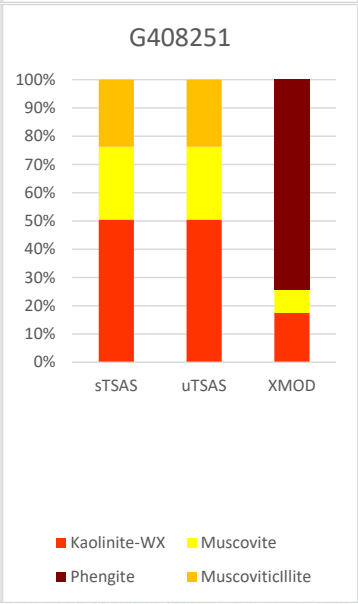

SWIR

Groups	sTSAS	uTSAS	XMOD
KAOLIN	50.5%	50.5%	17.1%
WHITE-MICA	49.5%	49.5%	80.7%

Minerals	sTSAS	uTSAS	XMOD
Kaolinite-WX	50.5%	50.5%	17.1%
Muscovite	25.8%	25.8%	7.9%
Phengite			72.6%
MuscoviticIllite	23.7%	23.7%	

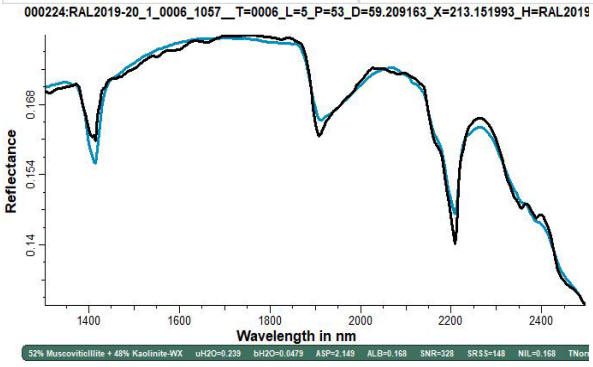

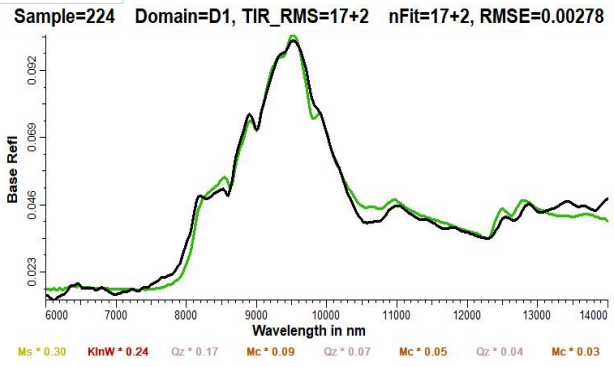

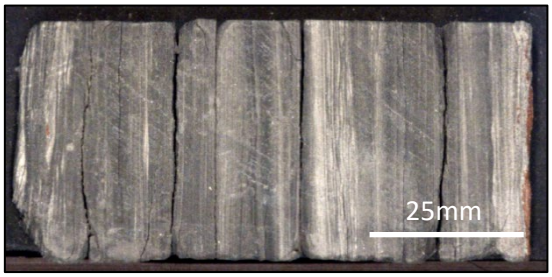

G408275 Altered granodiorite

Mineral Group

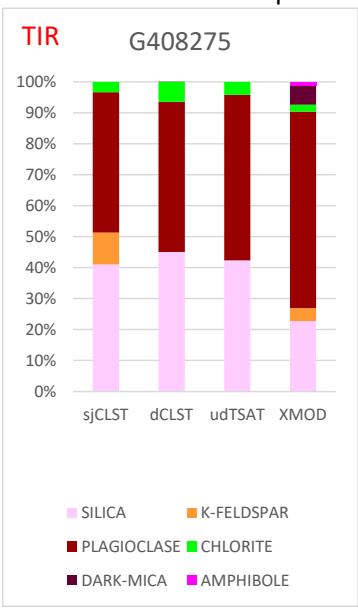

Mineral Species

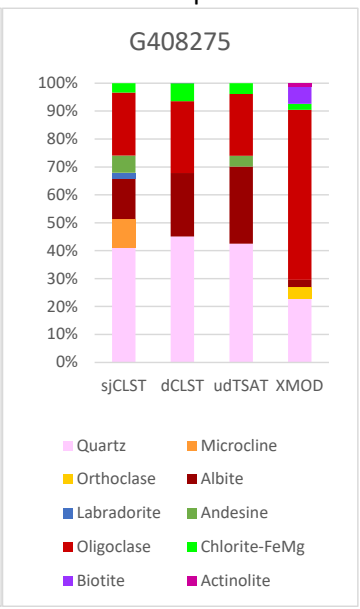

G408275
K-feldspar+Plag

TIR

Groups	sjCLST	dCLST	udTSAT	XMOD
SILICA	41.0%	45.0%	42.3%	22.2%
K-FELDSPAR	10.3%			4.1%
PLAGIOCLASE	45.3%	48.5%	53.4%	61.8%
CHLORITE	3.3%	6.5%	4.3%	2.2%
DARK-MICA		0.0%		6.1%
AMPHIBOLE				1.1%

Minerals	sjCLST	dCLST	udTSAT	XMOD
Quartz	41.0%	45.0%	42.3%	22.2%
Microcline	10.3%			
Orthoclase				4.1%
Albite	14.5%	22.8%	27.5%	2.5%
Labradorite	2.1%			
Andesine	6.2%		3.9%	
Oligoclase	22.6%	25.7%	22.0%	59.3%
Chlorite-FeMg	3.3%	6.4%	3.8%	2.1%
Biotite		0.0%		6.1%
Actinolite				1.1%

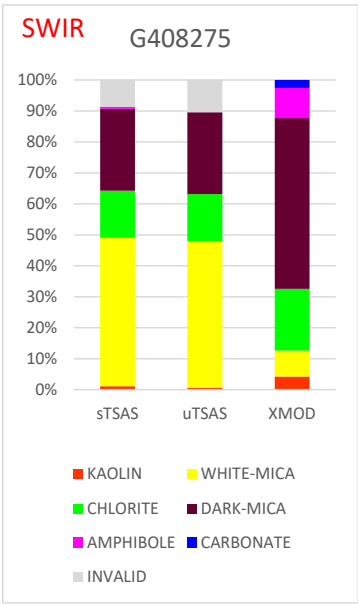

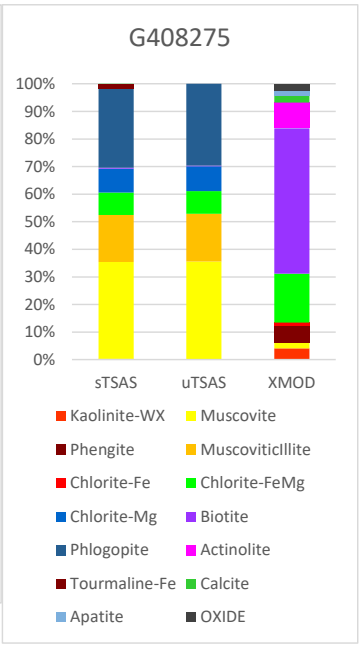

SWIR

Groups	sTSAS	uTSAS	XMOD
KAOLIN	1.1%	0.7%	4.3%
WHITE-MICA	46.9%	47.2%	8.4%
CHLORITE	15.0%	15.2%	19.9%
DARK-MICA	25.9%	26.4%	55.2%
AMPHIBOLE	0.3%		9.7%
CARBONATE	0.3%		2.6%
INVALID	8.6%	10.4%	

Minerals	sTSAS	uTSAS	XMOD
Kaolinite-WX	0.3%	0.2%	4.1%
Muscovite	34.2%	35.0%	2.2%
Phengite			5.9%
MuscoviticIllite	16.7%	17.1%	
Chlorite-Fe			1.3%
Chlorite-FeMg	7.9%	8.2%	17.7%
Chlorite-Mg	8.4%	8.9%	
Biotite	0.3%	0.2%	52.6%
Phlogopite	28.0%	29.3%	
Actinolite			9.3%
Tourmaline-Fe	1.6%		
Calcite	0.1%		2.4%
Apatite			2.0%
OXIDE			2.4%

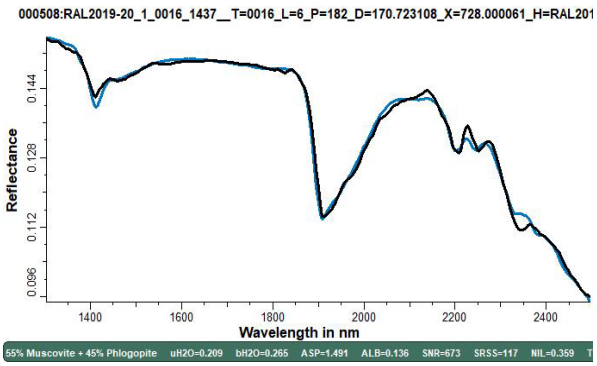

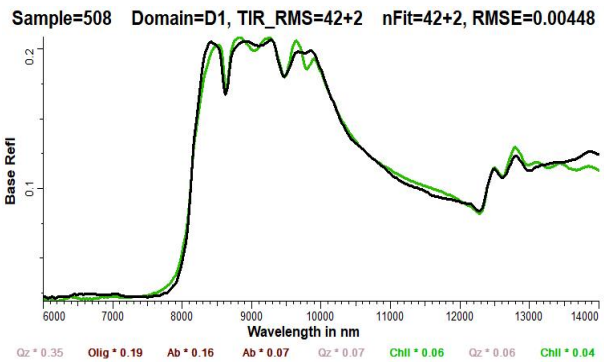

G408243 K-feldspar-altered dacite

Mineral Group

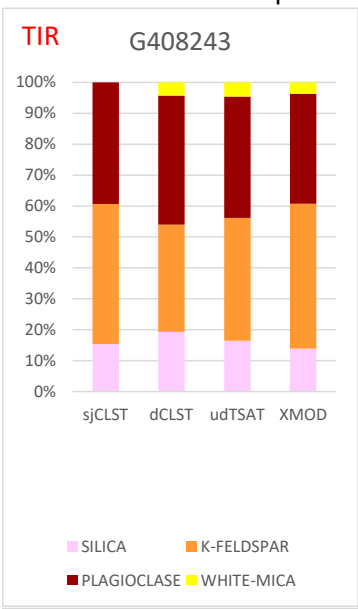

Mineral Species

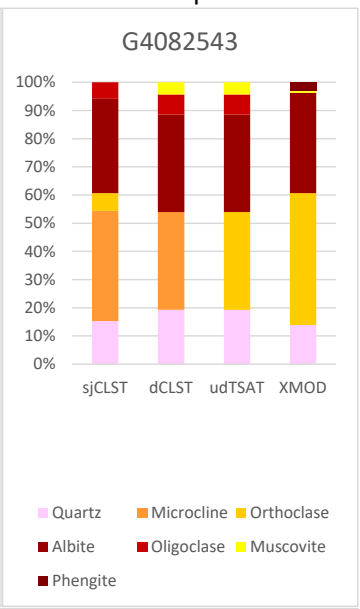

G408243
K-feldspar+Plag+White mica(+Qtz)

TIR

Groups	sjCLST	dCLST	udTSAT	XMOD
SILICA	15.2%	19.0%	16.1%	13.7%
K-FELDSPAR	44.9%	34.1%	39.0%	46.1%
PLAGIOCLASE	39.0%	41.1%	38.6%	35.0%
WHITE-MICA		4.2%	4.5%	3.7%

Minerals	sjCLST	dCLST	udTSAT	XMOD
Quartz	15.2%	19.0%	19.0%	13.7%
Microcline	38.7%	34.1%	0.0%	
Orthoclase	6.2%		34.1%	46.1%
Albite	33.2%	34.0%	34.0%	35.0%
Oligoclase	5.8%	7.1%	7.1%	
Muscovite		4.2%	4.2%	0.6%
Phengite				3.1%

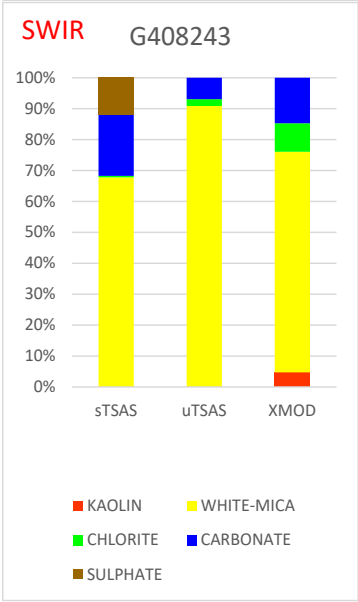

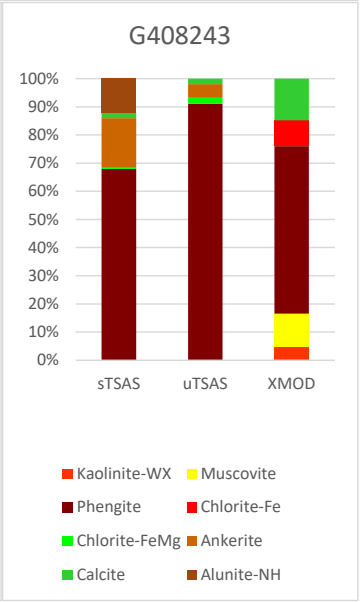

SWIR

Groups	sTSAS	uTSAS	XMOD
KAOLIN			4.7%
WHITE-MICA	66.9%	90.9%	71.4%
CHLORITE	0.5%	2.1%	9.2%
CARBONATE	19.4%	6.9%	14.7%
SULPHATE	11.8%		

Minerals	sTSAS	uTSAS	XMOD
Kaolinite-WX			4.6%
Muscovite			11.8%
Phengite	67.5%	90.9%	58.9%
Chlorite-Fe			9.1%
Chlorite-FeMg	0.5%	2.1%	
Ankerite	17.5%	4.8%	
Calcite	2.0%	2.0%	14.6%
Alunite-NH	11.9%		

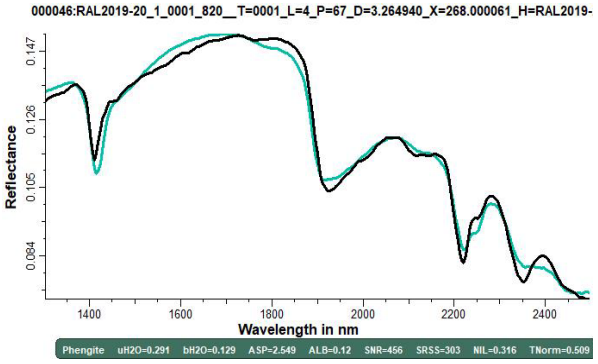

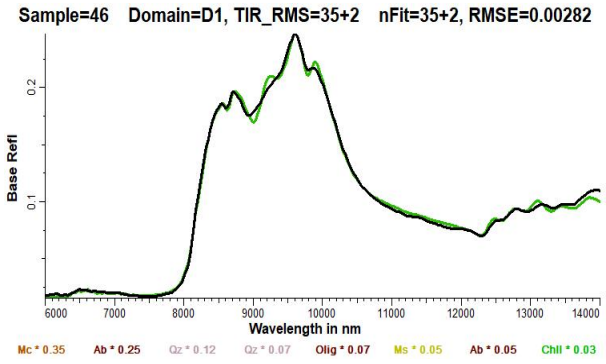

G408265 Biotite-garnet-altered mafic

Mineral Group

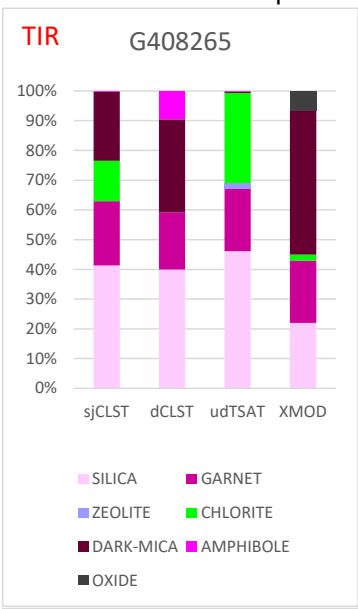

Mineral Species

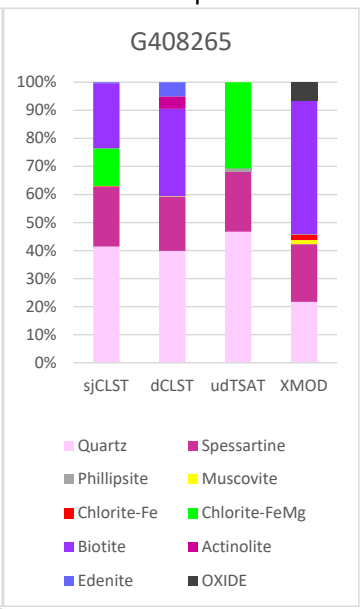

G408265
Biot+Epid+Amph

TIR

Groups	sjCLST	dCLST	udTSAT	XMOD
SILICA	41.1%	39.9%	46.0%	21.3%
GARNET	21.5%	19.3%	21.2%	20.3%
ZEOLITE			1.7%	
CHLORITE	13.5%		30.3%	1.9%
DARK-MICA	23.1%	31.2%	0.4%	46.7%
AMPHIBOLE	0.3%	9.5%	0.3%	0.0%
OXIDE				6.5%

Minerals	sjCLST	dCLST	udTSAT	XMOD
Quartz	41.1%	39.9%	46.0%	21.3%
Spessartine	21.2%	19.3%	21.2%	20.3%
Phillipsite			1.0%	
Muscovite	0.1%	0.2%		1.4%
Chlorite-Fe	0.1%			1.9%
Chlorite-FeMg	13.3%		30.3%	0.1%
Biotite	23.1%	31.2%		46.7%
Actinolite		4.4%		0.0%
Edenite	0.3%	5.0%		
OXIDE				6.5%

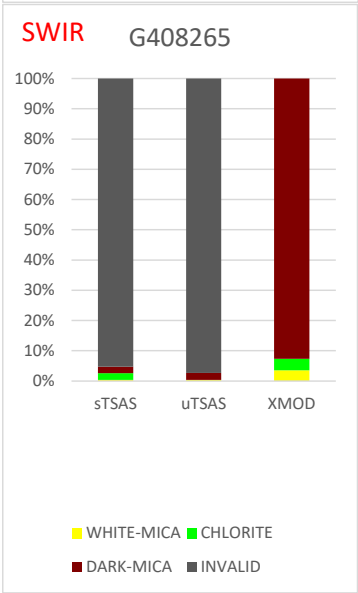

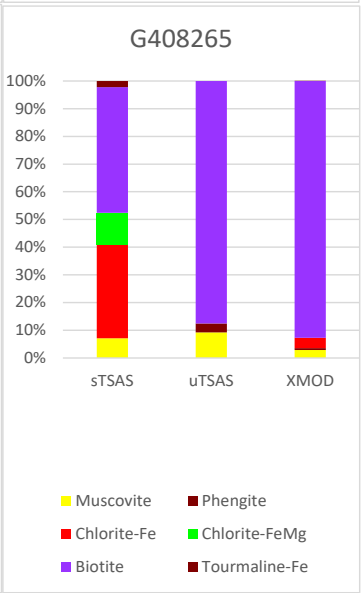

SWIR

Groups	sTSAS	uTSAS	XMOD
WHITE-MICA	0.3%	0.3%	3.5%
CHLORITE	2.2%		3.9%
DARK-MICA	2.2%	2.3%	92.6%
INVALID	95.1%	97.3%	

Minerals	sTSAS	uTSAS	XMOD
Muscovite	7.0%	9.2%	2.5%
Phengite		3.3%	0.6%
Chlorite-Fe	34.0%		3.3%
Chlorite-FeMg	11.3%		
Biotite	45.4%	87.5%	81.4%
Tourmaline-Fe	2.2%		0.0%

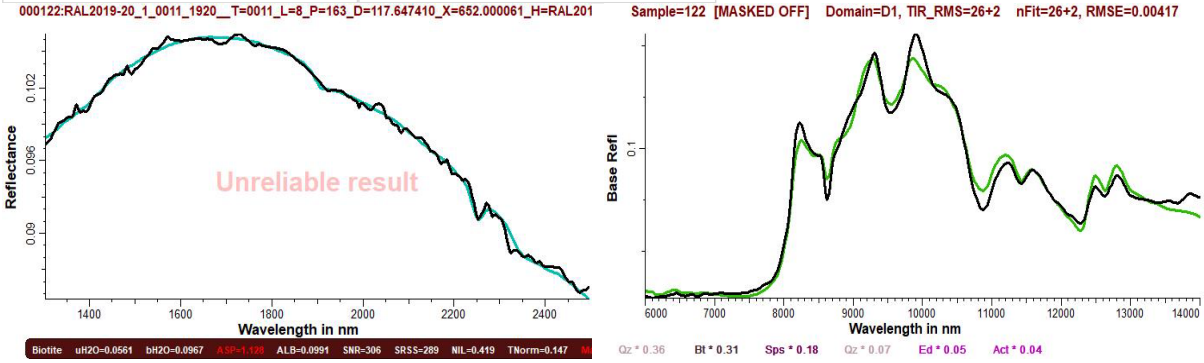

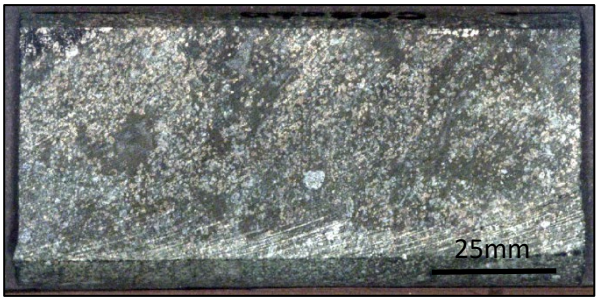

G408264 Biotite-altered mafic

Mineral Group

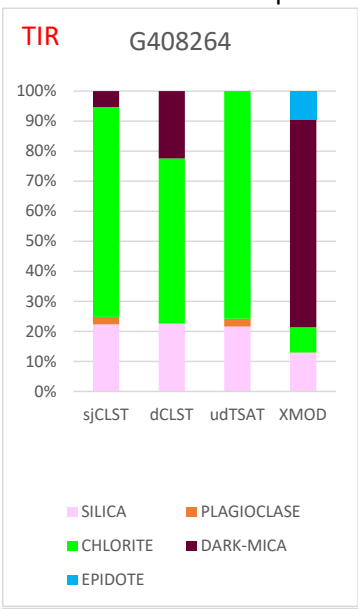

Mineral Species

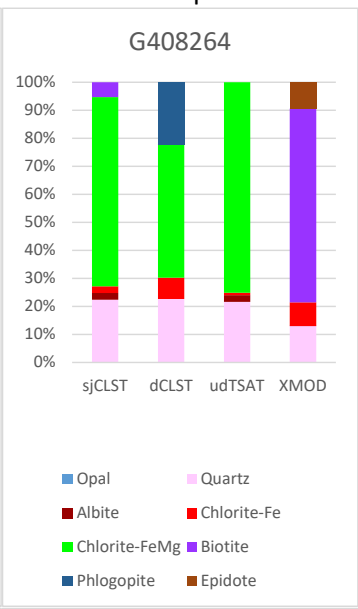

G408264
Chl+Biot

TIR

Groups	sjCLST	dCLST	udTSAT	XMOD
SILICA	22.1%	22.6%	21.6%	12.6%
PLAGIOCLASE	2.5%		2.6%	0.0%
CHLORITE	69.0%	55.0%	75.8%	8.1%
DARK-MICA	5.2%	22.4%		67.1%
EPIDOTE				9.1%

Minerals	sjCLST	dCLST	udTSAT	XMOD
Opal				
Quartz	22.1%	22.6%	21.6%	12.6%
Albite	2.3%		2.4%	0.0%
Chlorite-Fe	2.4%	7.6%	0.9%	8.1%
Chlorite-FeMg	66.6%	47.4%	74.9%	
Biotite	5.2%	0.0%		67.1%
Phlogopite		22.1%		
Epidote				9.1%

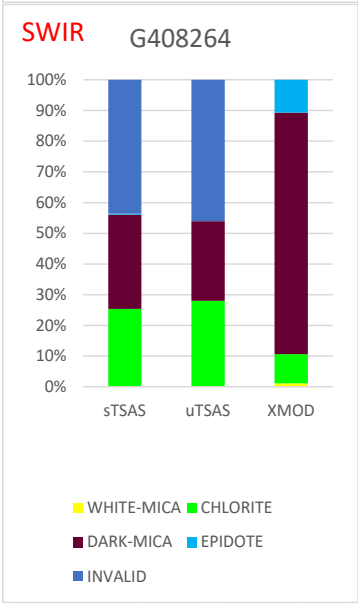

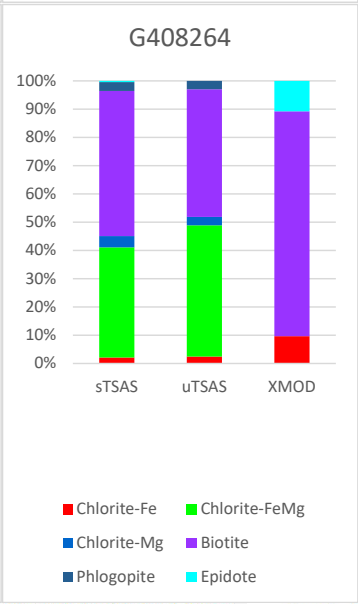

SWIR

Groups	sTSAS	uTSAS	XMOD
WHITE-MICA		0.1%	1.1%
CHLORITE	25.0%	27.7%	9.5%
DARK-MICA	30.2%	25.8%	78.3%
EPIDOTE	0.4%		10.6%
INVALID	42.9%	45.8%	

Minerals	sTSAS	uTSAS	XMOD
Chlorite-Fe	2.1%	2.4%	9.4%
Chlorite-FeMg	38.2%	45.8%	
Chlorite-Mg	4.0%	2.9%	
Biotite	50.4%	44.6%	77.8%
Phlogopite	3.1%	2.9%	
Epidote	0.4%		10.5%

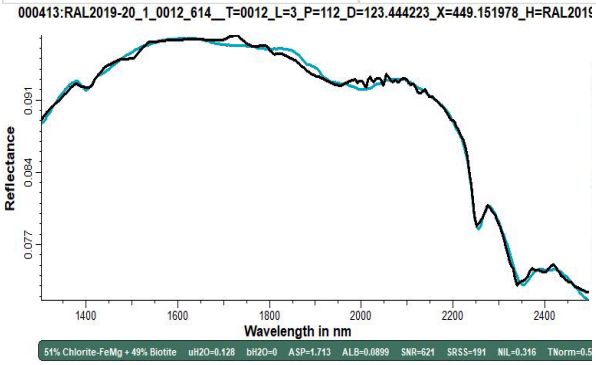

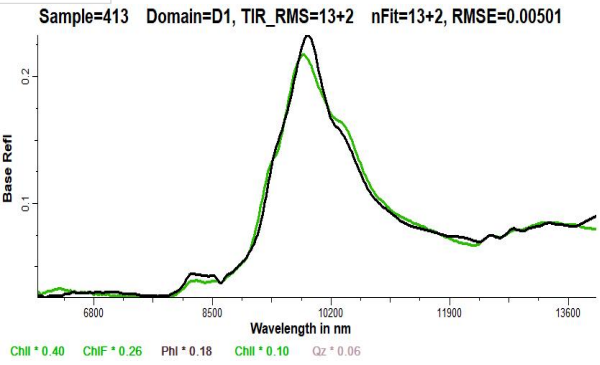

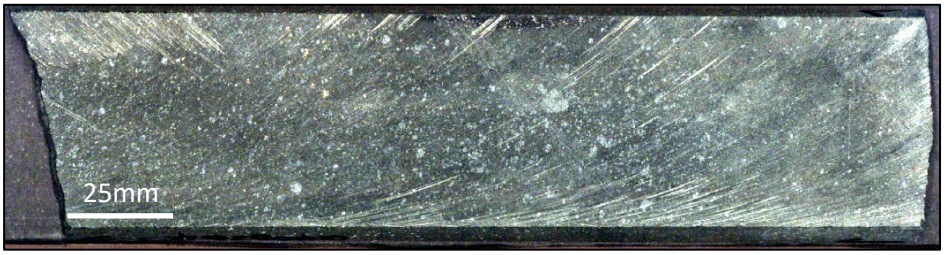

G408260 Micaceous grey shale

Mineral Group

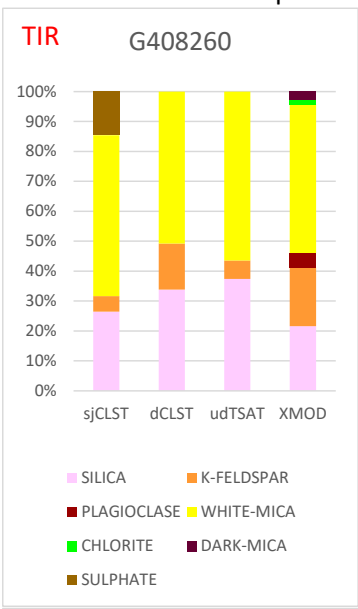

Mineral Species

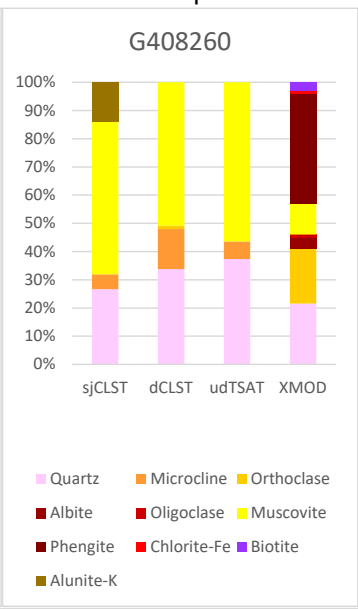

G408260
Shale - crypto-micaceous

TIR

Groups	sjCLST	dCLST	udTSAT	XMOD
SILICA	26.5%	33.8%	37.4%	21.2%
K-FELDSPAR	5.2%	15.4%	6.2%	19.2%
PLAGIOCLASE				4.9%
WHITE-MICA	53.8%	50.8%	56.4%	48.8%
CHLORITE				1.4%
DARK-MICA				2.8%
SULPHATE	14.6%			

Minerals	sjCLST	dCLST	udTSAT	XMOD
Quartz	26.5%	33.8%	37.4%	21.2%
Microcline	5.2%	14.1%	6.2%	
Orthoclase		1.2%		19.2%
Albite				3.7%
Oligoclase				1.2%
Muscovite	53.8%	50.8%	56.4%	10.7%
Phengite				38.1%
Chlorite-Fe				1.3%
Biotite				2.8%
Alunite-K	13.9%			

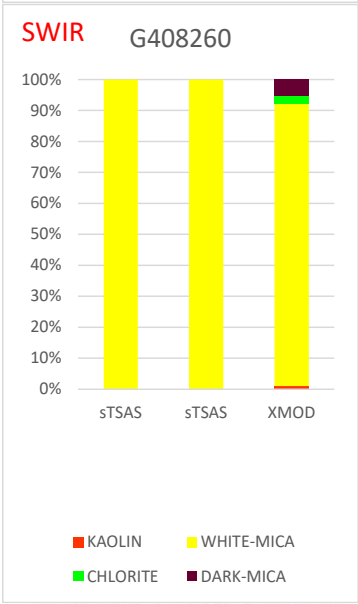

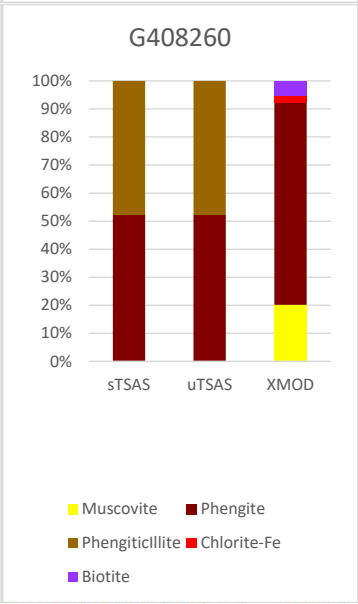

SWIR

Groups	sTSAS	sTSAS	XMOD
KAOLIN			1.0%
WHITE-MICA	99.8%	99.8%	92.1%
CHLORITE			2.6%
DARK-MICA			5.3%

Minerals	sTSAS	uTSAS	XMOD
Muscovite			20.0%
Phengite	52.1%	52.1%	71.4%
PhengiticIllite	47.7%	47.7%	
Chlorite-Fe			2.5%
Biotite			5.2%

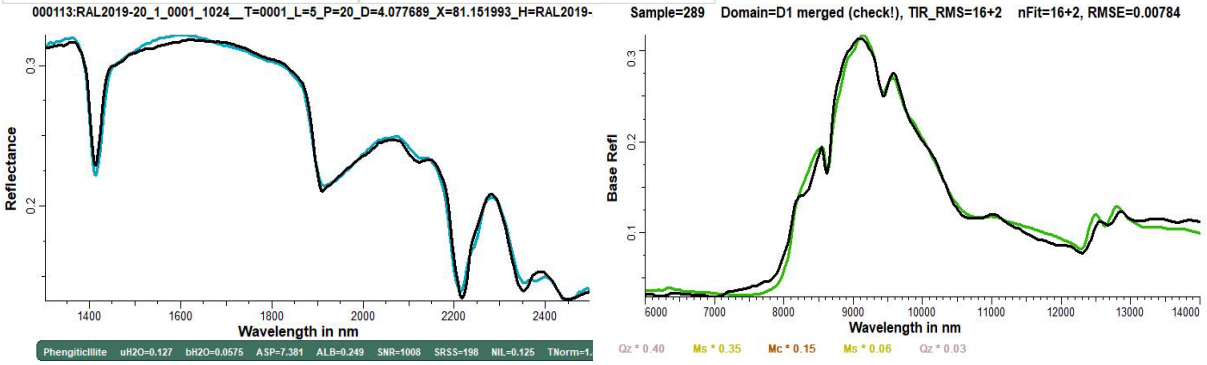

4. Discussion

The proportion of MLA spots classified as unknown were less than 0.12% for 4 of the 6 samples, with the other 2 resulting in 0.5% and 1.3% (respectively G408275 altered granite and G408243 K-feldspar-altered dacite). The finest grained samples G408251 mudstone and G408260 micaceous black shale resulted in 0.1% and 0.01% unknowns. These excellent results are due to adequate grain size and mineralogies well represented by the X-ray spectral libraries.

The accuracy of the HyLogger mineralogy using the five SWIR and TIR unmixing algorithms relative to that determined by MLA (XMOD) is best examined in terms of mineral identification, which is the primary goal of HyLogging. The HyLogging system is not necessarily designed to measure mineral proportions, partly because the HyLogger IR spectral library has been normalised so each mineral has a maximum reflectance of 1, jettisoning information on their relative reflectance. Nevertheless, the statistical power generated by the high level of over-sampling that the HyLogging system produces builds confidence in averaged mineral proportion estimates (e.g. a 200m drill hole typically returns 50,000 spectra from 4mm samples).

Sample interpretations

G408251 Mudstone

TSAS and CLST both correctly identified mineral groups. TSAS overestimated the proportion of white mica by a factor of 1.6 and apportioned all of it to muscovite (or illitic muscovite), but XMOD identified 90% of the white mica as phengitic.

CLST (and TSAT) correctly identified significant white mica, but like the SWIR algorithms, incorrectly identified the white mica as muscovite. A small proportion of plagioclase included in XMOD could not be justified in the RMS for the dCLST, although was not severely penalised if included in addition to, or instead of K-feldspar. The TIR algorithms over-estimated quartz by a factor of 1.8.

G408275 Altered granodiorite

TSAS and CLST both correctly identified mineral groups and mineral species. TSAS made a good estimate of the chlorite proportion, but overestimated white mica by a factor of 6 and underestimated dark mica by a factor of 2.

White mica or biotite was not used by CLS, even when feldspars, kaolin and each other were not made available. Similarly, biotite was not used, even though indicated by the SWIR interpretation. CLS overestimated quartz:plagioclase by a factor of 1.7. sjCLST identified a low proportion of K-feldspar that was not backed up by dCLST, but was validated by XMOD. A small proportion of chlorite (3-7%) interpreted by the TIR unmixing algorithms was a surprisingly good estimate of the true proportion (6%). CLST (and TSAT) interpreted plagioclase as albite plus oligoclase, but XMOD identified 96% as oligoclase.

G408243 K-feldspar-altered dacite

TSAS and CLST both correctly identified mineral groups and mineral species and their relative proportions (including quartz) to within 8%.

The carbonate was identified as siderite using the 14,000 and 11,300nm features.

G408265 Biotite-garnet-altered mafic

TSAS was unable to determine the mineralogy of over 90% of the spectra, interpreting them as aspectral, but MLA indicated a high proportion of biotite. Although a deep crystal field feature was apparent, features in the SWIR were noisy. Smoothing the spectra did reveal prominent FeOH and MgOH absorptions at 2252nm (biotite or chlorite) and 2339nm (more consistent with chlorite). When aspectral results were disregarded, as presented in the mineral species results, biotite becomes dominant.

In the TIR, sjCLST and dCLST did a good job at identifying mineral groups, including

biotite and garnet. However dTSAT favoured chlorite over biotite. Minor amphibole was incorrectly identified and used by dCLST, but not by dTSAT. Quartz was over-estimated by a factor of 1.9.

G408264 Biotite-altered mafic

Dark mica (biotite) and chlorite were correctly identified by the TSAS algorithms, but the chlorite proportion was over-estimated. Both SWIR and TIR algorithms were unable to see the epidote (9%).

sjCLST, dCLST and uTSAT all incorrectly interpreted chlorite over biotite. Quartz was over-estimated by a factor of 1.8.

G408260 Micaceous grey shale

The SWIR algorithms correctly identified white mica as the dominant mineral. MLA apportioned 70% to phengite (or illitic phengite) and 20% to muscovite, but TSA found only phengite (or illitic phengite).

sjCLST, dCLST and udTSAT all correctly identified white mica, quartz and K-feldspar, but sjCLST incorrectly added minor sulphate (alunite). The proportion of white mica was accurately estimated by all algorithms, K-feldspar was best estimated by dCLST and quartz was over-estimated by a factor of 1.6.

In summary, both SWIR and TIR consistently identified mineral groups correctly except for chlorite and biotite, which were commonly incorrectly misidentified as each other. White mica was consistently identified correctly at the group level, but the mineral species was commonly incorrectly identified as muscovite when the MLA interpreted it as phengite. Small proportions of kaolin, white mica, chlorite and carbonate were consistently identified in both the SWIR and TIR, but similar proportions of plagioclase, epidote, dark mica and K-feldspar were not.

Mineral proportions

Mineral proportions from the three HyLogging TIR unmixing algorithms are compared with MLA and also compared with each other in Figure 10. Improvements can be seen in moving from sjCLST to dCLST, but dTSAT resulted in poorer estimates, especially for chlorite + biotite and carbonate. dTSAT was perhaps compromised by a limited RMS constraining subset selection options and the TIR library not providing enough spectra to characterise spectral range.

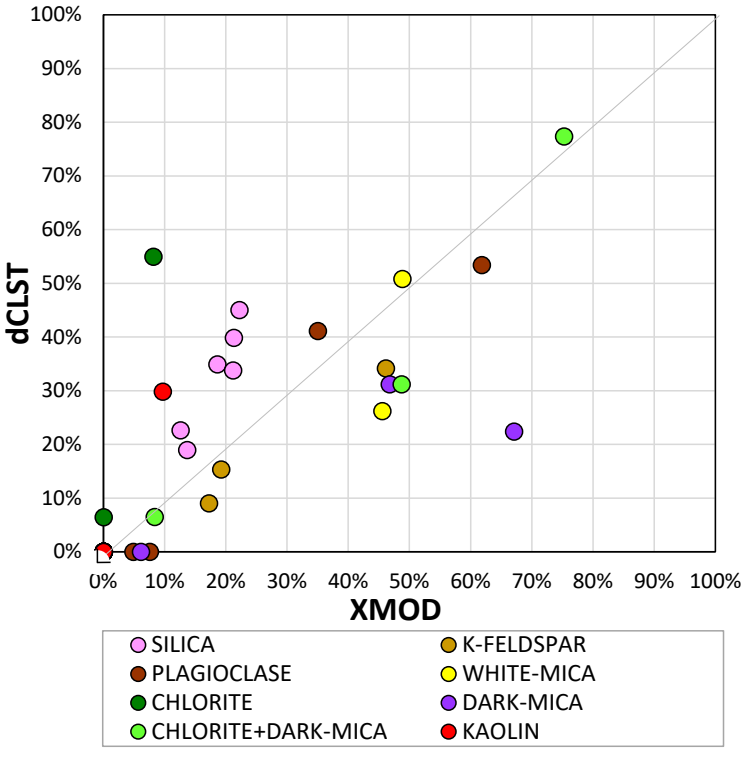

Figure 10a. Summary plot comparing mineral proportion estimates from TIR HyLogging (dCLST) with MLA (using XMOD). (This plot is repeated at a smaller scale in Figure 10b as part of a sequence of plots.)

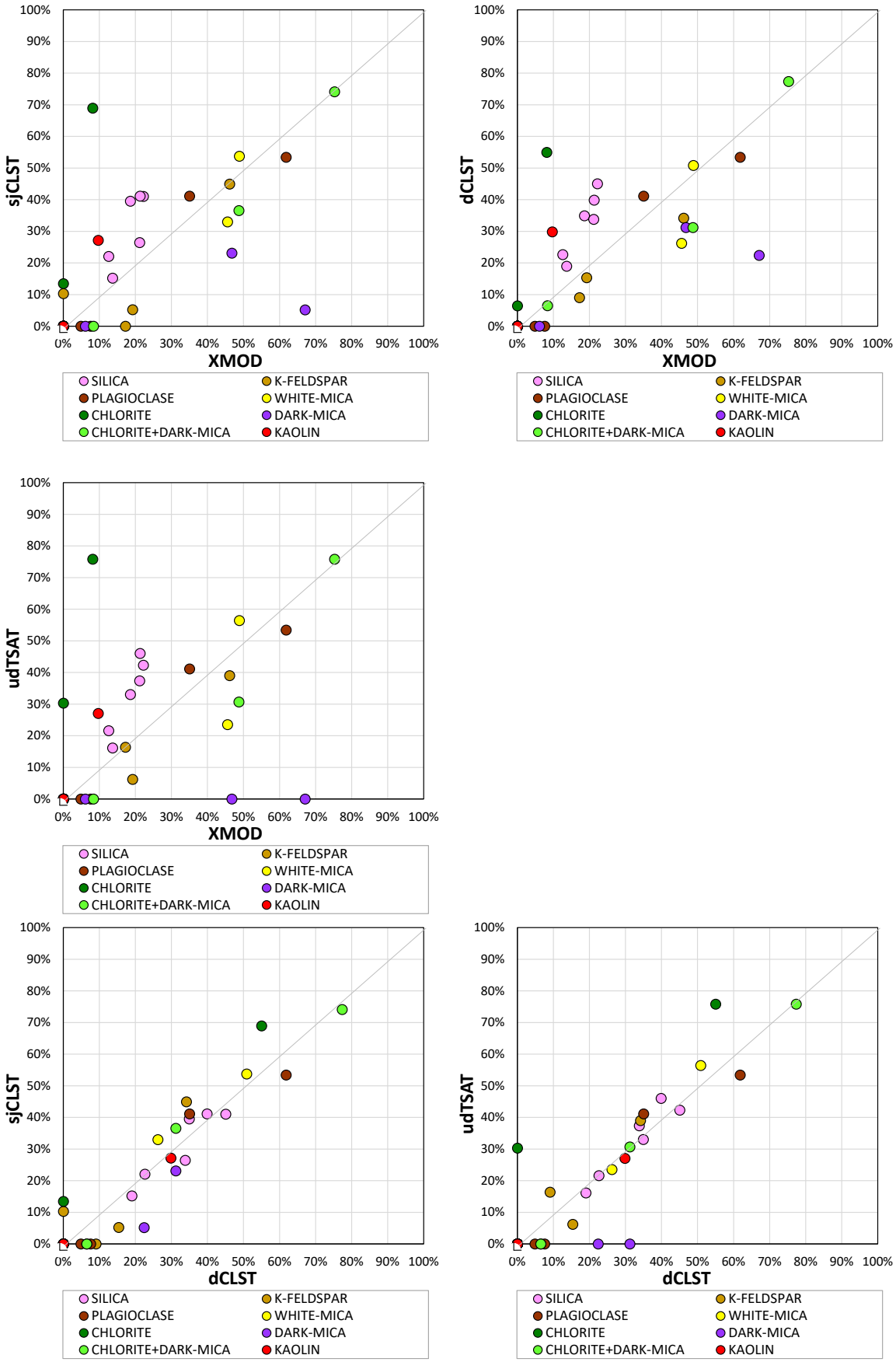

Figure 10b. Summary plots comparing mineral proportion estimates from three TIR unmixing algorithms with MLA (using XMOD) and comparing the algorithms with each other.

Mineral proportions from the two TSG SWIR unmixing algorithms are compared with MLA and also compared with each other in Figure 11. sTSAS and uTSAS produced similar results.

White mica proportions performed better than chlorite and kaolinite. Biotite was significantly under-estimated.

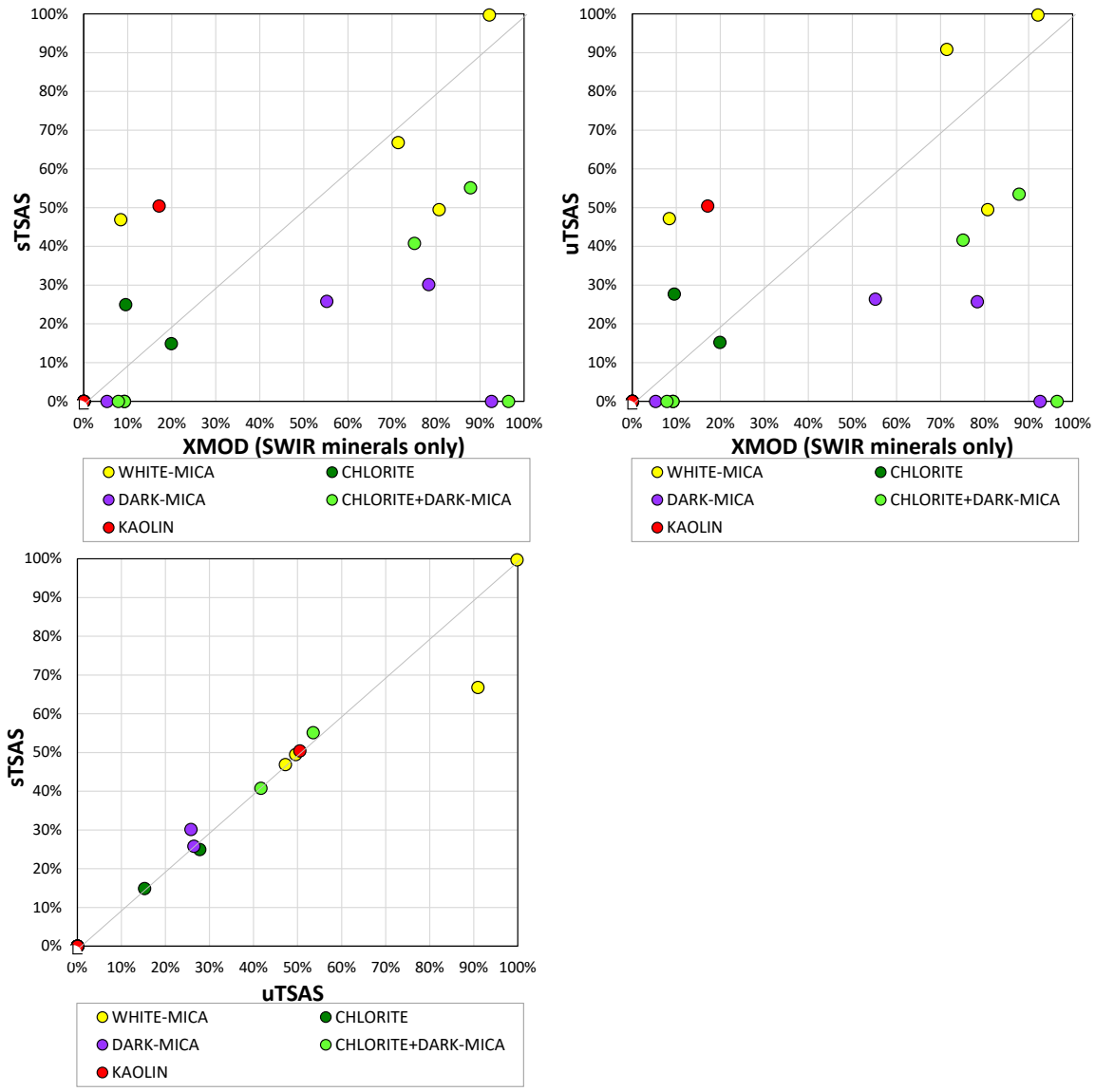

Figure 11. Summary plots comparing mineral proportion estimates from SWIR HyLogging with MLA (using XMOD) and comparing HyLogging unmixing algorithms with each other. MLA mineral proportions have been normalised so that the total of SWIR-active minerals sums to 100%.

Differences between the mineral proportions from the HyLogging unmixing algorithms and MLA are expressed as factors averaged across all 6 samples in Table 4. The comparison only includes occurrences in which minerals were reported in both the MLA and HyLogging algorithm and only for samples where the mineral comprises greater than 10% as measured by MLA.

- Quartz was consistently over-estimated by a factor of 1.8 (1.4 to 2.0).
- K-feldspar was under-estimated by a factor of 0.7.
- Plagioclase factors were close to 1.0 (0.8 and 1.2 for dCLST).
- Significant kaolin was reported only in the mudstone which was over-estimated by a factor of 3 in the SWIR. The kaolin proportion of TIR-active minerals for the shale was less than 10%, so was not included in Table 4, but was over-estimated by CLST by a factor of 3.
- White mica was accurately estimated by the SWIR algorithm, but was under-estimated by a factor of 0.8 by the TIR algorithms.
- Chlorite was under-estimated by the SWIR algorithms by a factor of 0.8. The proportion of chlorite among TIR-active minerals was less than 10% in all samples, so the TIR algorithms would struggle, but where chlorite was interpreted, it was over-estimated by a factor of 3 to 8.
- Biotite was under-estimated by the SWIR and TIR algorithms by a factor of 0.4 and 0.5 respectively.
- Chlorite + biotite was under-estimated by a factor of about 0.7.
- (Carbonate in 1 sample (15% siderite) was under-estimated by uTSAS by a factor of 0.5.)

Table 4. The differences between HyLogging results and MLA expressed as factors averaged for all 6 samples. e.g. The proportion of quartz (SILICA) estimated by sjCLST is 1.7 times that determined by MLA. The comparison only includes occurrences in which minerals were reported in both the MLA and HyLogging algorithm and only for samples where the mineral comprises greater than 10% as measured by MLA.

		SILICA (Quartz)	K-FELDSPAR	PLAGIOCLASE	KAOLIN	WHITE-MICA	CHLORITE	DARK-MICA (Biotite)	CHLORITE+ DARK-MICA	CARBONATE (Siderite)
sjCLST	Average	1.7	0.6	0.9		0.9		0.3	0.9	
	Std deviation	0.4	0.5	0.3		0.3		0.3	0.2	
dCLST	Average	1.8	0.7	1.0		0.8		0.5	0.8	
	Std deviation	0.2	0.1	0.3		0.3		0.2	0.3	
udTSAT	Average	1.8	0.7	1.0		0.8			0.8	
	Std deviation	0.3	0.3	0.2		0.5			0.3	
sTSAS	Average				3.0	0.9	0.8	0.4	0.6	1.3
	Std deviation					0.2		0.1	0.1	
uTSAS	Average				3.0	1.0	0.8	0.4	0.6	0.5
	Std deviation					0.3		0.1	0.0	0.0

Potential further work

Opportunities for further work on the data, or on the samples includes:

- Compare the performance of other unmixing methods e.g. MFEM scalars (Multiple Feature Extraction Method, Laukamp *et al.* 2010), sTSAT and uTSAT with all but black-listed minerals turned on.
- Use the polished, coated samples:
  - Microprobe minerals to compare with the spectrally interpreted composition e.g. white mica, chlorite, carbonate and amphibole.
  - Microprobe populations of each mineral species to measure the compositional range and compare with the spectral results using histograms of composition and feature wavelength respectively.
- Unpolish the samples:
  - MIR scanning.
- Destroy the polished, coated samples:
  - Compare MLA with the validation methods used previously: Crush the samples and analyse them by XRD, MINSQ (from XRD, XRF and microprobe analyses) and thin sections.

5. Conclusions

MLA produced estimates of mineral proportions accurate to within 2% and with an insignificant proportion that could not be identified. HyLogger data from surfaces matching the MLA samples were processed with 5 SWIR and TIR spectral unmixing algorithms. Minerals identified by the spectral unmixing algorithms were validated by the MLA at the mineral group level except for chlorite and biotite, which were commonly misidentified as one another. The identifications benefitted from applying the more advanced processing techniques. Small proportions of kaolin, white mica, chlorite and carbonate were consistently identified in both the SWIR and TIR, but similar proportions of plagioclase, epidote, dark mica and K-feldspar were not. At the mineral species level, muscovite and phengite were commonly incorrectly identified.

Estimates of mineral proportions improved from sjCLST to dCLST, but dTSAT resulted in poorer estimates, especially for chlorite + biotite and carbonate. The SWIR unmixing techniques sTSAS and uTSAS produced similar results for these mineralogically simple samples. The proportion of quartz was typically over-estimated relative to MLA by a factor of 1.8. White mica and plagioclase were accurately estimated by SWIR and TIR respectively. White mica and K-feldspar were under-estimated by factors of 0.7 to 0.8 in the TIR and biotite was under-estimated by a factor of 0.5. Chlorite was under-estimated in the SWIR by a factor of 0.8.

MLA validation of 6 samples analysed by HyLogger was a useful pilot study, with sample by sample interpretations providing interesting comparisons. However, generalisations would benefit from adding further samples (now underway) and incorporating data from previous HyLogger validation studies, including those that used the MINSQ method.

References

Berman, M., and Bishof, L. (1997) The algorithms underlying the Spectral Assistant software, CSIRO/AMIRA Project P435 report.

Berman, M., Bischof, L., Lagerstron, R., Guo, Y., Huntington, J., Mason, P. (2011) An unmixing algorithm based on a large library of shortwave infrared spectra, in: Technical Report EP117468, CSIRO Mathematics, Informatics and Statistics, URL: https://publications.csiro.au/rpr/pub?list=SEA&pid=csiro:EP117468.

Berman, M., Bischof, L., Lagerstrom, R., Guo, Y., Huntington, J., Mason, P., Green, A. (2017). A comparison between three sparse unmixing algorithms using a large library of shortwave infrared mineral spectra. IEEE Transactions on Geoscience and Remote Sensing, v.55 (6), p. 3588-3610.

Green, A. (2015) TSA+ and jCLST. URL: http://www.corstruth.com.au/information/FAQ.html#jCLST

Green, A. (2017) mineral occurrence maps of Australia – MOMAs. URL: http://www.corstruth.com.au/information/MOMAs.html

Green, D. and Schodlok, M. (2016) Characterisation of carbonate minerals from hyperspectral TIR scanning using features at 14 000 and 11 300 nm. Australian Journal of Earth Sciences, v. 63 (8), p.951-957.

Fandrich, R., Gu, Y., Burrows, D. and Moeller, K. (2007) Modern SEM-based mineral liberation analysis. Int. J. Miner. Process. v.84, p.310-320.

Gu, Y. and Sugden, T. (1995) A highly integrated SEM-EDS-IP system automated quantitative mineral analysis, Proceedings of the third biennial symposium on SEM imaging and analysis: applications and techniques, University of Melbourne. (Australian Society of Electron Microscopy)

Hermann, W. and Berry, R.F. (2002) MINSQ – A least squares spreadsheet method spreadsheet for calculating mineral proportions from whole rock major element analysis. Geochemistry: Exploration, Environment, Analysis, v.2, p, 361-368.

Huntington, J., Yang, K., Quigley, M., Schodlok. M. (2009) Validation of interpreted HyLogging mineralogical results: Parts 1 to 3. GeM^{III} (AMIRA P843) Technical Report 3, chapter 11.

Laukamp, C., Cudahy T., Caccetta M., *et al.* (2010). The uses, abuses and opportunities for hyperspectral technologies and derived geoscience information. AIG Bulletin, 51 (Geo-Computing 2010 Conference, Brisbane, September 2010): p.73-76.

Moltzen, J. and Bottrill, R. (2018): Rock assemblage Library – Report 2018.

J.K. Moltzen, J., Bottrill, R., Unwin, L. and Coyte, T. (2020) NVCL Activity 2: Spectral libraries and additional validation of rock assemblage data. Rock Assemblage Library: FY2019/20. NSW Geological Survey Report, June 2020. (In press.)

Schodlok, M., Whitbourn, L., Huntington, J., Mason, P., Green, A., Berman, M., Coward, D., Connor, P., Wright, W., Jolivet, M., Martinez, R. (2016a) HyLogger-3, a visible to shortwave and thermal infrared reflectance spectrometer system for drill core logging: functional description. Australian Journal of Earth Sciences, v. 63 (8), p.929-940.

Schodlok, M., Green, A., Huntington, J. (2016b). A reference library of thermal infrared mineral reflectance spectra for the HyLogger-3 drill core logging system. Australian Journal of Earth Sciences, v. 63 (8), p.941-949.

Appendix 1. HyLogging and MLA results

Tables 1 to 4 (below). Results of HyLogger analysis and MLA point counting. Full MLA results are included as Appendix 2.

Note: 0.0% indicates less than 0.1%, blank indicates not detected at all. XMOD sums to less than 100% when there are unlisted non-mineral classes, i.e. unknown, poor spectra, pen marks and sample holder.

	G408251 Kaol+White mica Tasmania Basin, Tas				G408275 K-feldspar+Plag Gramalote Project, Colombia				G408243 K-feldspar+Plag+White mica(+Qtz) White Spur, Tas			
Number of HyLogger spectra	165				338				149			
Number of MLA points	35025				38380				117816			
TIR												
Groups	sjCLST	dCLST	udTSAT	XMOD	sjCLST	dCLST	udTSAT	XMOD	sjCLST	dCLST	Cb	XMOD
MISC-SILICATE				0.0%				0.0%				
SILICA	39.5%	34.9%	33.0%	18.6%	41.0%	45.0%	42.3%	22.2%	15.2%	19.0%		13.7%
K-FELDSPAR		9.1%	16.4%	17.2%	10.3%			4.1%	44.9%	34.1%		46.1%
PLAGIOCLASE				7.6%	45.3%	48.5%	53.4%	61.8%	39.0%	41.1%		35.0%
GARNET												
OLIVINE												
ZEOLITE												
KAOLIN	27.2%	29.8%	27.0%	9.7%				0.5%				0.2%
WHITE-MICA	33.0%	26.2%	23.5%	45.5%				0.9%		4.2%		3.7%
SMECTITE	0.3%								0.4%			
OTHER-ALOH												
CHLORITE				0.3%	3.3%	6.5%	4.3%	2.2%		0.9%		0.5%
DARK-MICA				0.3%		0.0%		6.1%				
AMPHIBOLE								1.1%				
SERPENTINE												
OTHER-MGOH												
EPIDOTE				0.4%								
CARBONATE				0.2%				0.3%		0.7%		0.8%
SULPHATE									0.5%			
PHOSPHATE				0.0%				0.2%				0.0%
OXIDE				0.1%				0.3%				0.0%
	100.0%	100.0%		100.0%	100.0%	100.0%	100.0%	99.7%	100.0%	100.0%		100.0%
Minerals												
Opal												
Quartz	39.5%	34.9%	33.0%	18.6%	41.0%	45.0%	42.3%	22.2%	15.2%	19.0%		13.7%
Anorthoclase										0.0%		
Microcline		9.1%	16.4%		10.3%				38.7%	34.1%		
Orthoclase				17.2%				4.1%	6.2%			46.1%
Albite				7.6%	14.5%	22.8%	27.5%	2.5%	33.2%	34.0%		35.0%
Labradorite					2.1%							
Andesine					6.2%		3.9%					
Oligoclase					22.6%	25.7%	22.0%	59.3%	5.8%	7.1%		
Almandine												
Spessartine												
Analcime												
Natrolite												
Phillipsite												
Kaolinite-WX	27.2%	29.8%	27.0%	9.7%				0.5%				0.2%
Muscovite	33.0%	26.2%	23.5%	4.5%				0.3%		4.2%		0.6%
Phengite				41.1%				0.7%				3.1%
Glauconite												
Montmorillonite	0.3%											
Nontronite									0.4%			
Topaz												
Chlorite-Fe				0.3%		0.0%	0.4%	0.1%				0.5%
Chlorite-FeMg					3.3%	6.4%	3.8%	2.1%		0.9%		
Biotite				0.3%		0.0%		6.1%				
Phlogopite												
Stilpnomelane												
Actinolite								1.1%				
Edenite												
Hornblende												
Antigorite												
Lizardite												
Talc												
Epidote				0.4%								
Zoisite												
Siderite										0.7%	0.7%	
Aragonite												
Calcite				0.2%				0.3%				0.8%
Dolomite												
Alunite-K									0.5%			
Gypsum												
Apatite				0.0%				0.2%				0.0%
Zircon				0.0%				0.0%				
OXIDE				0.1%				0.3%				0.0%
	100.0%	100.0%		100.0%	100.0%	100.0%	100.0%	99.7%	100.0%	100.0%	0.7%	100.0%

	G408251 Kaol+White mica Tasmania Basin, Tas			G408275 K-feldspar+Plag Gramalote Project, Colombia			G408243 K-feldspar+Plag+White mica(+Qtz) White Spur, Tas		
Number of HyLogger spectra	165			338			149		
Number of MLA points	35025			38380			117816		
SWIR									
Groups	sTSAS	uTSAS	XMOD	sTSAS	uTSAS	XMOD	sTSAS	uTSAS	XMOD
KAOLIN	50.5%	50.5%	17.1%	1.1%	0.7%	4.3%			4.7%
WHITE-MICA	49.5%	49.5%	80.7%	46.9%	47.2%	8.4%	66.9%	90.9%	71.4%
OTHER-ALOH									
CHLORITE			0.6%	15.0%	15.2%	19.9%	0.5%	2.1%	9.2%
DARK-MICA			0.6%	25.9%	26.4%	55.2%			
AMPHIBOLE				0.3%		9.7%			
SERPENTINE				0.1%					
EPIDOTE			0.7%	0.4%			0.5%		
TOURMALINE				1.4%					
CARBONATE			0.3%	0.3%		2.6%	19.4%	6.9%	14.7%
SULPHATE							11.8%		
NOTAROK				0.1%			0.9%		
INVALID				8.6%	10.4%				
	100.0%	100.0%	100.0%	100.0%	100.0%	100.0%	100.0%	100.0%	100.0%
Minerals									
Kaolinite-PX				0.9%	0.6%				
Kaolinite-WX	50.5%	50.5%	17.1%	0.3%	0.2%	4.1%			4.6%
Muscovite	25.8%	25.8%	7.9%	34.2%	35.0%	2.2%			11.8%
Paragonite				0.5%	0.7%				
Phengite			72.6%			5.9%	67.5%	90.9%	58.9%
MuscoviticIllite	23.7%	23.7%		16.7%	17.1%				
PhengiticIllite									
Topaz									
Chlorite-Fe			0.6%			1.3%			9.1%
Chlorite-FeMg				7.9%	8.2%	17.7%	0.5%	2.1%	
Chlorite-Mg				8.4%	8.9%				
Biotite			0.6%	0.3%	0.2%	52.6%			
Phlogopite				28.0%	29.3%				
Actinolite						9.3%			
Hornblende				0.2%					
Riebeckite				0.1%					
Serpentine				0.1%					
Epidote			0.7%	0.4%					
Zoisite							0.5%		
Tourmaline-Fe				1.6%					
Ankerite				0.1%			17.5%	4.8%	
Siderite				0.1%					
Calcite			0.3%	0.1%		2.4%	2.0%	2.0%	14.6%
Dolomite							0.2%	0.2%	
Alunite-NH							11.9%		
Jarosite									
Apatite			0.1%			2.0%			0.4%
Zircon			0.0%			0.2%			
OXIDE			0.1%			2.4%			0.6%
	100.0%	100.0%	100.0%	100.0%	100.0%	100.0%	100.0%	100.0%	100.0%

	G408265 Biot+Epid+Amph Cethana, Tas				G408264 Chl+Biot Cethana, Tas				G408260 Shale - crypto-micaceous Oonah Prospect, Tas			
Number of HyLogger spectra	183				364				219			
Number of MLA points	39091				37025				35465			
TIR												
Groups	sjCLST	dCLST	udTSAT	XMOD	sjCLST	dCLST	udTSAT	XMOD	sjCLST	dCLST	udTSAT	XMOD
MISC-SILICATE				0.0%				0.1%				0.0%
SILICA	41.1%	39.9%	46.0%	21.3%	22.1%	22.6%	21.6%	12.6%	26.5%	33.8%	37.4%	21.2%
K-FELDSPAR				0.2%	0.4%			0.9%	5.2%	15.4%	6.2%	19.2%
PLAGIOCLASE				0.1%	2.5%		2.6%	0.0%				4.9%
GARNET	21.5%	19.3%	21.2%	20.3%								
OLIVINE												
ZEOLITE			1.7%									
KAOLIN				0.0%				0.1%				0.0%
WHITE-MICA	0.1%	0.2%	0.1%	1.8%				0.9%	53.8%	50.8%	56.4%	48.8%
SMECTITE												
OTHER-ALOH	0.4%											
CHLORITE	13.5%		30.3%	1.9%	69.0%	55.0%	75.8%	8.1%				1.4%
DARK-MICA	23.1%	31.2%	0.4%	46.7%	5.2%	22.4%		67.1%				2.8%
AMPHIBOLE	0.3%	9.5%	0.3%	0.0%	0.5%							0.0%
SERPENTINE					0.4%							
OTHER-MGOH												
EPIDOTE	0.1%							9.1%				
CARBONATE				0.0%				0.4%				
SULPHATE									14.6%			
PHOSPHATE				0.4%				0.5%				0.0%
OXIDE				6.5%				0.0%				0.3%
	100.0%	100.0%	100.0%	99.3%	100.0%	100.0%	100.0%	99.8%	100.0%	100.0%	100.0%	98.7%
Minerals												
Opal												
Quartz	41.1%	39.9%	46.0%	21.3%	22.1%	22.6%	21.6%	12.6%	26.5%	33.8%	37.4%	21.2%
Anorthoclase												
Microcline					0.4%				5.2%	14.1%	6.2%	
Orthoclase				0.2%				0.9%		1.2%		19.2%
Albite				0.0%	2.3%		2.4%	0.0%				3.7%
Labradorite												
Andesine												
Oligoclase				0.1%	0.2%		0.2%					1.2%
Almandine	0.2%											
Spessartine	21.2%	19.3%	21.2%	20.3%								
Analcime			0.2%									
Natrolite			0.5%									
Phillipsite			1.0%									
Kaolinite-WX				0.0%				0.1%				0.0%
Muscovite	0.1%	0.2%		1.4%				0.3%	53.8%	50.8%	56.4%	10.7%
Phengite				0.3%				0.6%				38.1%
Glauconite			0.1%									
Montmorillonite												
Nontronite												
Topaz	0.4%											
Chlorite-Fe	0.1%			1.9%	2.4%	7.6%	0.9%	8.1%				1.3%
Chlorite-FeMg	13.3%		30.3%	0.1%	66.6%	47.4%	74.9%					0.0%
Biotite	23.1%	31.2%		46.7%	5.2%	0.0%		67.1%				2.8%
Phlogopite						22.1%						
Stilpnomelane			0.4%			0.2%						
Actinolite		4.4%		0.0%	0.0%							0.0%
Edenite	0.3%	5.0%			0.4%							
Hornblende		0.1%	0.3%		0.1%							
Antigorite												
Lizardite					0.4%							
Talc												
Epidote								9.1%				
Zoisite	0.1%											
Siderite												
Aragonite												
Calcite				0.0%				0.4%				
Dolomite												
Alunite-K									13.9%			
Gypsum									0.7%			
Apatite				0.4%				0.5%				0.0%
Zircon				0.0%				0.1%				0.0%
OXIDE				6.5%				0.0%				0.3%
	100.0%	100.0%	100.0%	99.3%	100.0%	100.0%	100.0%	99.8%	100.0%	100.0%	100.0%	98.7%

	G408265 Biot+Epid+Amph Cethana, Tas			G408264 Chl+Biot Cethana, Tas			G408260 Shale - crypto-micaceous Oonah Prospect, Tas		
Number of HyLogger spectra	183			364			219		
Number of MLA points	39091			37025			35465		
SWIR									
Groups	sTSAS	uTSAS		sTSAS	sTSAS		sTSAS	sTSAS	
KAOLIN			0.0%			0.1%			0.1%
WHITE-MICA	0.3%	0.3%	3.5%		0.1%	1.1%	99.8%	99.8%	92.1%
OTHER-ALOH	1.6%								
CHLORITE	0.5%		3.9%	25.0%	27.7%	9.5%			2.6%
DARK-MICA	2.2%	2.3%	92.6%	30.2%	25.8%	78.3%			5.3%
AMPHIBOLE			0.0%	0.3%					0.0%
SERPENTINE				0.1%					
EPIDOTE				0.4%		10.6%			
TOURMALINE	0.1%			0.1%					
CARBONATE			0.0%	0.4%		0.4%	0.2%	0.2%	
SULPHATE				0.1%					
NOTAROK	0.1%	0.1%		0.6%	0.6%				
INVALID	95.1%	97.3%		42.9%	45.8%				
	100.0%	100.0%	100.0%	100.0%	100.0%	100.0%	100.0%	100.0%	100.0%
Minerals									
Kaolinite-PX									
Kaolinite-WX			0.0%			0.1%			0.1%
Muscovite		9.2%	2.5%			0.3%			20.0%
Paragonite									
Phengite	67.5%	3.3%	0.6%		0.1%	0.7%	52.1%	52.1%	71.4%
MuscoviticIllite									
PhengiticIllite							47.7%	47.7%	
Topaz									
Chlorite-Fe			3.3%	2.1%	2.4%	9.4%			2.5%
Chlorite-FeMg	0.5%		0.1%	38.2%	45.8%				0.1%
Chlorite-Mg				4.0%	2.9%				
Biotite		87.5%	81.4%	50.4%	44.6%	77.8%			5.2%
Phlogopite				3.1%	2.9%				
Actinolite			0.0%	0.1%					0.0%
Hornblende				0.4%					
Riebeckite				0.1%					
Serpentine				0.1%					
Epidote				0.4%		10.5%			
Zoisite	0.5%			0.2%					
Tourmaline-Fe				0.2%					
Ankerite	17.5%			0.5%			0.2%	0.2%	
Siderite				0.2%					
Calcite	2.0%		0.0%			0.4%			
Dolomite	0.2%								
Alunite-NH	11.9%								
Jarosite				0.1%					
Apatite			0.7%			0.6%			0.0%
Zircon			0.0%			0.1%			0.0%
OXIDE			11.4%			0.0%			0.6%
	100.0%	100.0%	100.0%	100.0%	98.8%	100.0%	100.0%	100.0%	100.0%

Appendix 2. Full MLA results

MLA was acquired at the University of Tasmania Central Science Laboratory using a FEI MLA650 SEM with Bruker Quantax Esprit 1.9 EDS system using two XFlash 5030 SDD detectors with MnKα 133 eV resolution and combined throughput up to 800kcps.

Operating conditions were 20keV, dead time around 30%, 400 kcps throughput, 13 mm working distance. The spot size was less than 1 μm.

The MLA analytical settings were 5ms count time per spot and 210-450 μm step size (70 and 150 pixels) depending on the overall sample area. BSE imagery was acquired with a CBS solid state detector.

Mineral		Al (%)	C (%)	Ca (%)	Ce (%)	Cl (%)	F (%)	Fe (%)	H (%)	K (%)	La (%)	Mg (%)	Mn (%)	Na (%)	Nd (%)	O (%)	P (%)	Pb (%)	RE (%)	S (%)	Si (%)	Ti (%)	Zr (%)	Density
Quartz	SiO2	0.00	0.00	0.00	0.00	0.00	0.00	0.00	0.00	0.00	0.00	0.00	0.00	0.00	0.00	53.26	0.00	0.00	0.00	0.00	46.74	0.00	0.00	2.63
Albite	NaAlSi3O8	10.77	0.00	0.76	0.00	0.00	0.00	0.00	0.00	0.00	0.00	0.00	0.00	8.30	0.00	48.66	0.00	0.00	0.00	0.00	31.50	0.00	0.00	2.62
Plagioclase	Ca0.4Na0.6Al1.4Si2.6O8	14.06	0.00	5.97	0.00	0.00	0.00	0.00	0.00	0.00	0.00	0.00	0.00	5.14	0.00	47.65	0.00	0.00	0.00	0.00	27.19	0.00	0.00	2.67
Pl_or_Ab-Cal mix	Ca0.4Na0.6Al1.4Si2.6O8Ca(CO3)	10.24	3.26	15.22	0.00	0.00	0.00	0.00	0.00	0.00	0.00	0.00	3.74	0.00	47.73	0.00	0.00	0.00	0.00	19.81	0.00	0.00	0.00	2.70
K-Feldspar	KAlSi3O8	9.69	0.00	0.00	0.00	0.00	0.00	0.00	0.00	14.04	0.00	0.00	0.00	0.00	0.00	45.99	0.00	0.00	0.00	0.00	30.28	0.00	0.00	2.56
Actinolite	Ca2Mg3Fe2+2Si8O22(OH)2	1.39	0.00	8.59	0.00	0.00	0.00	8.57	0.23	0.00	0.00	9.71	0.12	0.59	0.00	35.34	0.00	0.00	0.00	0.00	35.34	0.11	0.00	3.04
Muscovite	KAl3Si3O10(OH)1.9F0.1	20.30	0.00	0.00	0.00	0.00	0.95	0.00	0.45	9.80	0.00	0.00	0.00	0.00	0.00	47.36	0.00	0.00	0.00	0.00	21.13	0.00	0.00	2.83
Muscovite_minorFe	KAl3Si3O10(OH)1.9F0.1	20.30	0.00	0.00	0.00	0.00	0.95	0.00	0.45	9.80	0.00	0.00	0.00	0.00	0.00	47.36	0.00	0.00	0.00	0.00	21.13	0.00	0.00	2.83
Biotite	KMg2.5Fe2+0.5AlSi3O10(OH)1.75F0.25	6.22	0.00	0.00	0.00	0.00	1.09	6.44	0.40	9.01	0.00	14.02	0.00	0.00	0.00	43.38	0.00	0.00	0.00	0.00	19.44	0.00	0.00	3.10
Chlorite	(Mg,Fe)3(Si,Al)4O10(OH)2·(Mg,Fe)3(OH)6	8.34	0.00	0.00	0.00	0.00	0.00	25.91	1.25	0.00	0.00	11.28	0.00	0.00	0.00	44.53	0.00	0.00	0.00	0.00	8.69	0.00	0.00	2.95
Chlorite_Fe	(Fe2+,Mg,Fe3+)5Al[Si3Al]O10·(OH,O)8	8.21	0.00	0.00	0.00	0.00	0.00	28.34	0.61	0.00	0.00	6.17	0.00	0.00	0.00	43.84	0.00	0.00	0.00	0.00	12.83	0.00	0.00	2.80
Kaolinite	Al2Si2O5(OH)4	20.90	0.00	0.00	0.00	0.00	0.00	0.00	1.56	0.00	0.00	0.00	0.00	0.00	0.00	55.78	0.00	0.00	0.00	0.00	21.75	0.00	0.00	2.60
Epidote-Allanite	Ca2Al2(Fe3+,Al)(SiO4)(Si2O7)O(OH)	14.39	0.00	17.10	0.00	0.00	5.96	0.22	0.00	0.00	0.00	0.00	0.00	44.37	0.00	0.00	0.00	17.97	0.00	0.00	0.00	0.00	0.00	3.45
Spessartine	Mn2+3Al2(SiO4)3	10.90	0.00	0.00	0.00	0.00	0.00	0.00	0.00	0.00	0.00	33.29	0.00	0.00	38.78	0.00	0.00	0.00	0.00	17.02	0.00	0.00	0.00	4.18
Calcite	Ca(CO3)	0.00	12.00	40.04	0.00	0.00	0.00	0.00	0.00	0.00	0.00	0.00	0.00	0.00	0.00	47.95	0.00	0.00	0.00	0.00	0.00	0.00	0.00	2.71
Dolomite	CaMg(CO3)2	0.00	13.02	21.73	0.00	0.00	0.00	0.00	0.00	0.00	0.00	13.18	0.00	0.00	0.00	52.06	0.00	0.00	0.00	0.00	0.00	0.00	0.00	2.85
Ca-REE carbonate	Ca(Ce,Nd,La)(CO3)2F	0.00	7.50	12.52	14.59	0.00	5.93	0.00	0.00	0.00	14.46	0.00	0.00	0.00	15.02	29.98	0.00	0.00	0.00	0.00	0.00	0.00	0.00	4.00
Alumina-Cal		0.00	0.00	0.00	0.00	0.00	0.00	0.00	0.00	0.00	0.00	0.00	0.00	0.00	0.00	0.00	0.00	0.00	0.00	0.00	0.00	0.00	0.00	1.00
Ca-Al-Fe-Mg silicate	Ca2(Mg,Fe,Al)5(Al,Si)8O22(OH)2	17.68	0.00	9.27	0.00	0.00	10.76	0.23	0.00	0.00	4.68	0.00	0.00	0.00	44.39	0.00	0.00	0.00	0.00	12.99	0.00	0.00	0.00	2.90
Titanite	CaTiSiO5	2.72	0.00	19.26	0.00	0.00	0.96	1.41	0.00	0.00	0.00	0.00	0.00	0.00	0.00	39.65	0.00	0.00	3.64	0.00	14.20	18.16	0.00	3.48
Apatite	Ca5(PO4)(F,Cl,OH)	0.00	0.00	39.37	0.00	2.32	1.24	0.00	0.06	0.00	0.00	0.00	0.00	0.00	0.00	38.76	18.25	0.00	0.00	0.00	0.00	0.00	0.00	3.19
Ilmenite-Mn	Fe0.7Mn0.3TiO3	0.00	0.00	0.00	0.00	0.00	0.00	25.81	0.00	0.00	0.00	0.00	10.88	0.00	0.00	31.69	0.00	0.00	0.00	0.00	0.00	31.62	0.00	4.72
Rutile	TiO2	0.00	0.00	0.00	0.00	0.00	0.00	0.00	0.00	0.00	0.00	0.00	0.00	0.00	0.00	40.05	0.00	0.00	0.00	0.00	0.00	59.95	0.00	4.25
Fe-oxide	Fe3O4	0.00	0.00	0.00	0.00	0.00	0.00	72.36	0.00	0.00	0.00	0.00	0.00	0.00	0.00	27.64	0.00	0.00	0.00	0.00	0.00	0.00	0.00	5.15
Pyrite	Fe2+S2	0.00	0.00	0.00	0.00	0.00	0.00	46.54	0.00	0.00	0.00	0.00	0.00	0.00	0.00	0.00	0.00	0.00	0.00	53.46	0.00	0.00	0.00	5.01
Galena	PbS	0.00	0.00	0.00	0.00	0.00	0.00	0.00	0.00	0.00	0.00	0.00	0.00	0.00	0.00	0.00	0.00	86.60	0.00	13.40	0.00	0.00	0.00	7.40
Zircon	ZrSiO4	0.00	0.00	0.00	0.00	0.00	0.00	0.00	0.00	0.00	0.00	0.00	0.00	0.00	0.00	34.91	0.00	0.00	0.00	0.00	15.32	0.00	49.76	4.65

Table A2.1. Mineral compositions used in the XMOD reference mineral library.

Data Source: G40851_XMOD_STD			
Mineral Groupings: Ungrouped			
Filter: Unfiltered			
Mineral	Wt%	Area%	Point Count
Unknown	0.00	0.11	38
Quartz	18.58	19.12	6696
Albite	7.56	7.79	2729
K-Feldspar	17.23	18.18	6366
Muscovite	4.48	4.28	1500
Muscovite_minorFe	41.07	39.27	13753
Biotite	0.32	0.28	97
Chlorite_Fe	0.34	0.33	116
Kaolinite	9.66	10.03	3514
Epidote-Allanite	0.42	0.33	116
Calcite	0.18	0.18	62
Dolomite	0.00	0.00	0
Rutile	0.06	0.04	13
Apatite	0.04	0.03	12
Ca-REE carbonate	0.01	0.01	2
Zircon	0.02	0.01	5
Pyrite	0.03	0.01	5
Galena	0.01	0.00	1
Total	100.00	100.00	35025

Data Source: G408243_XMOD_STD			
Mineral Groupings: Ungrouped			
Filter: Unfiltered			
Mineral	Wt%	Area%	Point Count
Unknown	0.00	1.28	1504
Low_Counts	0.00	0.00	0
No_XRay	0.00	0.00	0
Quartz	13.66	13.37	15748
Albite	35.03	34.34	40455
K-Feldspar	46.12	46.26	54507
Muscovite	0.61	0.56	655
Muscovite_minorFe	3.06	2.78	3273
Chlorite_Fe	0.47	0.43	512
Kaolinite	0.24	0.24	279
Calcite	0.74	0.70	828
Dolomite	0.00	0.00	0
Rutile	0.03	0.02	24
Apatite	0.02	0.02	19
Ca-REE carbonate	0.02	0.01	12
Total	100.00	100.00	117816

Data Source: G408275_XMOD_STD			
Mineral Groupings: Ungrouped			
Filter: Unfiltered			
Mineral	Wt%	Area%	Point Count
Unknown	0.00	0.51	197
Low_Counts	0.00	0.00	0
No_XRay	0.00	0.00	0
Quartz	22.19	22.66	8695
Albite	2.47	2.52	968
Plagioclase	59.32	59.54	22853
K-Feldspar	4.08	4.27	1638
Actinolite	1.08	0.95	365
Muscovite	0.25	0.24	92
Muscovite_minorFe	0.68	0.65	248
Biotite	6.13	5.30	2033
Chlorite	2.06	1.87	717
Chlorite_Fe	0.15	0.14	55
Kaolinite	0.47	0.49	187
Titanite	0.28	0.21	82
Calcite	0.28	0.27	105
Dolomite	0.00	0.00	0
Rutile	0.00	0.00	0
Apatite	0.23	0.20	75
Ca-REE carbonate	0.01	0.01	2
Zircon	0.03	0.02	6
Pyrite	0.30	0.16	62
Galena	0.00	0.00	0
Pen	0.00	0.00	0
Pen_2	0.00	0.00	0
Alumina-Cal	0.00	0.00	0
NiP_holder	0.00	0.00	0
Total	100.00	100.00	38380

Data Source: G408265_XMOD_STD			
Mineral Groupings: Ungrouped			
Filter: Unfiltered			
Mineral	Wt%	Area%	Point Count
Unknown	0.00	0.02	7
Quartz	21.30	26.09	10197
Albite	0.01	0.01	5
Plagioclase	0.06	0.07	26
K-Feldspar	0.24	0.31	120
Spessartine	20.25	15.57	6087
Ca-Al-Fe-Mg silicate	0.53	0.59	230
Actinolite	0.02	0.02	7
Muscovite	1.42	1.62	633
Muscovite_minorFe	0.35	0.39	154
Biotite	46.75	48.47	18947
Chlorite	0.07	0.08	30
Chlorite_Fe	1.87	2.15	841
Kaolinite	0.01	0.02	7
Titanite	0.00	0.00	0
Ilmenite-Mn	0.16	0.11	43
Fe-oxide	6.37	3.97	1553
Calcite	0.01	0.01	5
Dolomite	0.00	0.00	0
Rutile	0.00	0.00	1
Apatite	0.38	0.38	149
Ca-REE carbonate	0.00	0.00	0
Zircon	0.02	0.01	5
Pyrite	0.18	0.11	44
Galena	0.00	0.00	0
Total	100.00	100.00	39091

Data Source: G408264_XMOD_STD			
Mineral Groupings: Ungrouped			
Filter: Unfiltered			
Mineral	Wt%	Area%	Point Count
Unknown	0.00	0.07	26
Quartz	12.58	14.49	5365
Albite	0.02	0.02	7
K-Feldspar	0.91	1.08	399
Muscovite	0.28	0.30	110
Muscovite_minorFe	0.64	0.68	252
Biotite	67.09	65.43	24226
Chlorite_Fe	8.15	8.80	3257
Kaolinite	0.08	0.09	34
Epidote-Allanite	9.09	7.97	2951
Calcite	0.35	0.39	146
Dolomite	0.00	0.00	0
Rutile	0.00	0.00	0
Apatite	0.54	0.51	190
Ca-REE carbonate	0.00	0.00	0
Zircon	0.06	0.04	14
Pyrite	0.21	0.13	47
Galena	0.01	0.00	1
Total	100.00	100.00	37025

Data Source: G408260_XMOD_STD			
Mineral Groupings: Ungrouped			
Filter: Unfiltered			
Mineral	Wt%	Area%	Point Count
Unknown	0.00	0.01	4
Quartz	21.17	22.12	7846
Albite	3.70	3.87	1372
Plagioclase	1.16	1.19	421
K-Feldspar	19.21	20.58	7299
Actinolite	0.01	0.01	3
Muscovite	10.70	10.39	3685
Muscovite_minorFe	38.14	37.03	13133
Biotite	2.79	2.47	876
Chlorite	0.03	0.03	9
Chlorite_Fe	1.35	1.32	469
Kaolinite	0.04	0.04	14
Titanite	0.00	0.00	0
Ilmenite-Mn	0.00	0.00	0
Fe-oxide	0.32	0.17	61
Calcite	0.00	0.00	0
Dolomite	0.00	0.00	0
Rutile	0.02	0.01	5
Apatite	0.02	0.01	5
Ca-REE carbonate	0.00	0.00	0
Zircon	0.00	0.00	1
Pyrite	1.35	0.74	262
Galena	0.00	0.00	0
Total	100.00	100.00	35465

Appendix 3. MLA method

Figure A3.1. A polished and carbon-coated sample mounted in a holder that has been minutely adjusted, aligning the sample so it is level in the SEM.

Figure A3.2. The sample being mounted in the SEM measurement chamber.

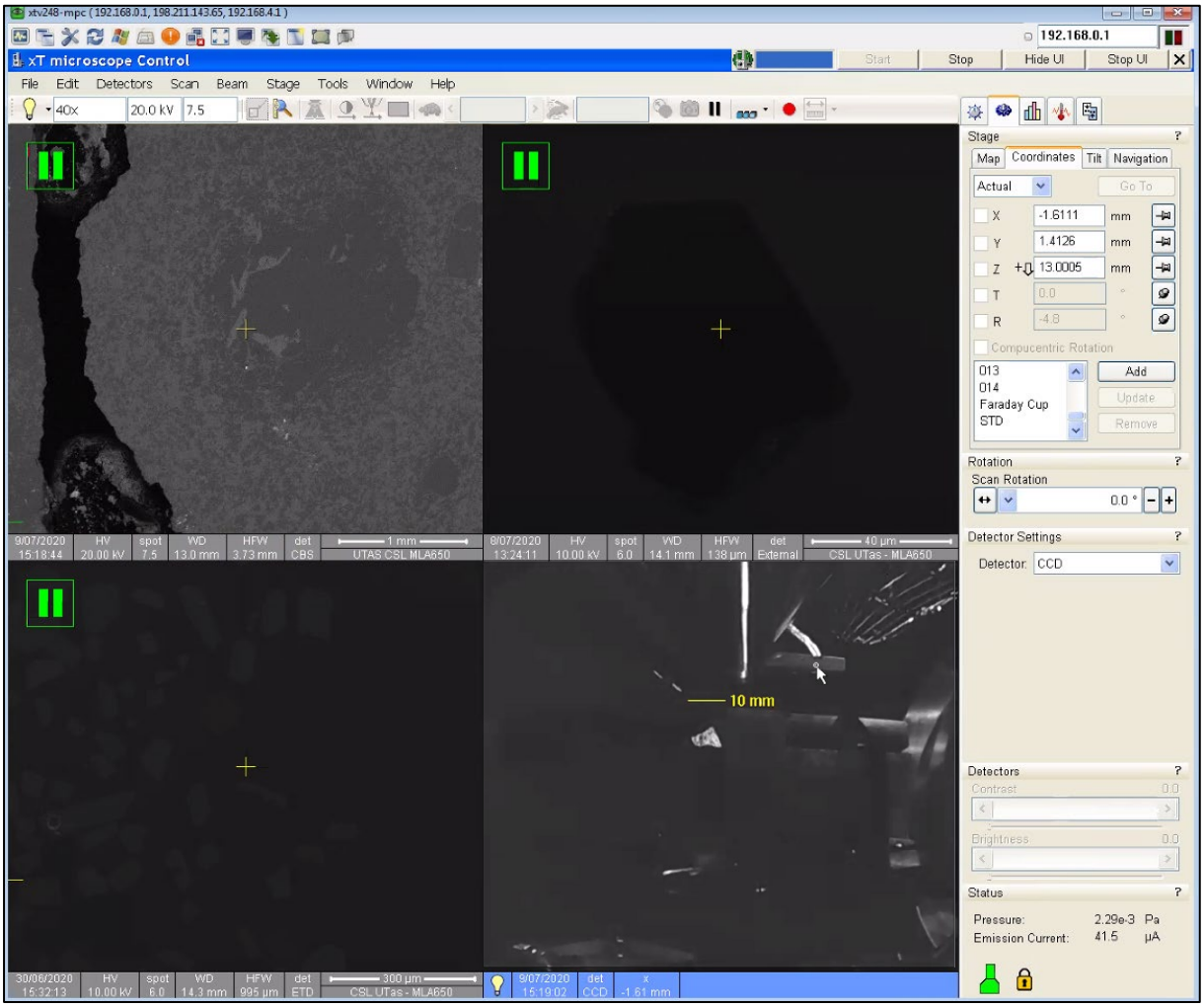

Figure A3.3. SEM control interface showing a reflected light image at various magnifications and a side view of the sample in the holder at bottom right. The cursor indicates the backscatter detector and the 10mm scale is used to monitor the gap between the sample and electron focusing objective lens. The actual working distance (distance final lens-sample surface) used for MLA measurements on this system is 13 mm.

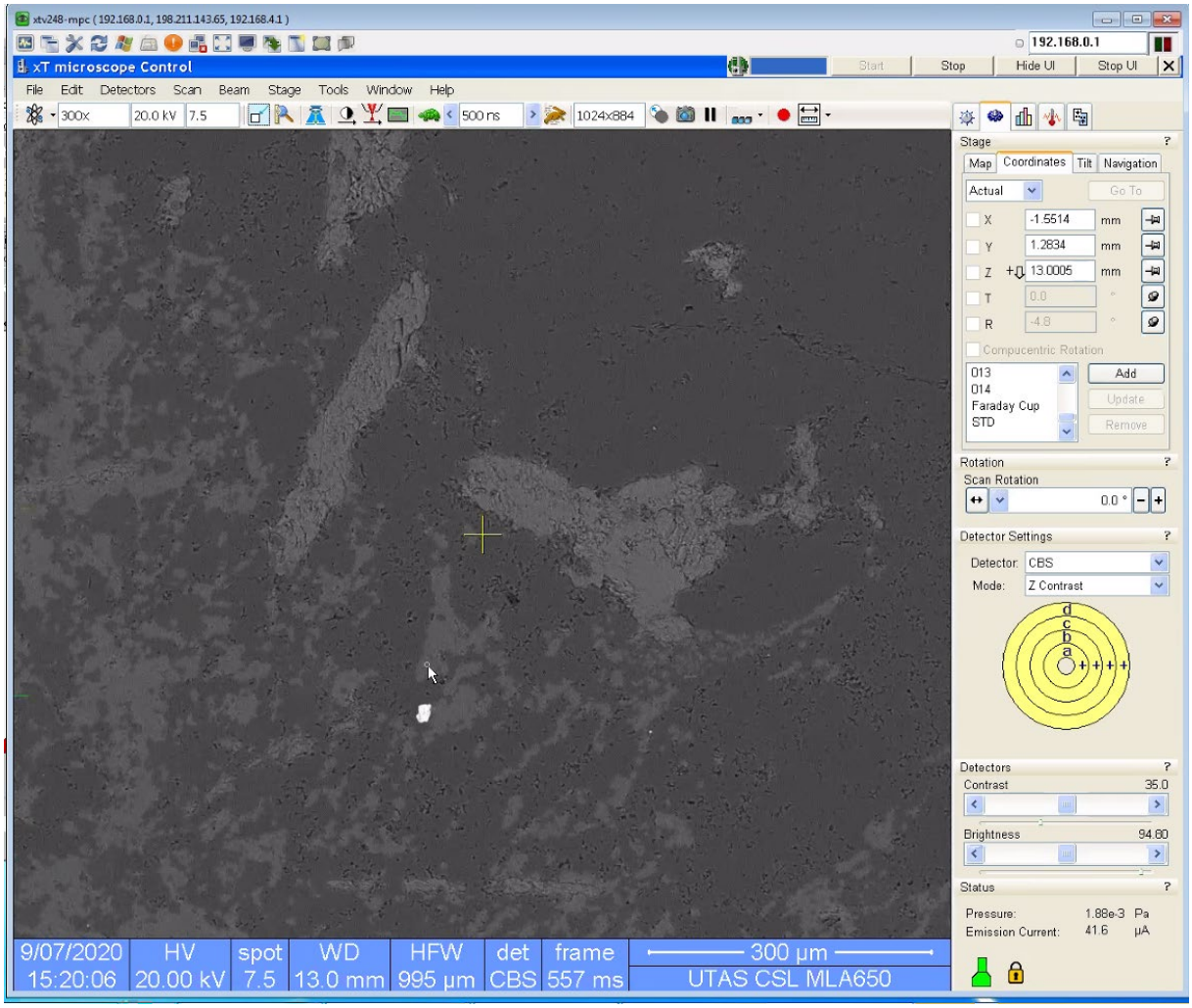

Figure A3.4. SEM control interface showing a backscatter image and the detector settings.

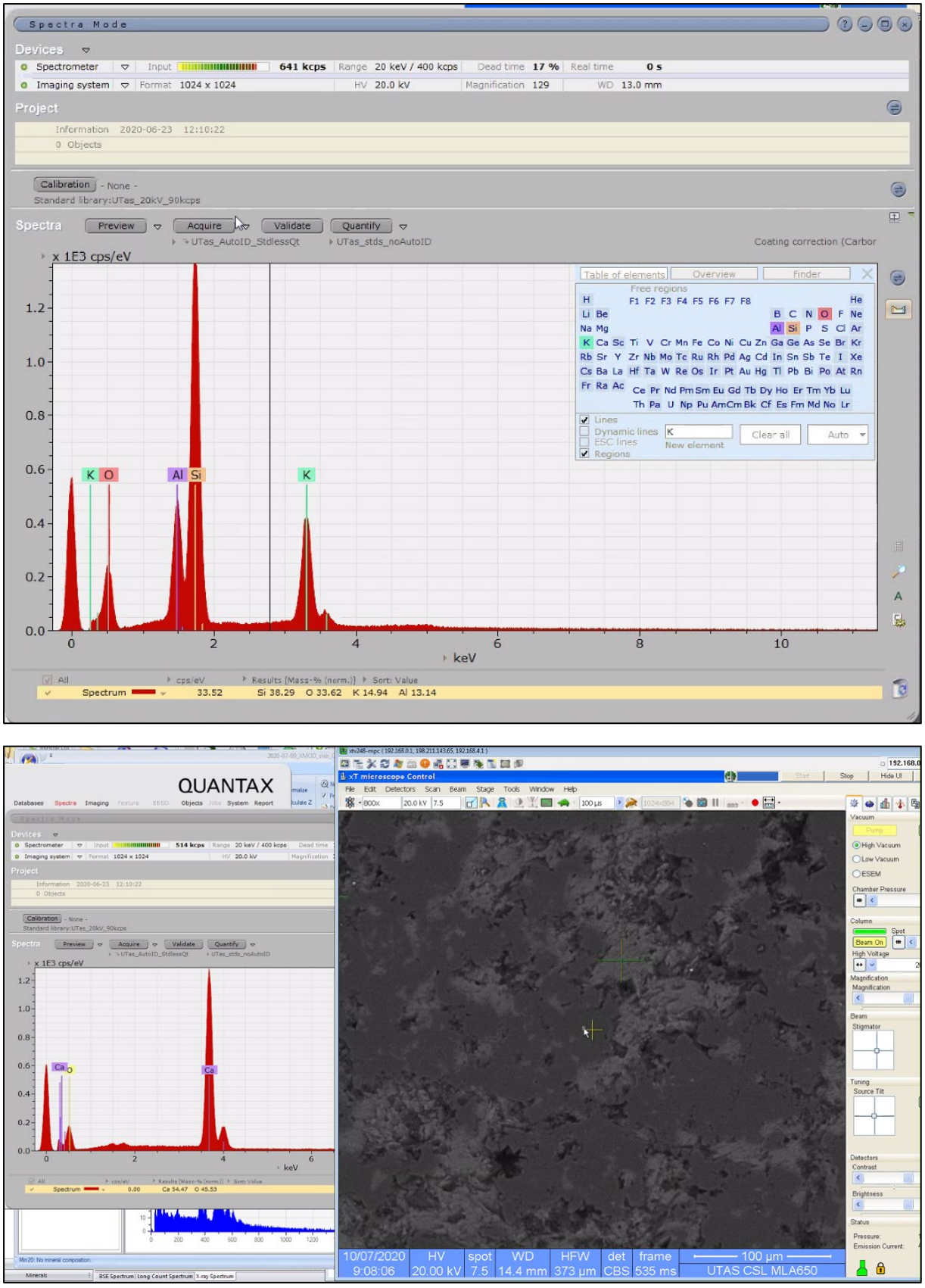

Figure A3.5. SEM spectral interfaces showing an X-ray energy spectrum (top image and at the left of the bottom image) of the current spot on a backscatter image (on the right).

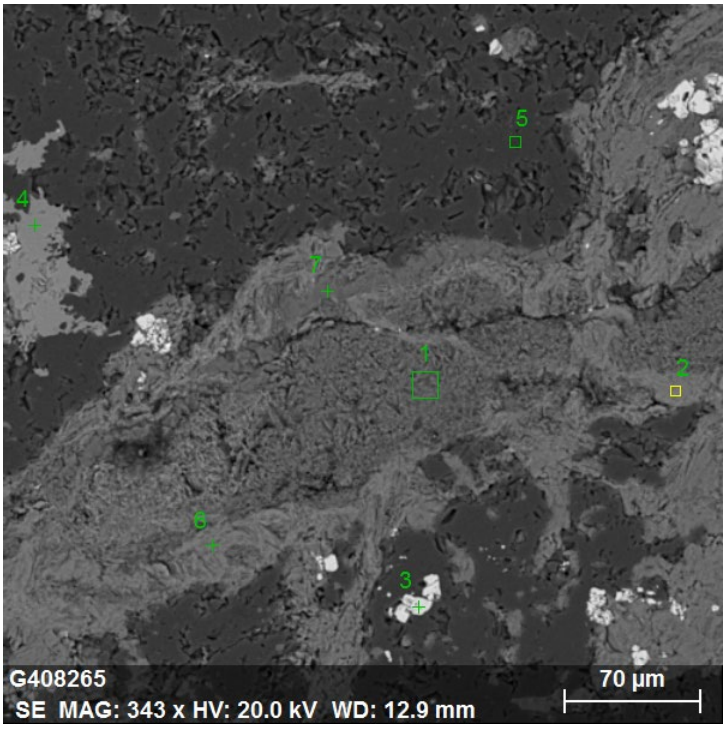

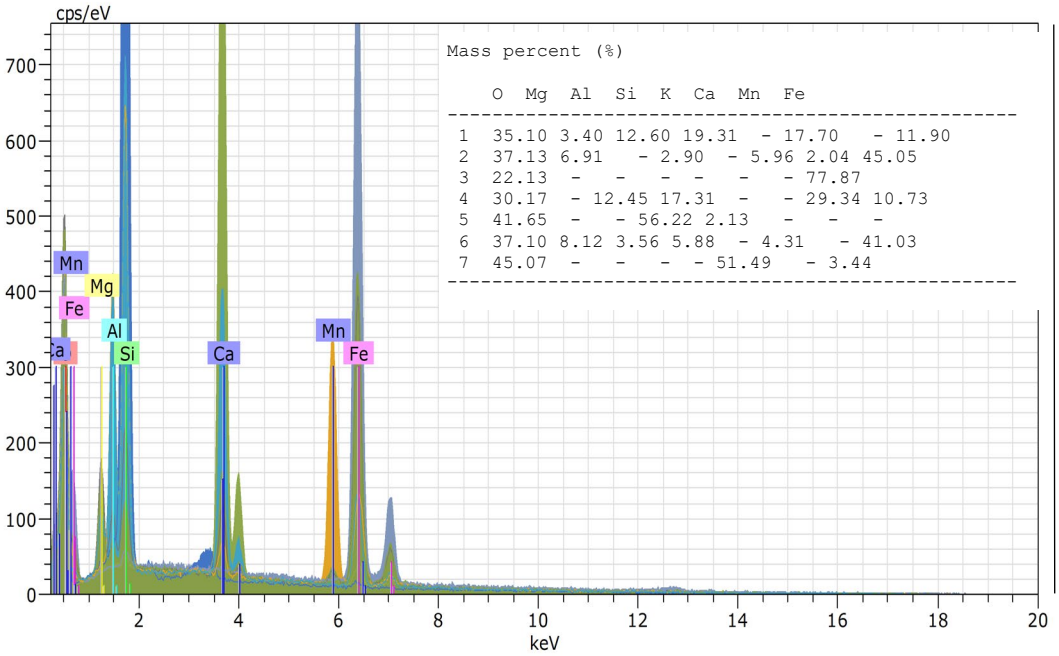

Figure A3.6. SEM spectral interface showing the results of several X-ray spectra located in the BSE image.

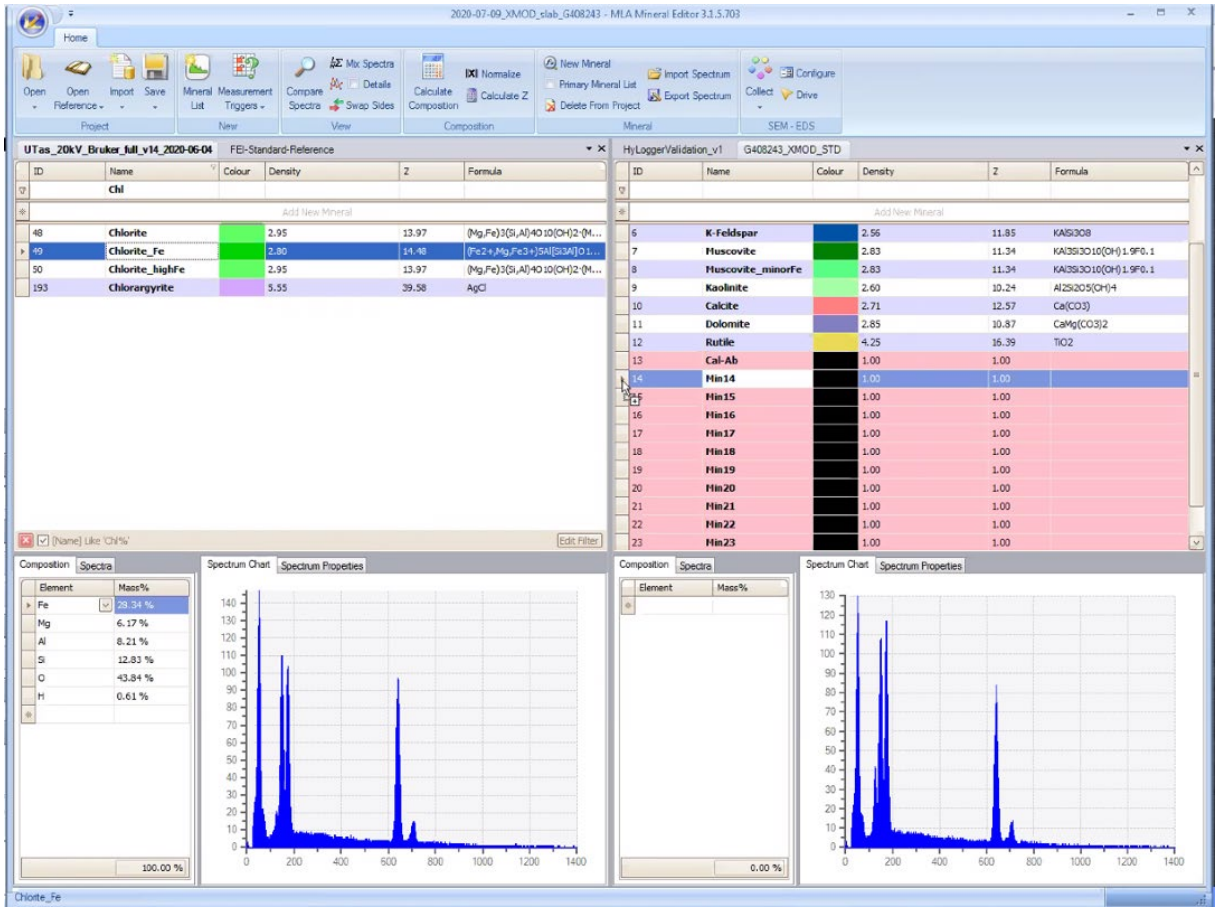

Figure A3.7. XMOD mineral editor interface showing the X-ray energy spectrum of a chlorite from the standard library minerals on the left and a comparable candidate spectrum from the sample on the right. The interface is used before MLA scanning to build a working library of mineral X-ray spectra for the sample, but the library is finalised (or completely built from scratch) after scanning. All of the data acquired in the MLA are retained for some time by the laboratory, enabling complete re-processing.

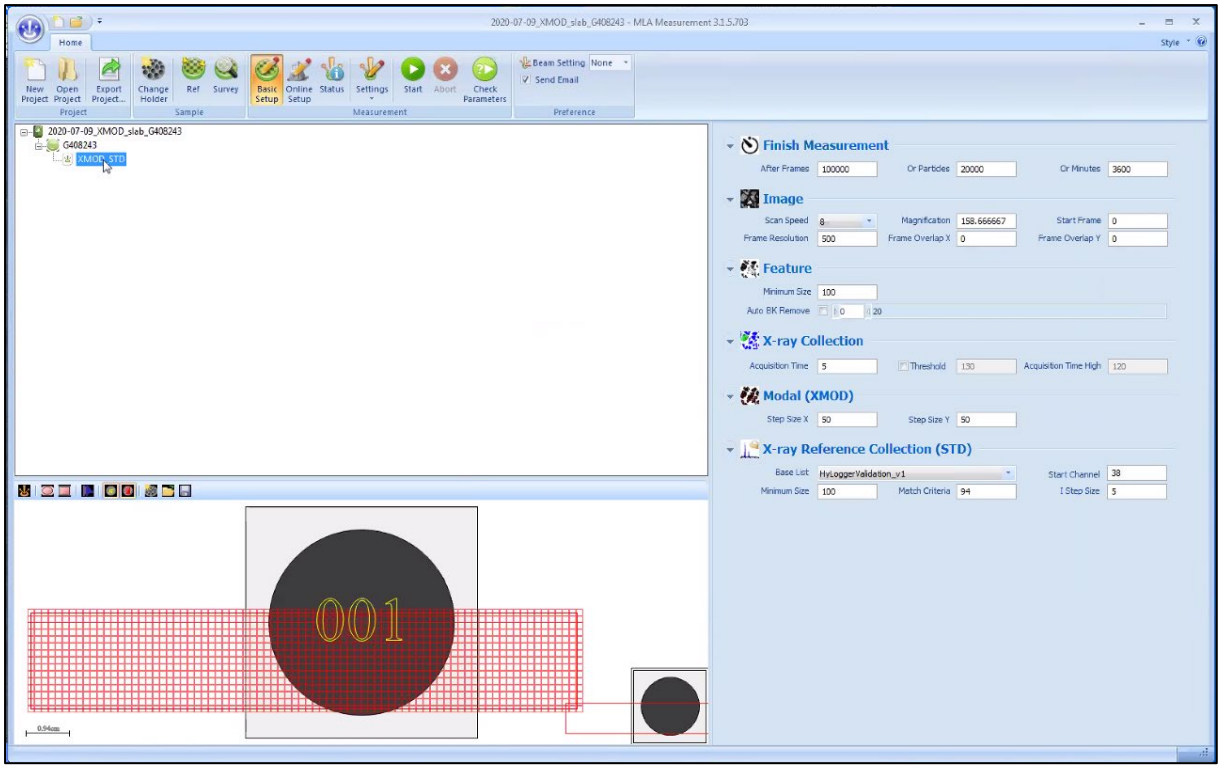

Figure A3.8. XMOD MLA measurement setup interface showing the settings for scanning a sample, including backscatter image resolution, X-ray acquisition time (5μs), point spacing (50 pixels) and the standard X-ray spectral library with matching threshold and step-out distances for instances when a match cannot be made (5 pixels).

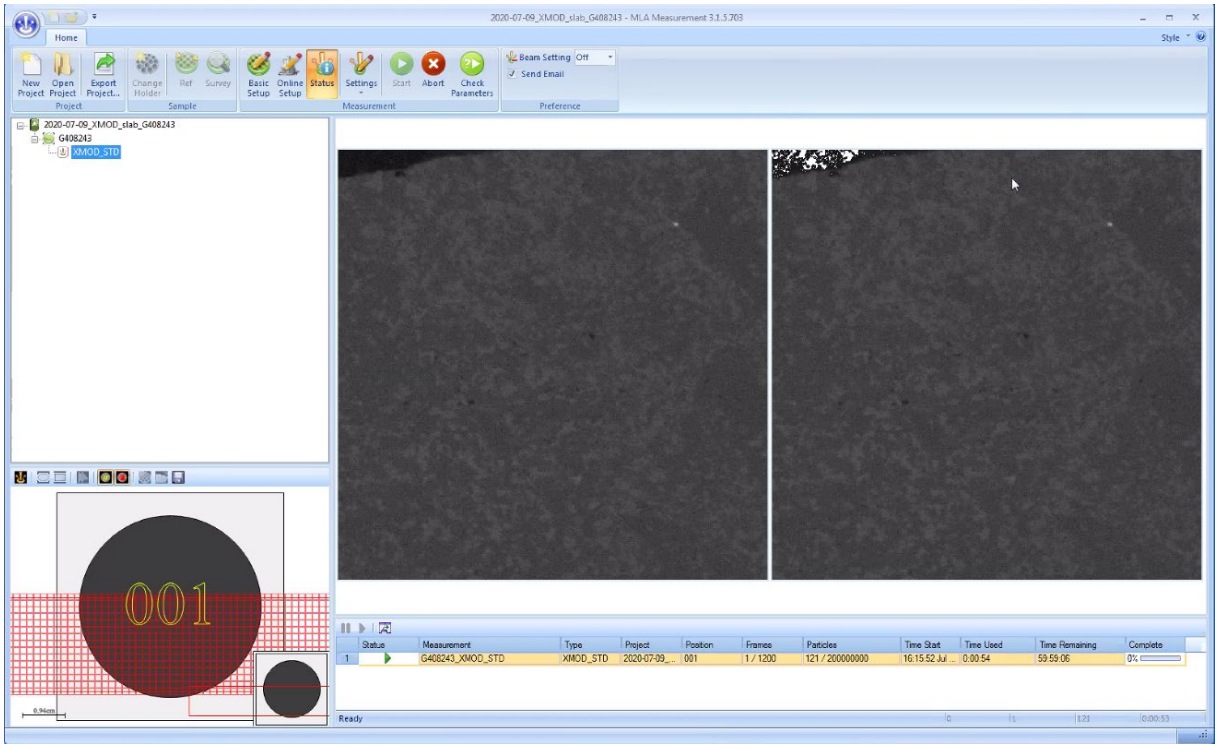

Figure A3.9. XMOD MLA measurement status window showing the current backscatter images and the location on a diagram of the scanning plan.

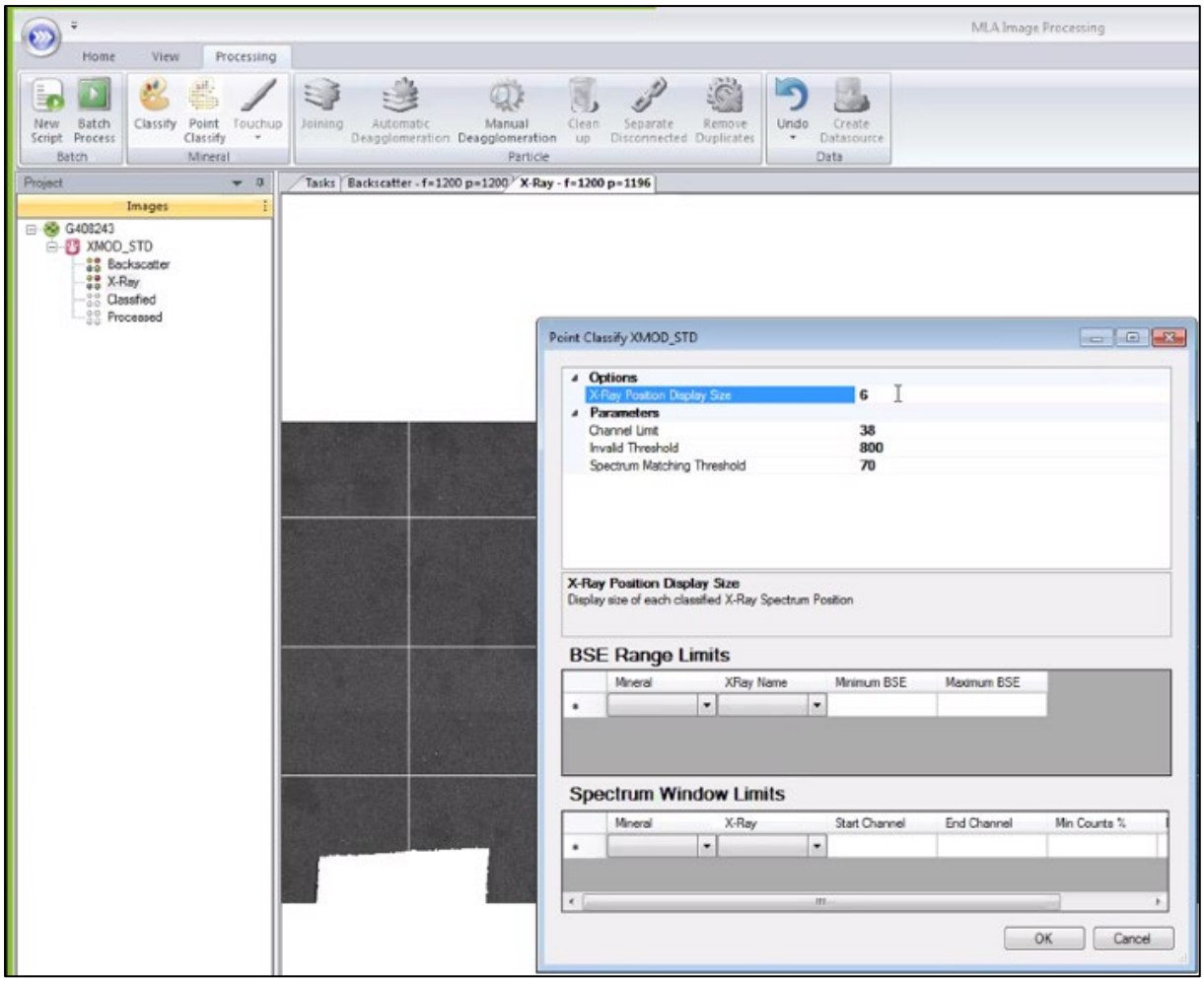

Figure A3.10. XMOD MLA image processing interface showing the workflow on the left (backscatter image, X-ray spectra, classified, processed) and the classification dialog featuring thresholds for classifying invalid spectra and matching to library spectra.

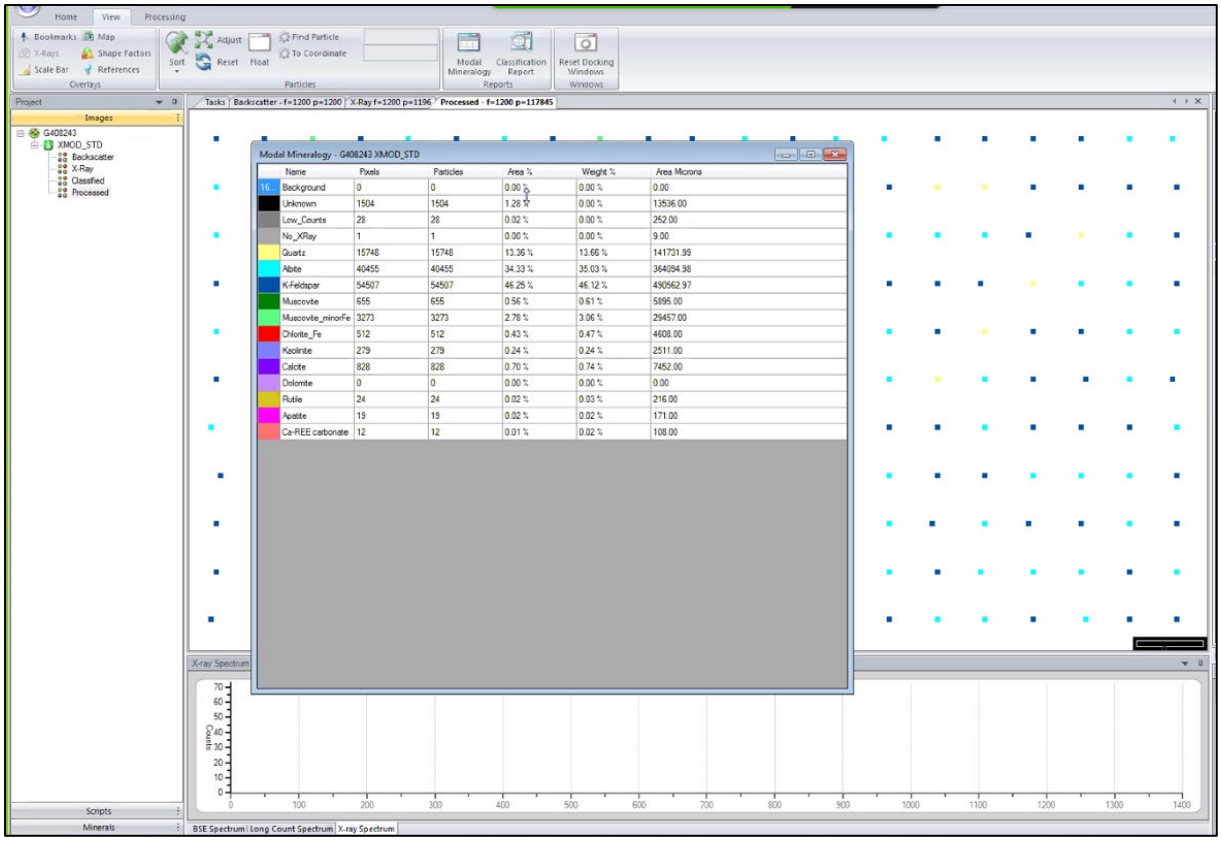

Modal Mineralogy - G408243 XMOD_STD

	Name	Pixels	Particles	Area %	Weight %	Area Microns
16...	Background	0	0	0.00 %	0.00 %	0.00
	Unknown	1504	1504	1.28 %	0.00 %	13536.00
	Low_Counts	28	28	0.02 %	0.00 %	252.00
	No_XRay	1	1	0.00 %	0.00 %	9.00
	Quartz	15748	15748	13.36 %	13.66 %	141731.99
	Albite	40455	40455	34.33 %	35.03 %	364094.98
	K-Feldspar	54507	54507	46.25 %	46.12 %	490562.97
	Muscovite	655	655	0.56 %	0.61 %	5895.00
	Muscovite_minorFe	3273	3273	2.78 %	3.06 %	29457.00
	Chlorite_Fe	512	512	0.43 %	0.47 %	4608.00
	Kaolinite	279	279	0.24 %	0.24 %	2511.00
	Calcite	828	828	0.70 %	0.74 %	7452.00
	Dolomite	0	0	0.00 %	0.00 %	0.00
	Rutile	24	24	0.02 %	0.03 %	216.00
	Apatite	19	19	0.02 %	0.02 %	171.00
	Ca-REE carbonate	12	12	0.01 %	0.02 %	108.00

Figure A3.11. XMOD MLA image processing interface showing results of classification, with a summary modal mineralogy table in the foreground (and below) and a high magnification classification image of the scanning raster in the background.

Appendix 4. Spatial analysis of Sample G408243

Robert Reid

Aim

XMOD data includes mineral classification together with spatial information, which can be combined to build thematic maps of sample mineralogy. Sample G408243 was selected for developing a workflow and initial spatial analysis.

Data wrangling

Supplied was a .CSV file with XY coordinates and mineral classifications. The XY values were in micrometers. The origin (XY = 0) was the centre of the sample stage (so somewhere in the middle of the sample). X values increase from left to right (West to East), Y from South to North. The source file G408243_XMOD_STD.csv was modified, removing line spaces and the data hungry field "SpectrumFileName" resulting in G408243_XMOD_STD1.xlsx for Mapinfo georeferencing.

XMOD results for sample G408243.

Minerals Original	Count of Mineral Name
Albite	40455
Apatite	19
Calcite	828
Ca-REE carbonate	12
Chlorite_Fe	512
Kaolinite	279
K-Feldspar	54507
Muscovite	655
Muscovite_minorFe	3273
Quartz	15748
Rutile	24
Unknown	1504
Grand Total	117816

Georeferencing XMOD data

The points were projected as a Non Earth coordinate system with millimetre units (which are actually μm in the sample).

Georeferencing bounds for the plot were determined by calculating descriptive statistics in Excel, then allowing an extra (+/-10% + rounding to the nearest 100) bounding edge to accommodate BSE sample edges outside the mineral sample point bounds. The sample was evidently located somewhat "west" and well "south" of the sample stage center.

	Xray_X	*Xray_Y*	*BSE*	*TotalCounts*	*MatchScore*
Mean	-11975.3	-7991.73	79.05902	2590.51027	96.66653308
Standard Error	101.2452	18.73374	0.037789	0.525594834	0.033458959
Median	-12105	-7907	80	2613	99.43239897
Mode	-19615	2436	82	2630	0
Standard Deviation	34751.75	6430.23	12.97092	180.4069335	11.48456529
Sample Variance	1.21E+09	41347860	168.2448	32546.66164	131.8952398
Kurtosis	-1.21348	-1.18495	1.719407	7.325490553	61.13858073
Skewness	-0.00769	-0.01433	-0.40539	-1.633809901	-7.647580196
Range	119786	22336	221	2659	99.99999941
Minimum	-72080	-19300	14	814	0
Maximum	47706	3036	235	3473	99.99999941
Sum	-1.4E+09	-9.4E+08	9314418	305203558	11388864.26
Count	117816	117816	117816	117816	117816

Georeferencing associated images

The mapped XMOD data provided points for georeferencing the associated BSE image and mineral classification images (G408243_XMOD_STD_BSE_SAMPLE.tif and G408243_XMOD_STD_MINERAL_SAMPLE.tif). Combining these images effectively replicated the BSE image overlain with points coloured to match the mineral colour legend (Mineral_colour_legend_v1.tif) as supplied by the SEM analyst (G408243_overlay.png).

Notably the resolution of the Mineral Sample image was very high, allowing the near exact location of sample points to be selected during georeferencing.

Figure A4.1. Mineral Colour legend

Mineral maps

MLA data points were re-sized to build a continuous map image to illustrate mineral distribution. The initial plot of Albite revealed a streaked pattern, likely related to symbology aliasing. A plot of Albite and K-Feldspar also shows these features, but adding Chlorite_Fe removed them (Figure A4.2). Zooming in on the features removes the effect, confirming that the phenomenon is a software induced artefact (or possibly a charging issue in the SEM).

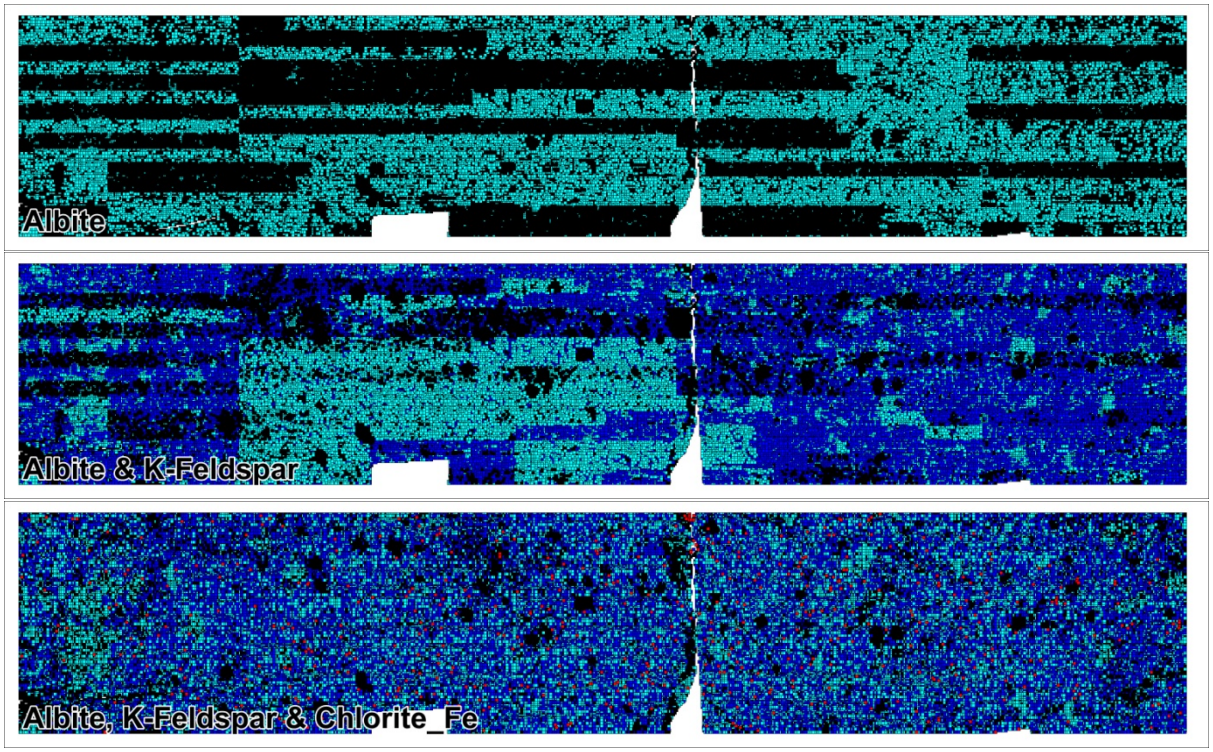

Figure A4.2. Maps of Albite, Albite and K-Feldspar and Albite, K-Feldspar and Chlorite_Fe. The colour legend is Figure A4.1.

When white mica and kaolin are added, a smear zone obvious in the BSE image is revealed (lower left of Figure A4.3). The smear is discussed further in Appendix 5. The smear largely plots as Muscovite (dark green), whereas Muscovite_minorFe (pale bright green) is more even and widespread. Kaolinite similarly appears to mimic the Muscovite smear with a further cluster in the top right.

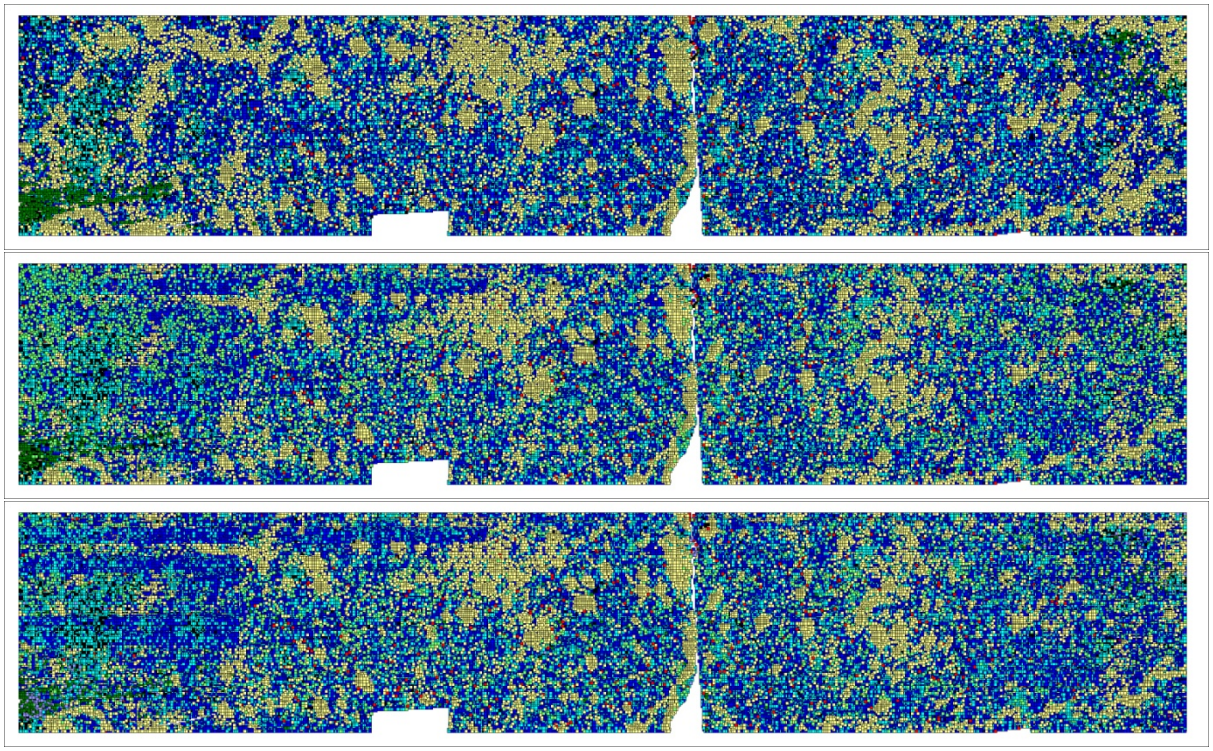

Figure A4.3. Maps highlighting Muscovite (green in top), Muscovite_minorFe (pale bright green) and Kaolinite (mauve in bottom).

When carbonate is added, the mineral map does not visually change, but when the occurrences of calcite are enhanced, the image reveals that calcite is commonly localised in veins (Figure A4.4).

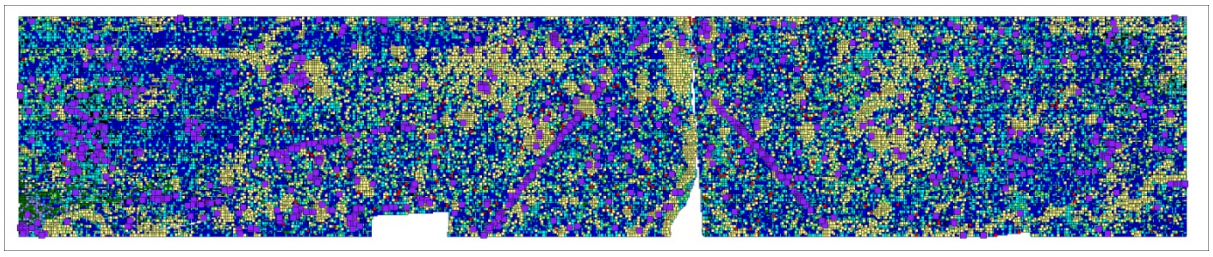

Figure A4.4. Map of all minerals, but enhancing Calcite (purple). Calcite is concentrated in planar veins.

A final map showing all minerals illustrates a fairly homogeneous texture (Figure A4.5).

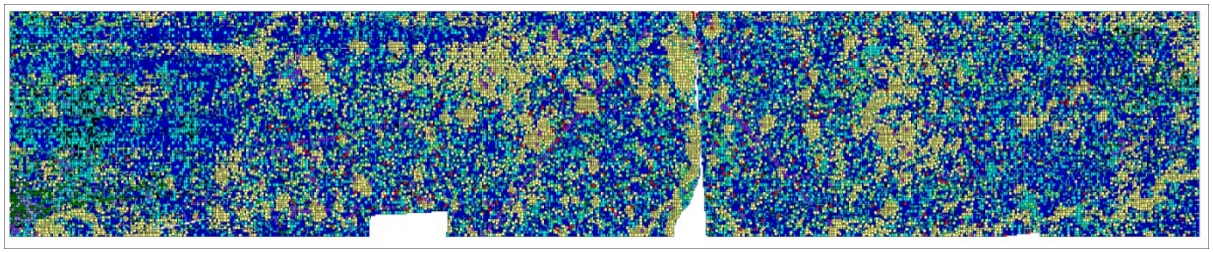

Figure A4.5: Final point MLA image. The colour legend is Figure A4.1.

Uncertainty maps

Nearest neighbour gridded plots of BSE image intensity, total X-ray counts and match score provide information relating to mineral reliability or confidence across the sample (Figure A4.6).

Total Counts are higher in the central west and lower at the west and east edges, due to inaccuracy in mounting a level sample, leading to variation in the sample distance. Total Counts are very low over the smear, suggesting that the smear interfered with the penetration of electrons or X-rays

Surprising variability in match score is evident with lower scores in the northern and outer west and east areas. More highly matched scores are focused across the southern part of the map.

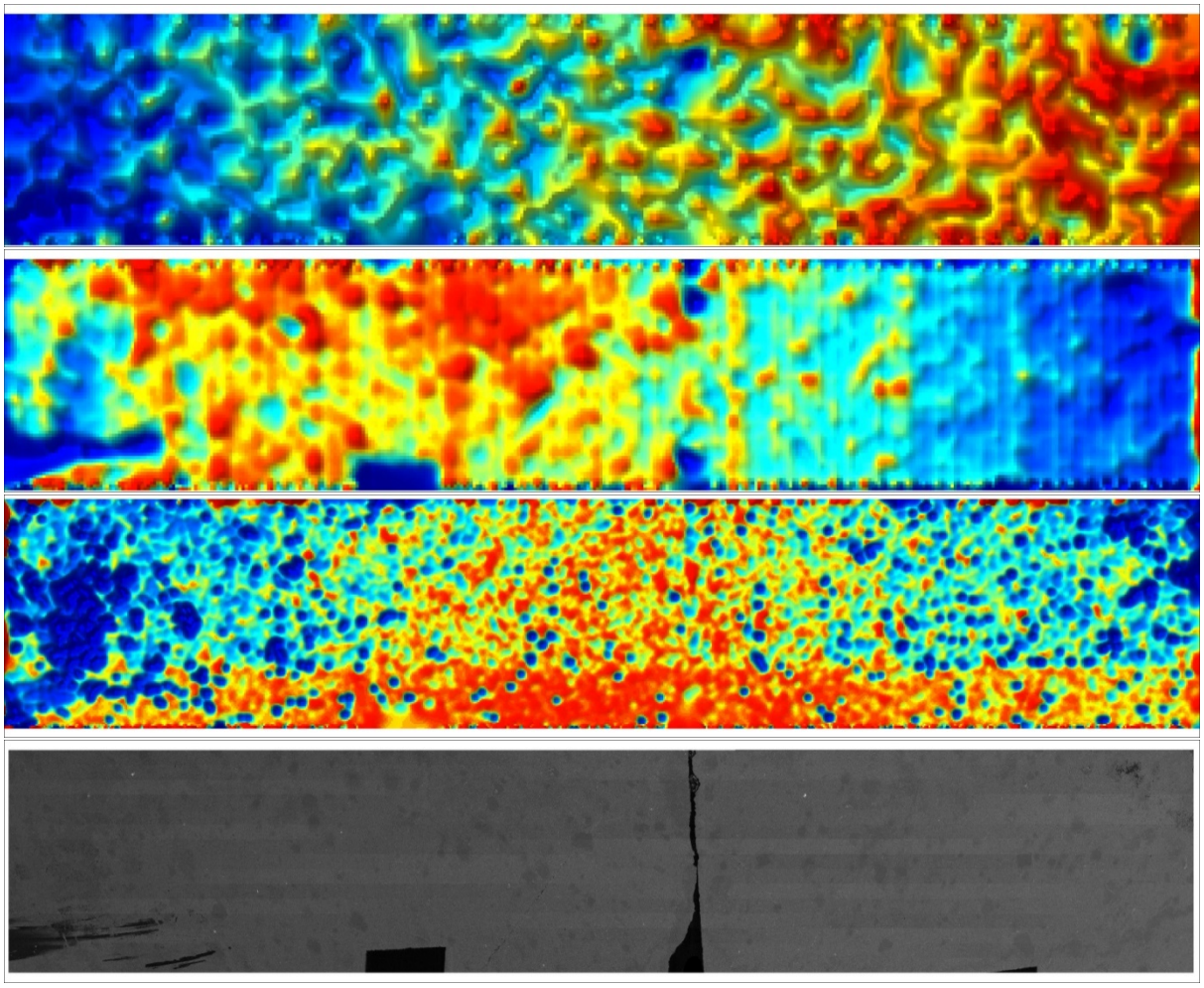

Figure A4.6. Nearest neighbour grids of BSE (top), Total_Counts, MatchScore and the BSE image (bottom).

Appendix 5. Investigation of removing smear on G408243

Robert Reid

Sample G408243 appeared to have a smear on the polished and carbon-coated surface. The mineralogy interpreted for the smeared areas appeared to differ from the adjacent un-smeared sample, with anomalously greater muscovite and a higher proportion of 'unknown'. This section describes a study to examine the effect of masking the smear on the XMOD results. It is a useful exercise to establish a masking workflow, calculate the effects on mineral proportions and highlights the usefulness of quantified uncertainty in the XMOD results.

Standard XMOD results provide point counts and derived area percentage and weight percentage (Table A5.1).

Behind the standard results is information that allows count statistics to be calculated at various uncertainty thresholds. Using >95 and >97.5% and >99% thresholds results in progressively more matching failures (resulting in unknowns), but little change in the mineral percentages (Table A5.2). This provides confidence in the standard statistics provided by the analyst.

Mineral	Wt%	Area%	Point Count
Unknown	0.00	1.28	1504
Low_Counts	0.00	0.00	0
No_XRay	0.00	0.00	0
Quartz	13.66	13.37	15748
Albite	35.03	34.34	40455
K-Feldspar	46.12	46.26	54507
Muscovite	0.61	0.56	655
Muscovite_minorFe	3.06	2.78	3273
Chlorite_Fe	0.47	0.43	512
Kaolinite	0.24	0.24	279
Calcite	0.74	0.70	828
Dolomite	0.00	0.00	0
Rutile	0.03	0.02	24
Apatite	0.02	0.02	19
Ca-REE carbonate	0.02	0.01	12
Total	100.00	100.00	117816

Table A5.1.
Summarised XMOD results for G408243 as provided by the SEM analyst. (Data Source: G408243_XMOD_STD, Mineral Groupings: Ungrouped, Filter: Unfiltered)

MLA Mineral	Count of Mineral Name (ALL)	% of Mineral Name (ALL)	Count of Mineral Name (>95% Match Score)	% of Mineral Name (>95% Match Score)	Count of Mineral Name (>97.5% Match Score)	% of Mineral Name (>97.5% Match Score)
Albite	40455	34.34	36401	36.31	31423	36.27
Apatite	19	0.02	10	0.01	5	0.01
Calcite	828	0.70	513	0.51	422	0.49
Ca-REE carbonate	12	0.01	8	0.01	6	0.01
Chlorite_Fe	512	0.43	473	0.47	397	0.46
Kaolinite	279	0.24	138	0.14	45	0.05
K-Feldspar	54507	46.26	46078	45.96	39760	45.89
Muscovite	655	0.56	457	0.46	350	0.40
Muscovite_minorFe	3273	2.78	2468	2.46	1719	1.98
Quartz	15748	13.37	13685	13.65	12490	14.42
Rutile	24	0.02	21	0.02	16	0.02
Unknown	1504	1.28				
Grand Total	117816		**100252**		**86633**	

Table A5.2
XMOD statistics for G408243 for various match scores.

Removing the smear

The aim was to re-calculate MLA mineral proportions after masking out the smear and the join between the 2 sample pieces. The task utilised the spreadsheet detailing x, y and matched mineral with the backscatter electron image (BSE) where obvious dark zones were the key basis for masking.

Stage 1 masking: Removal based on the BSE dark zones image and strong clusters of 'unknown' mineral. Muscovite clusters were another guide with strong spatial correlation with the dark zones.

Removed by analyst

Points removed as part of standard MLA processing fall in zones of low match score. Most zones featured partial removal, but one zone (centre east) was nearly totally removed via a mineral match to "?"(known mineral library).

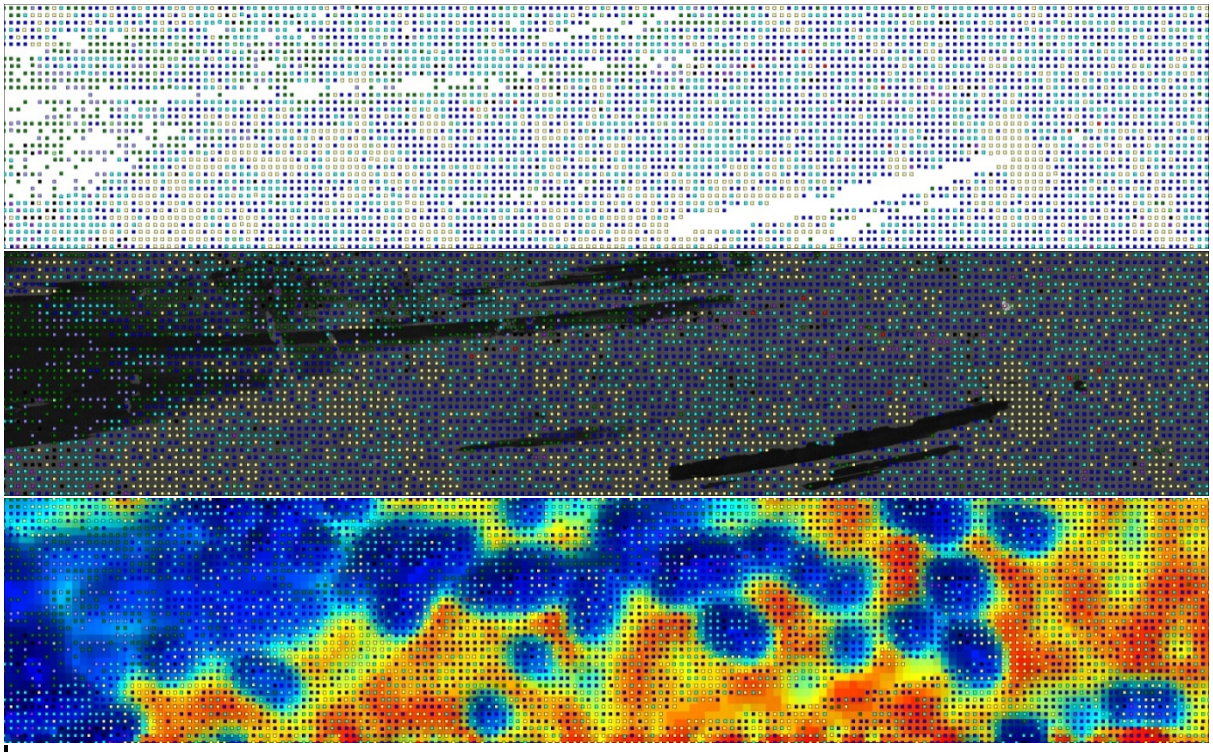

Figure A5.1. MLA Sample points (top), overlain on SEM (middle) and MatchScore (bottom). MLA mineral points have been selectively removed from zones of strong smearing in the east and especially in the southern middle east.

Staged masking

Stage 1 masking: Removal of points in weaker smear zones and checking join and clamp masking

The SEM analyst had already removed sample points within the join and under the sample clamps, which included islands of spurious Chlorite-Fe. Checking by georeferencing the BSE image to the sample points indicated that the masking was accurate. Points were removed from the strongest smear zones based on the BSE image.

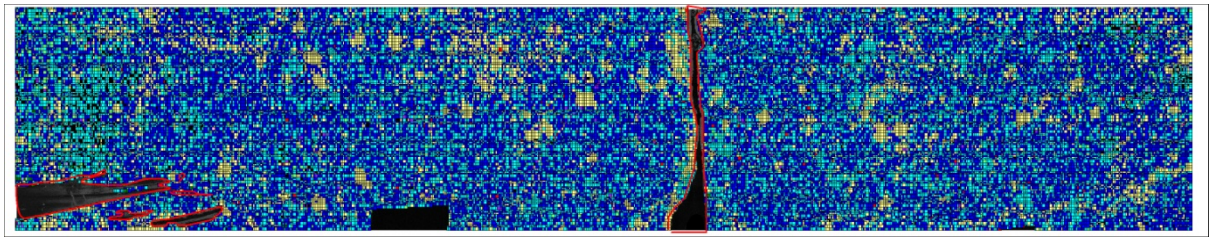

Figure A5.2. Stage 1 masking is shown in black, grey and outlined red.

Stage 2 masking: Removal of points in weaker smear zones.

Some areas of weaker smear appeared to correlate with more hackly textured mineral, and were linked to more obvious smearing by a very weak stripe effect.

Stage 3 masking: Completely remove all smear zone areas.

All muscovite and unknowns with <80% confidence were removed from the smeared areas.

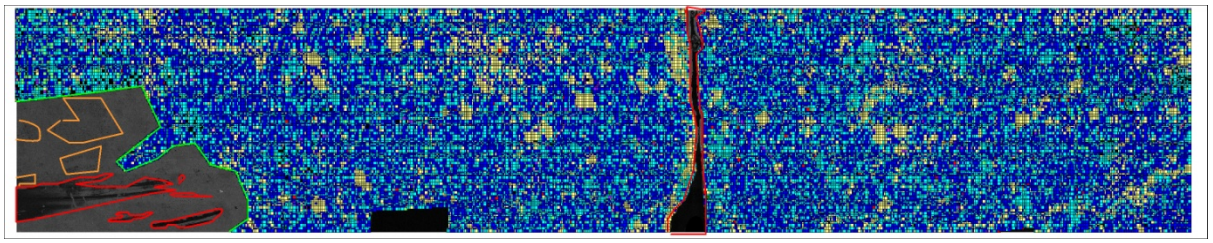

Figure A5.3. Stage 3 smear masking is shown in green, along with earlier stages (see Figure A5.4).

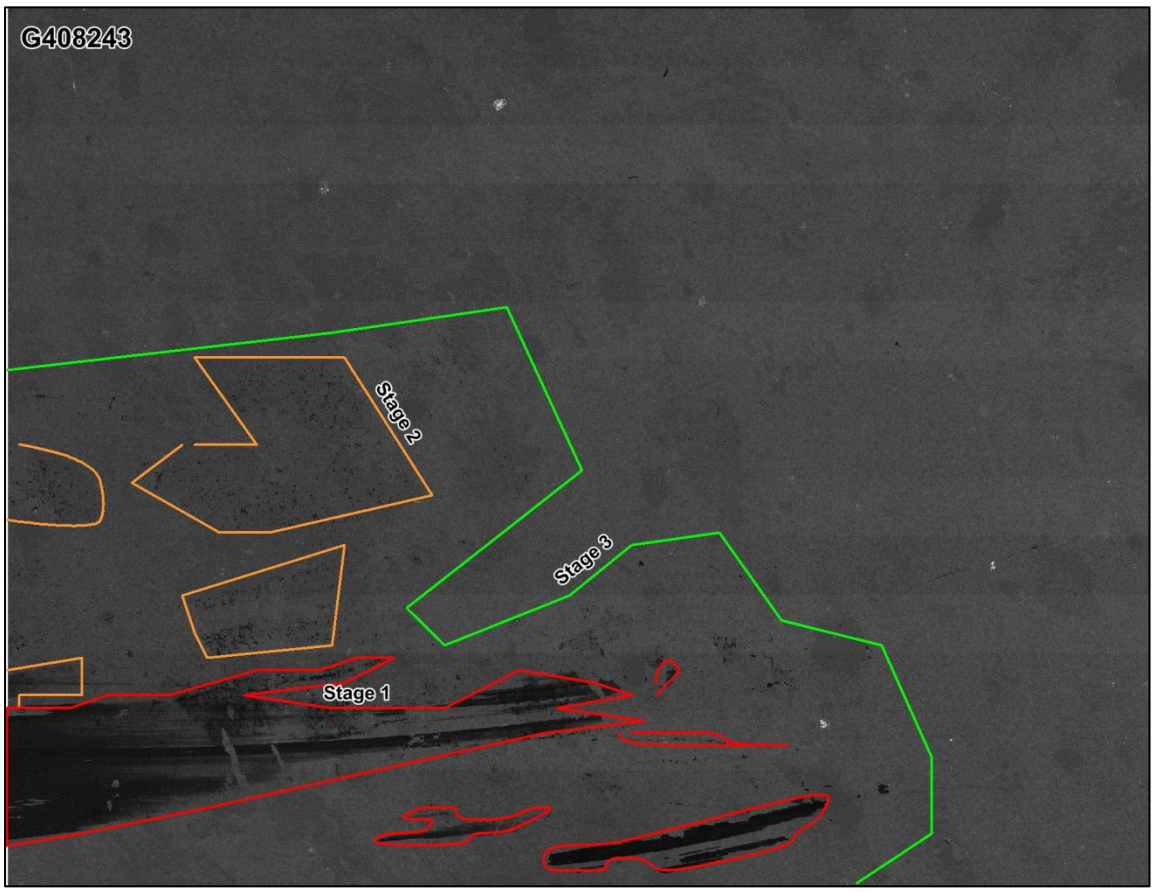

Figure A5.4. BSE image showing outlines of the 3 stages of smear removal.

Results

Mineral proportions did not change significantly as the 3 stages of masking progressed (Table A5.3).

Table A5.3. Recalculated Mineral % with progressive "Smear" removal.

Row Labels	Original	Stage 1	Stage 2	Stage 3
Albite	34.34%	34.46%	34.21%	34.35%
Apatite	0.02%	0.02%	0.02%	0.02%
Calcite	0.70%	0.69%	0.67%	0.66%
Ca-REE carbonate	0.01%	0.01%	0.01%	0.01%
Chlorite_Fe	0.43%	0.43%	0.43%	0.44%
Kaolinite	0.24%	0.13%	0.11%	0.10%
K-Feldspar	46.26%	46.64%	47.09%	47.49%
Muscovite	0.56%	0.23%	0.21%	0.17%
Muscovite_minorFe	2.78%	2.78%	2.78%	2.74%
Quartz	13.37%	13.35%	13.45%	13.14%
Rutile	0.02%	0.02%	0.02%	0.02%
Unknown	1.28%	1.25%	1.00%	0.85%

Appendix 6. BSE images

G408251

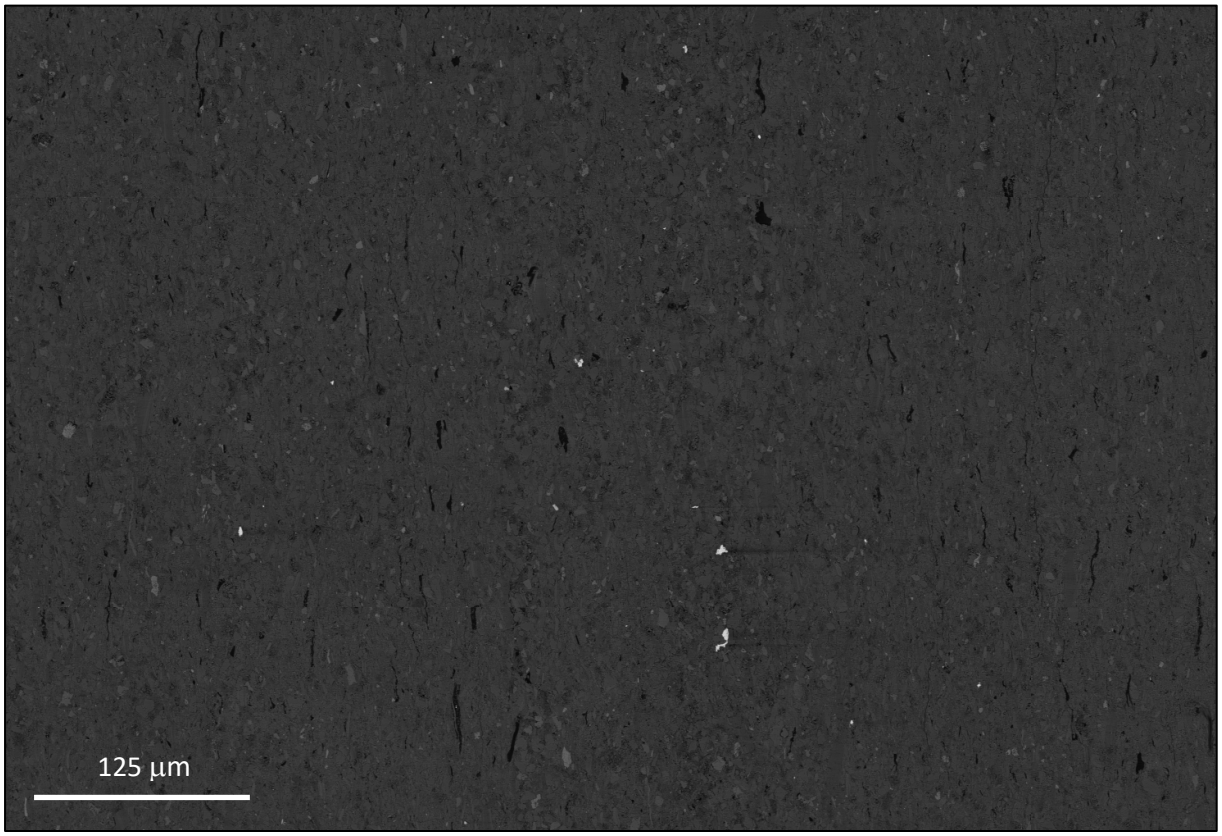

G408275

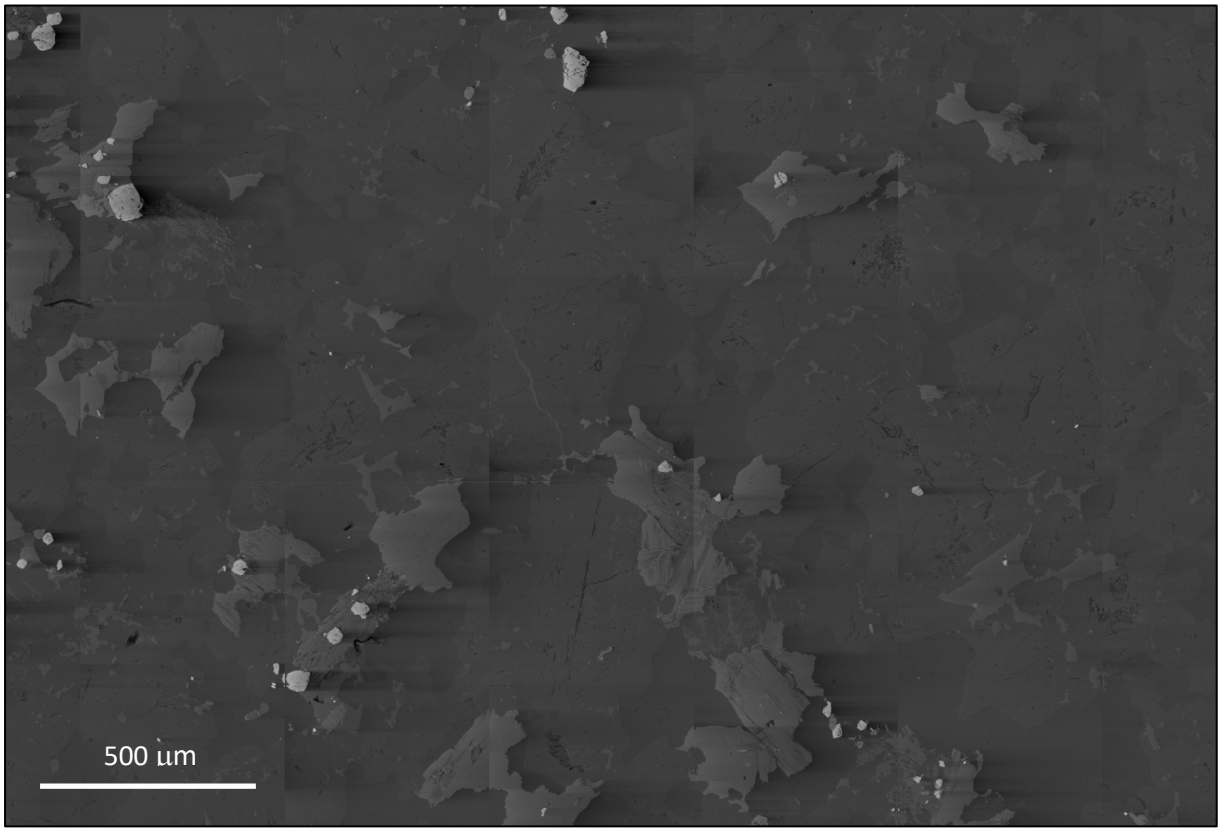

G408243

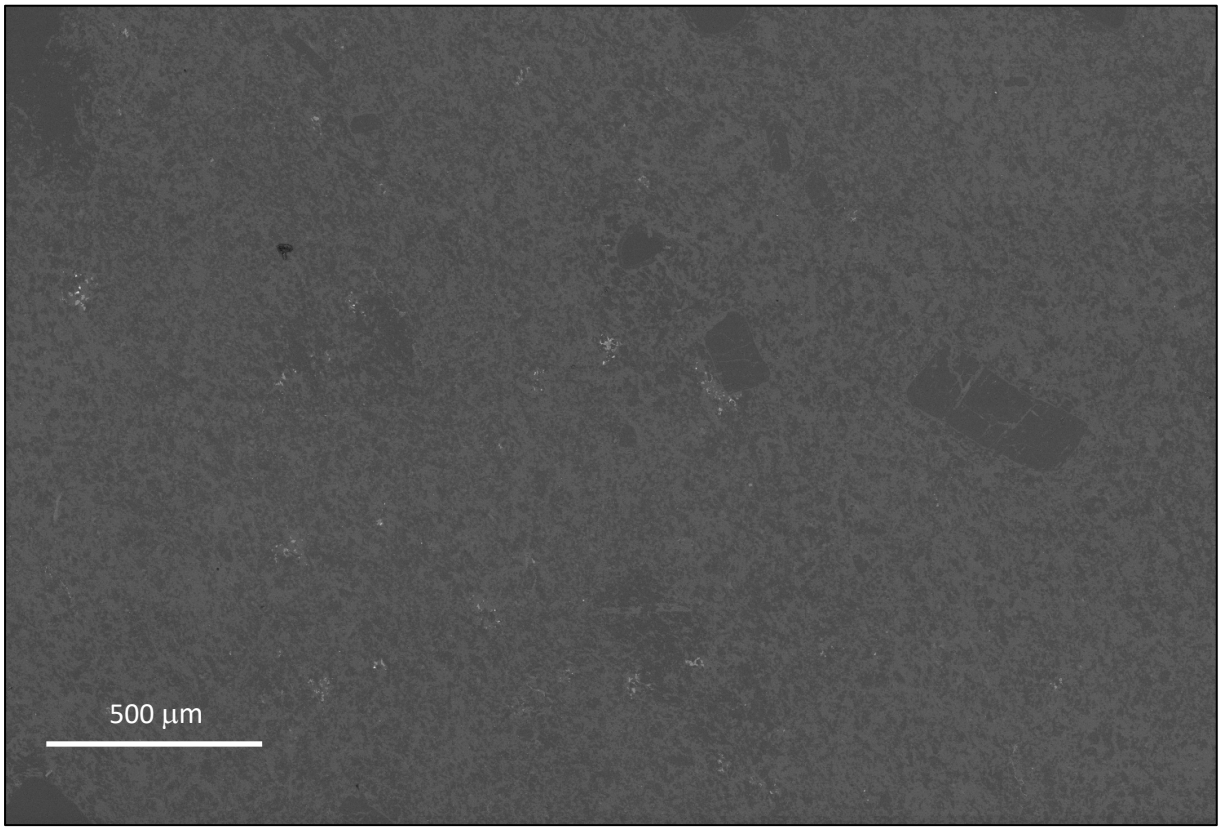

G408265

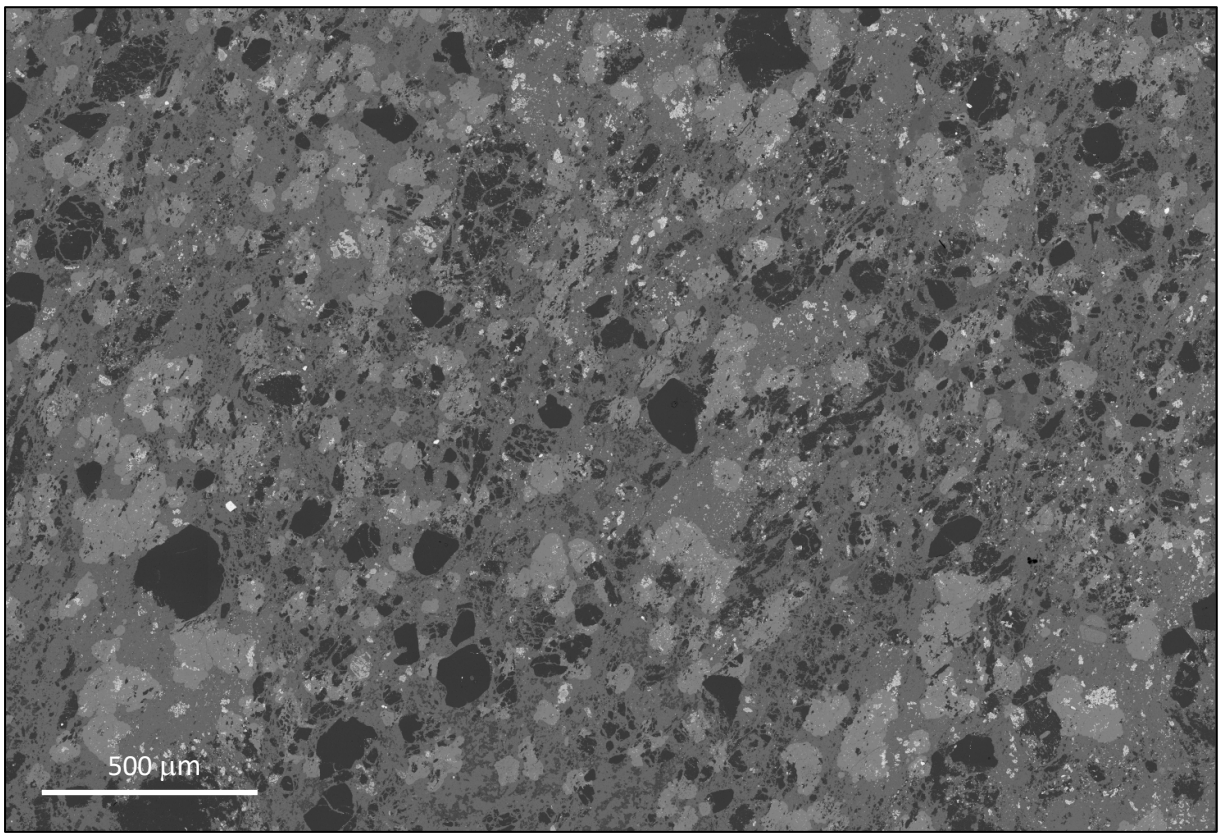

G408264

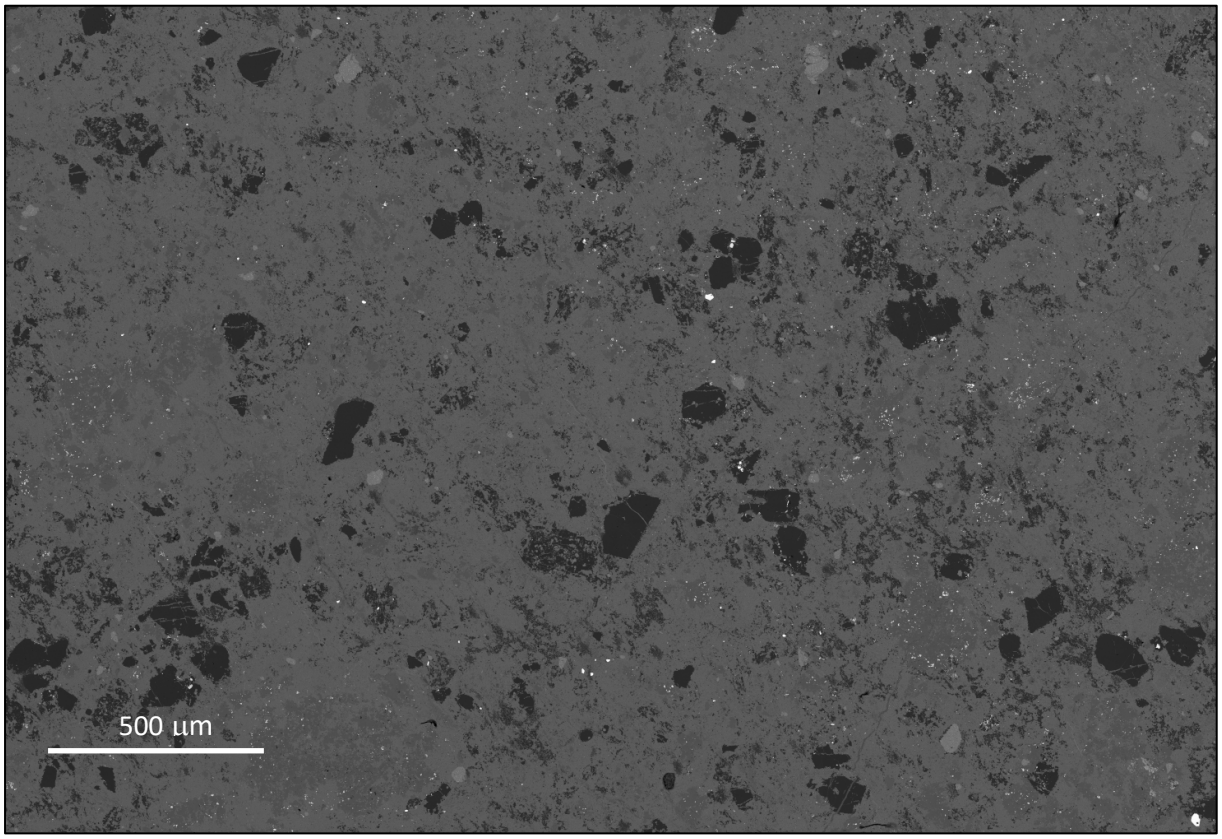

G408260

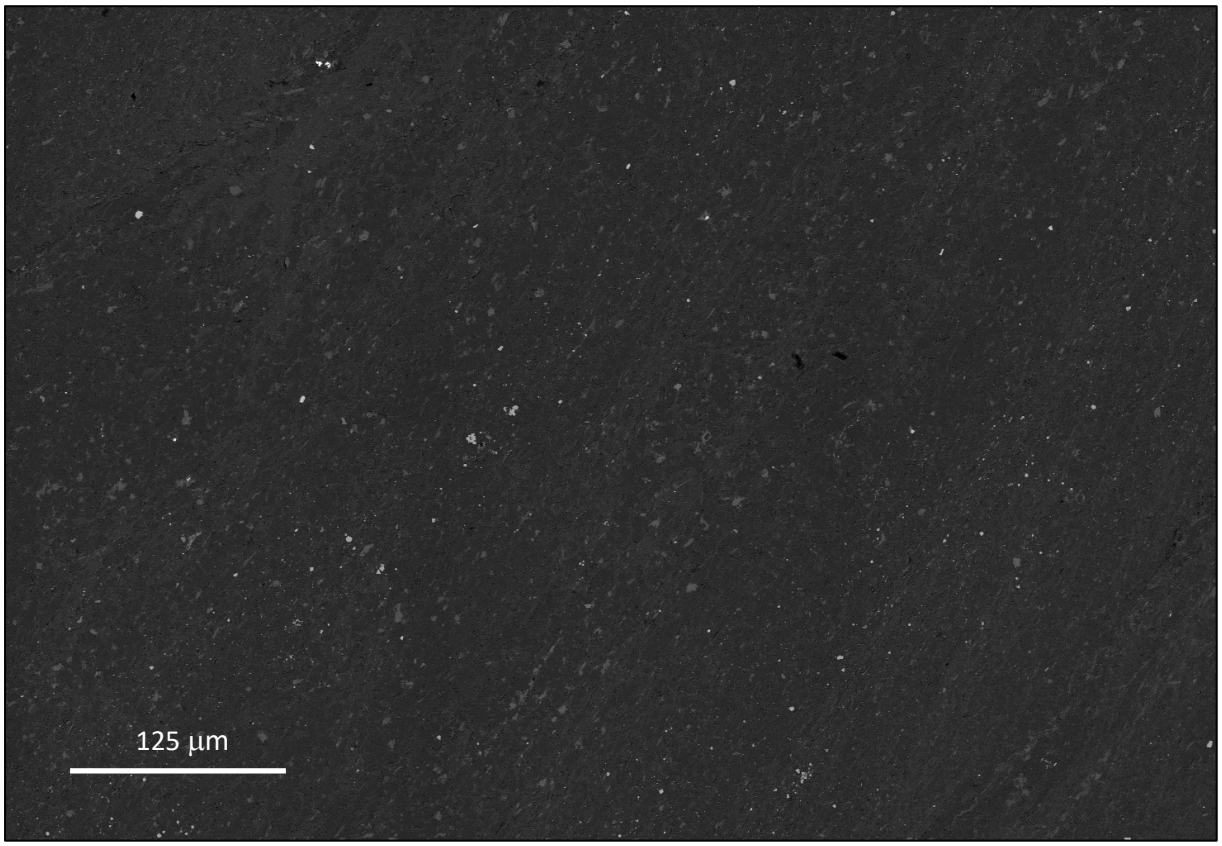

G408251

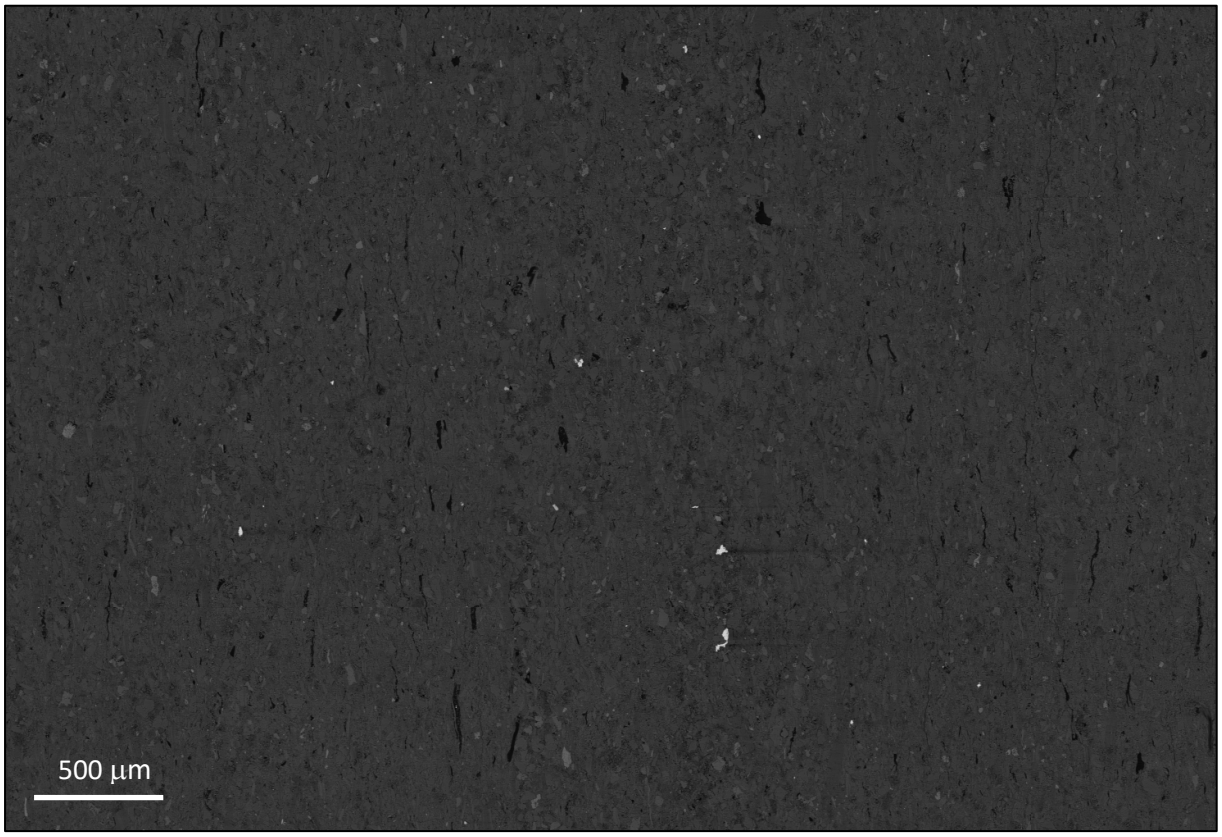

G408275

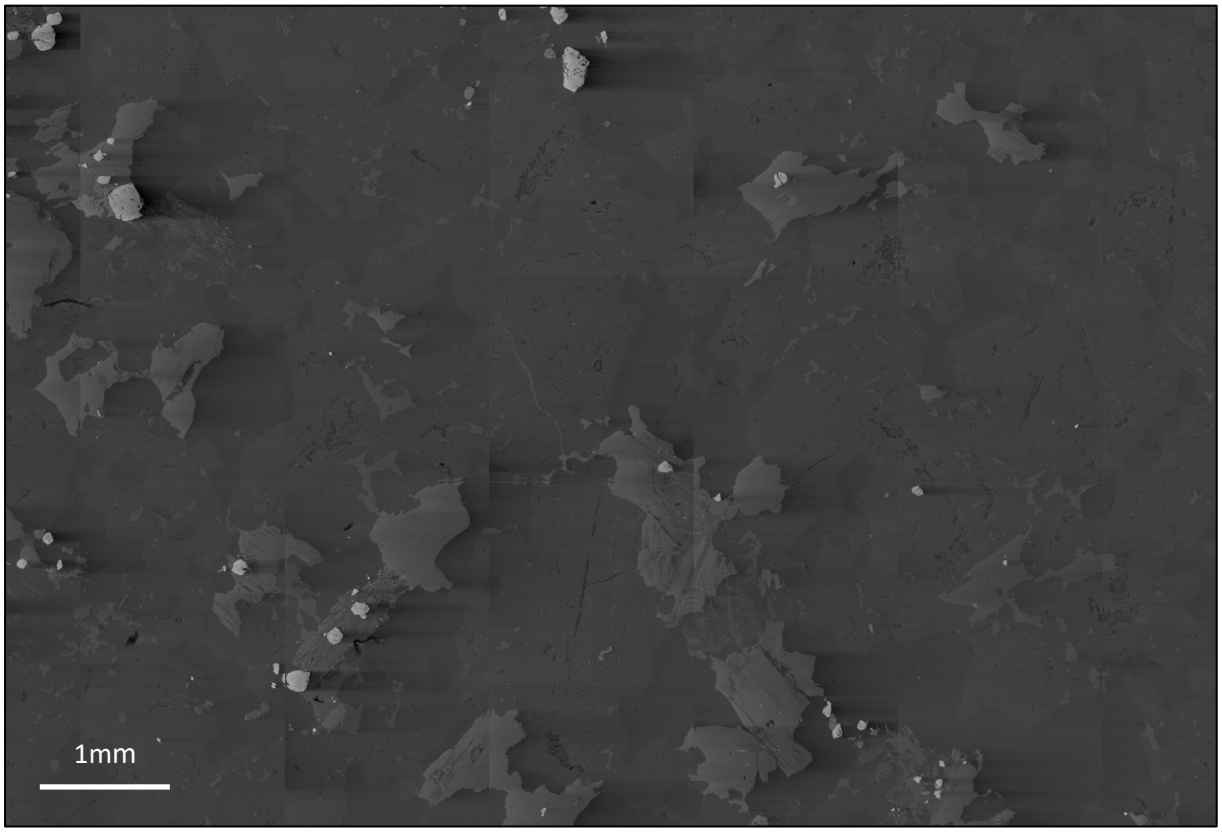

G408243

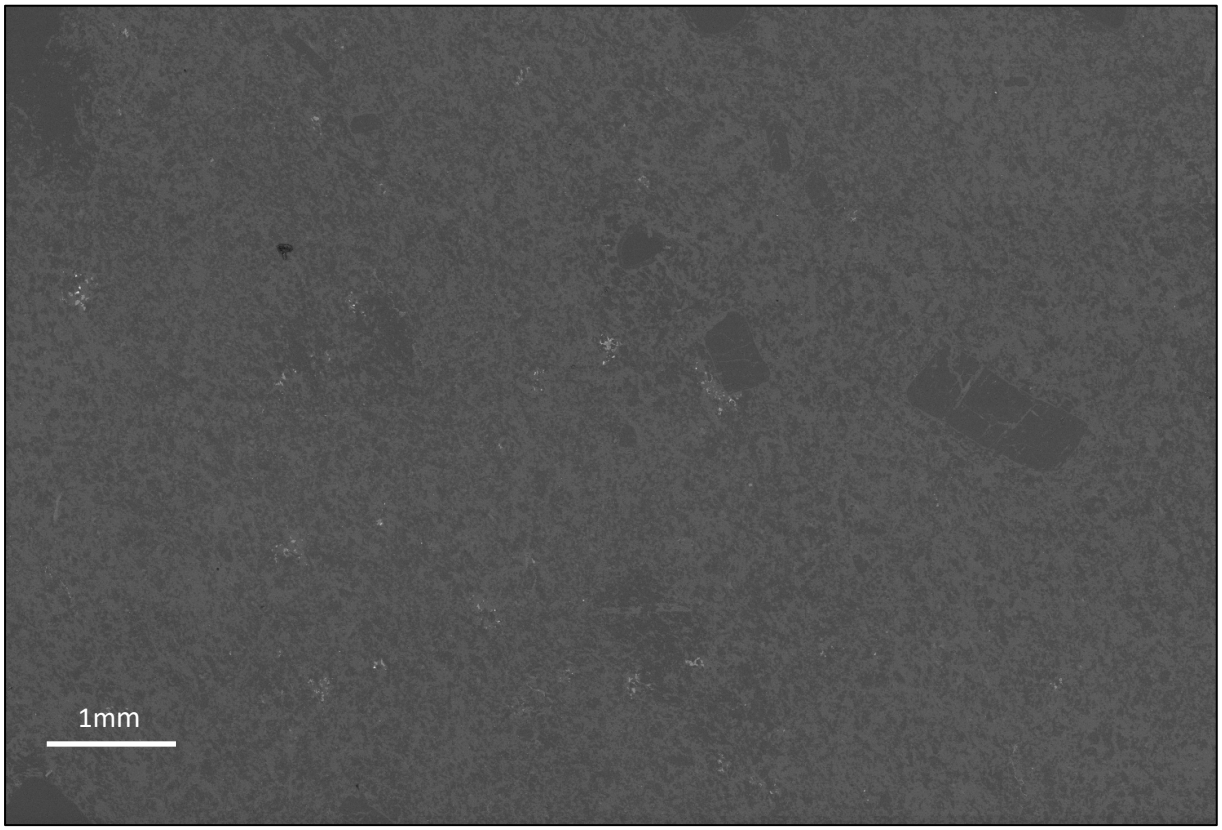

G408265

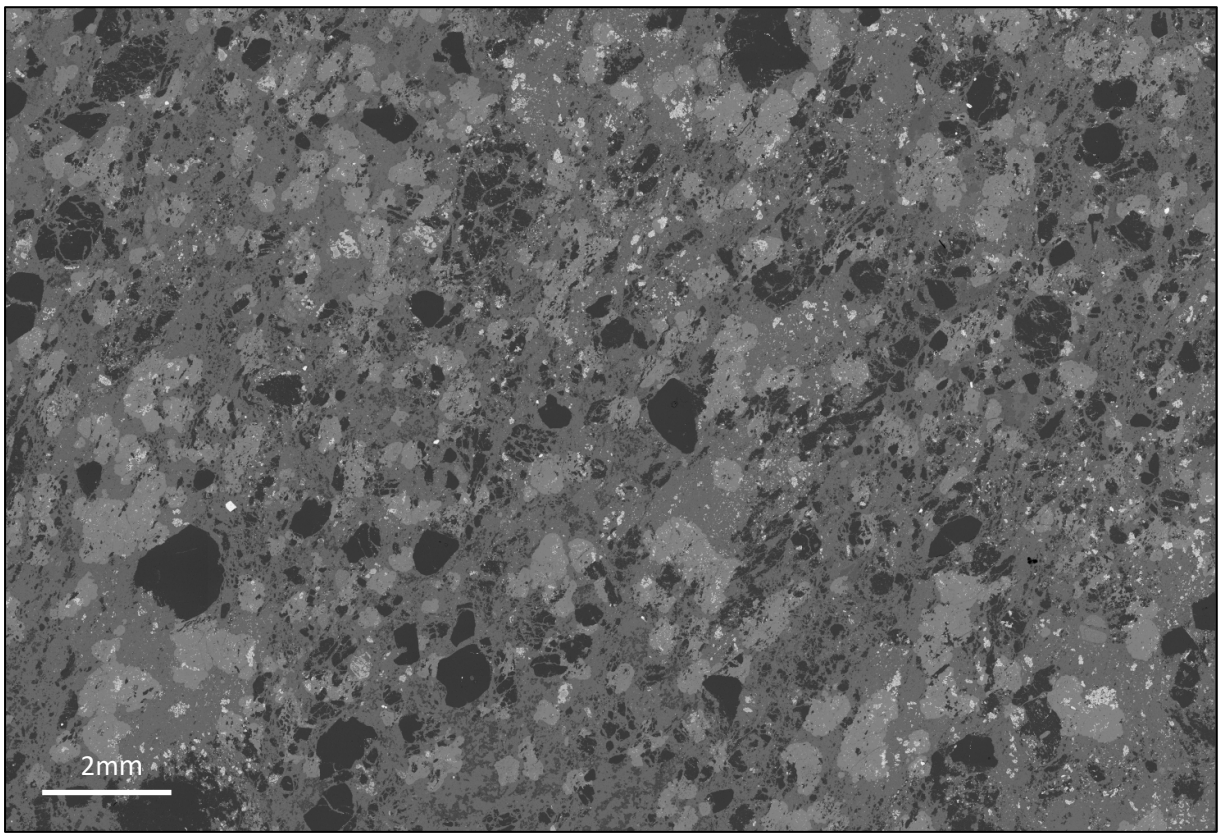

G408264

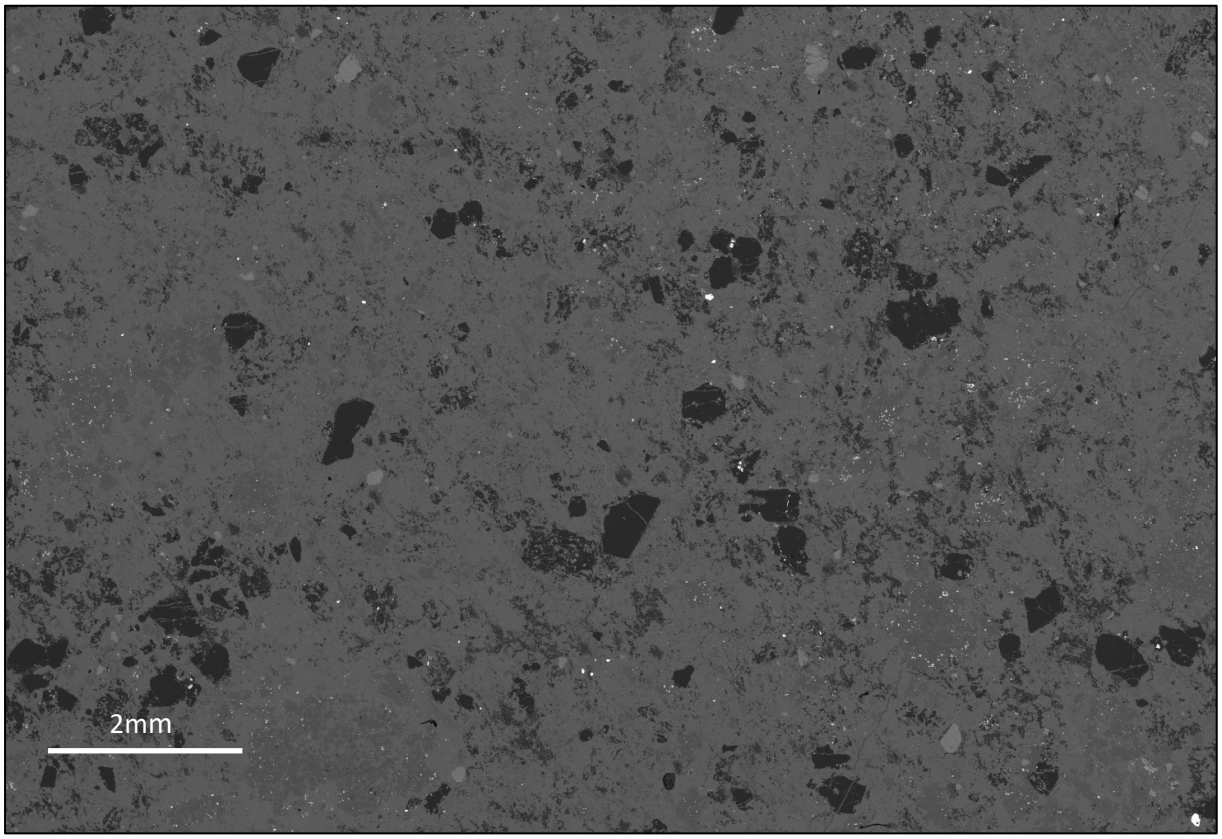

G408260

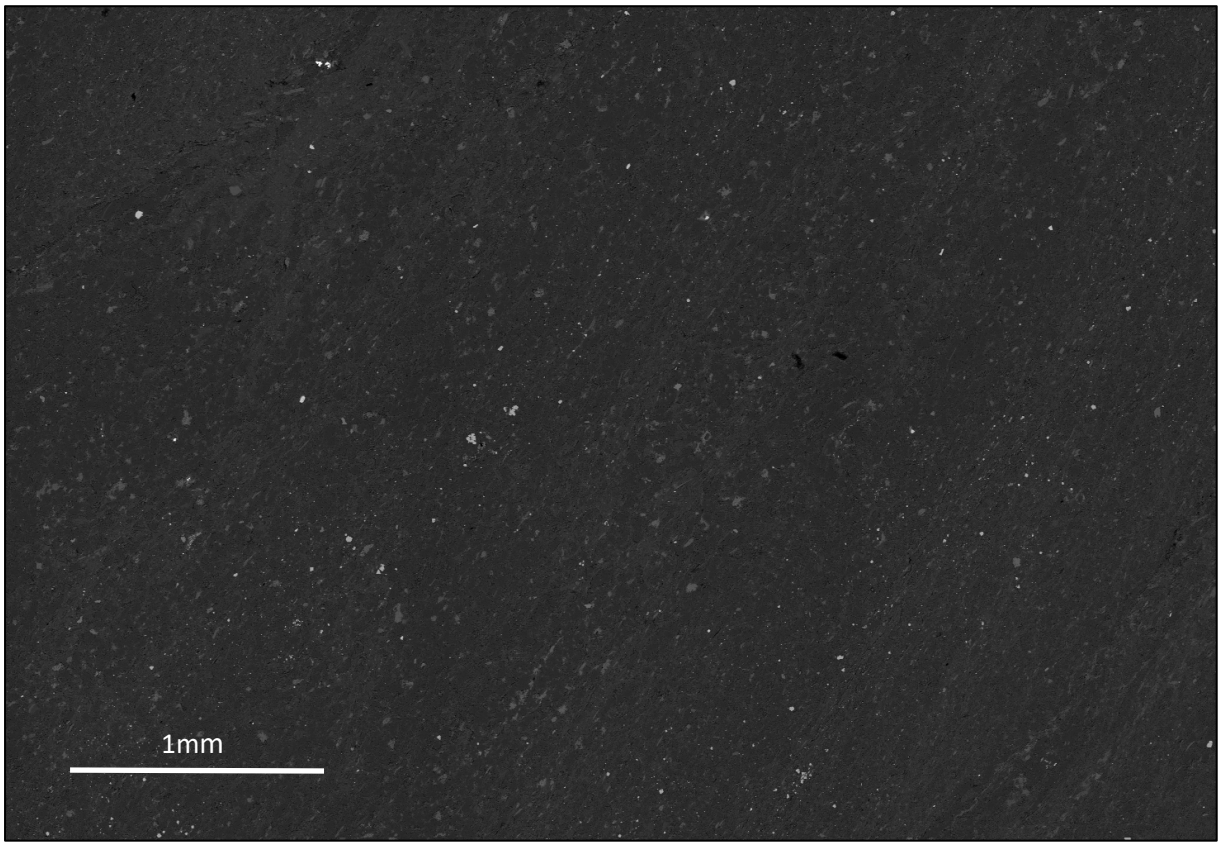

Appendix 7. Digital Files

Excel Tables

TSG Datasets

XMOD

Tasmanian
Government

Mineral Resources Tasmania
PO Box 56 Rosny Park
Tasmania Australia 7018
Ph: +61 3 6165 4800

info@mrt.tas.gov.au www.mrt.tas.gov.au